

Studies into the structural basis of the DNA uridine
endonuclease activity of exonuclease III homolog Mth212

Dissertation
zur Erlangung des Doktorgrades
der Mathematisch-Naturwissenschaftlichen Fakultäten
der Georg-August Universität zu Göttingen

Vorgelegt von
Khaliun Tseden
aus Greifswald, Deutschland

Göttingen 2011

D7

Referent:

Prof. Dr. Hans-Joachim Fritz

Korreferent:

PD Dr. Wilfried Kramer

Tag der mündlichen Prüfung:

02. Mai 2011

Table of Contents

1	Introduction	1
1.1.	Background to the study	1
1.1.1.	Necessity of mutation avoidance.....	1
1.1.2.	Mutations arising in DNA during replication	1
1.1.3.	Exogenous sources of DNA damage	2
1.1.4.	Endogenous sources of DNA damage	2
1.1.4.1.	Hydrolytic DNA deamination	4
1.1.5.	Repair of uracil in DNA	5
1.1.5.1.	Uracil-initiated base excision repair	5
1.1.5.2.	Uracil-initiated nucleotide incision repair	7
1.2.	Objective and methodology of the study	9
1.2.1.	Objective of the study.....	9
1.2.2.	Methodology of the study	9
1.2.2.1.	Necessity of screening or selection methodology in directed evolution of enzymes	11
1.2.2.2.	Selection of a protein with acquired DNA uridine endonuclease activity	11
2.	Materials and Methods	13
2.1.	Materials	13
2.1.1.	Bacterial strains	13
2.1.1.1.	<i>Escherichia coli</i>	13
2.1.1.2.	<i>Bacillus subtilis</i>	14
2.1.2.	Bacteriophage strains	14
2.1.3.	Plasmid vectors	15
2.1.4.	2' Desoxyriboseoligonucleotides	17
2.1.5.	Molecular ladders and markers	21
2.1.6.	Enzymes and proteins	22
2.1.7.	Chemicals and reagents	22
2.1.8.	Molecular biology kits	24
2.1.9.	Buffers and solutions	24

2.1.10. Bacterial growth media	29
2.1.11. Equipment and hardware	29
2.1.12. Other materials	31
2.1.13. Software	31
2.1.14. Databanks	32
2.2. Methods	32
2.2.1. Microbiological methods	32
2.2.2. Molecular biological methods	37
2.2.3. Protein biochemical methods	47
3. Results and Discussion	53
3.1. Production and characterization of ExoA from <i>Bacillus subtilis</i>	53
3.1.1. Production and purification of ExoA	54
3.1.2. Biochemical characterization of ExoA	55
3.2. Attempted genetic selection of a protein carrying DNA uridine endonuclease activity with the use of PBS1 bacteriophage	57
3.2.1. Design of a selection procedure	57
3.2.2. Construction of a mutant gene library	58
3.2.2.1. Optimisation of error-prone PCR conditions	59
3.2.2.2. Cloning of the library and transformation of <i>E. coli</i>	61
3.2.2.3. Investigation of transformation efficiencies of different <i>B.</i> <i>subtilis</i> strains	62
3.2.3. Investigation of PBS1 bacteriophage	63
3.2.3.1. Verification of presence of uridine residues in PBS1 bacteriophage genome	63
3.2.3.1.1. Processing of PBS1 DNA <i>in vivo</i>	65
3.2.3.2. Experiments to obtain clear-plaque mutant of PBS1 bacteriophage	67
3.3. Attempted genetic selection of a protein carrying U-Endo activity with the use <i>E. coli</i> bacteriophage	71
3.3.1. Design of a selection procedure	71
3.3.2. Construction of a mutant gene library	72
3.3.3. Construction of <i>E. coli</i> mutant strains C1a <i>Δung</i> and C520 <i>Δung</i> ..	73

3.3.4. Cloning of an amber-suppressor tRNA gene	74
3.3.5. Cultivation of bacteriophage P2vir1Ram3 on <i>dut- ung-</i> strain ...	75
3.3.6. Survey of inability of P2vir1Ram3 bacteriophage to finish infection	76
3.4. Attempted genetic selection based on heteroduplex DNA of phagemid pBluescriptII with uracil containing mismatch	80
3.4.1. Construction of mutant gene library	81
3.4.2. Construction of heteroduplex DNA	81
3.5. ExoA triple mutant and selection of its stable variant by genetic complementation.....	88
3.5.1. Generation and purification of the ExoA S110G_R111K_R120K triple and R120K single mutants	89
3.5.2. Activity assays with ExoA variants	93
3.5.3. Attempts to optimize production of ExoA triple mutant protein ...	95
3.5.4. ExoA quadruple (S110G_R111K_D145N_R120K) mutant production, purification and activity assays	96
3.5.5. Design of selection procedure of a stable variant of ExoA triple mutant	99
3.5.6. <i>E. coli</i> $\Delta xthA$ strain and cytotoxicity of overproduced proteins ...	99
4. Summary	104
5. Abbreviations	106
6. Literature	109
7. Appendix.....	121
7.1. Sequences (attached CD)	

Acknowledgements

Curriculum vitae

1 Introduction

1.1. Background to the study

1.1.1. Necessity of mutation avoidance

DNA, the carrier of genetic information in all cells and many viruses, is a dynamic molecule, subject to changes that alter this information (Lindahl, 1993). This genetic variability is essential for the adaptation and survival processes and drives the evolution. At the same time, an organism requires the correct functioning of lots of genes, damaging each of whose could have fatal consequences. Mutations in DNA can arise from natural cellular functions, like replication and recombination. In addition, the chemical instability of DNA under physiological conditions and susceptibility to reaction with various endogenous and exogenous compounds contribute to mutation pool. These mutations affect the structure of the genetic material and are considered to be DNA damage (Friedberg *et al.*, 2006). Much of these mutations change the coding properties of DNA, leading to expression of defect proteins; some modifications alter the efficiency of transcription, stall the replication fork, which at large can lead to cell death. Therefore, existence of DNA damage recognition and removal processes is of crucial importance in mutation avoidance and viability. In the following subsections sources of DNA mutations are briefly discussed.

1.1.2. Mutations arising in DNA during replication

DNA replication is a highly precise process with fidelity of about one error per 10^9 - 10^{10} nucleotides (Kunkel, 1992). This high fidelity of DNA synthesis is achieved through cooperative action of DNA polymerase, exonucleolytic proofreading and post-replicative mismatch repair processes. DNA polymerase synthesizes the DNA with only one mistake per 10^4 - 10^5 nucleotides as a result of a tight control on the stability of the newly formed hydrogen bonds in the active center of the enzyme. However, bias in the nucleotide pool and base tautomerisation can lead to various misincorporations (Roberts and Kunkel, 1996). In addition, polymerases are prone to “strand slippage” when copying sections of DNA that contain a large number of repeating nucleotides or repeating sequences which leads to deletions or insertions (Bichara *et al.*, 2006). 3'-5' exonucleolytic proofreading activity associated with replicative polymerases usually increases the fidelity of DNA synthesis 100-fold (Benkovic and Cameron, 1995). Replication errors that were not corrected by the proofreading process are

subject to post-replicative mismatch repair (MMR) thus increasing the fidelity of DNA synthesis by around three orders of magnitude (Friedberg *et al.*, 2006).

1.1.3. Exogenous sources of DNA damage

DNA damage causing physical and chemical agents that are generated outside of the cell are covered in this sub-section. Physical mutagens are primarily radiation sources, including UV- and ionizing radiation. Cyclobutane pyrimidine dimers (CPD) are the most common lesions produced in DNA when irradiated with UV. If not repaired, these lesions lead to replication arrest (Yoon *et al.*, 2000). Ionizing radiation generates reactive oxygen species (ROS) which cause a variety of DNA lesions among of which hazardous DNA strand breaks are prevalent (Rastogi *et al.*, 2010). Generally, enzymes involved in nucleotide excision repair (NER) pathway recognize and repair these DNA damages. Alkylating agents are the most abundant exogenous chemical mutagens. Abnormal base methylation, or AP-site formation are the results of their interaction with DNA. In addition, bifunctional alkylating agents can react with two different nucleophilic centers in DNA causing DNA cross-links. Chemicals, such as bleomycin and calicheamicin, cause DNA breaks or base modifications (Friedberg, 2006).

1.1.4. Endogenous sources of DNA damage

Normal metabolic processes also generate ROS, which, in addition to single-strand break formations, can modify DNA bases by oxidation (De Bont and van Larebeke, 2004). Both purine and pyrimidine bases are subject to oxidation. One of the most prevalent lesions in DNA is guanine oxidized to 8-oxo-7,8-dihydroguanine, which is capable of base pairing with adenine, resulting in a G→T transversion mutation following the replication (Ruiz-Laguna *et al.*, 2000). Products of unsaturated lipids oxydation can react with bases in DNA resulting in exocyclic etheno adducts such as etheno-dC or etheno-dA. Generally, base alterations produced by oxidizing agents are substrates of the base excision repair (BER).

Intracellular S-adenosylmethionine (SAM), which is a methyl group donor in enzymatic methylation reactions, is known as a weak non-enzymatic DNA-methylating agent (Lindahl, 1993). One of the products of its reaction with DNA bases is O⁶-methylguanine (O⁶-MeG) which base pairs with thymine rather than with cytosine. This point mutation is repaired by

damage reversal system by recruiting O⁶-MeG DNA methyltransferase, which removes the methyl group (E. C. Friedberg *et al.*, 2006).

Another principal source of DNA damage is spontaneous hydrolysis reaction (Figure 1.1). Especially susceptible is the N-glycosidic bond of the purines. Depyrimidination also occurs, but about 30 times slower. The resulting apurinic/apyrimidinic (AP) sites, if not repaired, can lead to DNA chain rupture. It was estimated that 10000 depurination events occur daily in a diploid mammalian cell (Friedberg, 2006). Not only glycosidic bonds, but also DNA bases suffer from hydrolytic attacks. The exocyclic amino groups of the bases are labile and readily undergo reactions of hydrolytic deamination (Lindahl, 1993). Formation and repair of these DNA damages, especially of cytosine deamination, will be described in more details as it has direct relation to this work.

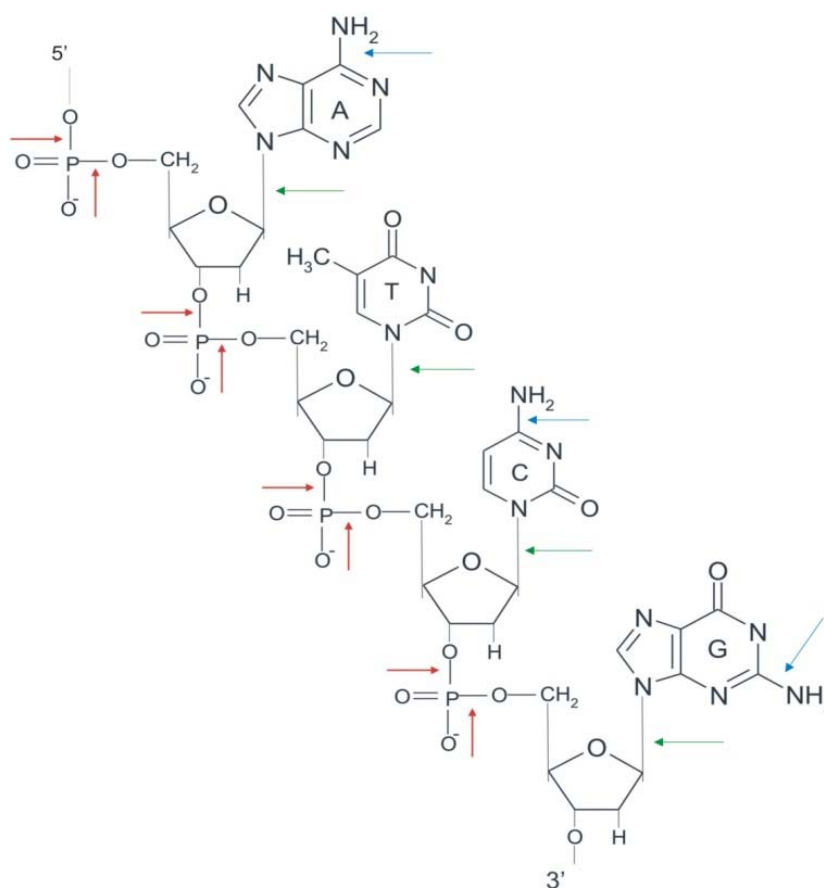


Figure 1.1: DNA primary structure with four principal DNA bases and major sites of spontaneous hydrolytic attack. Green arrows indicate N-glycosidic bonds; red arrows: phosphodiester bonds; blue arrows: bonds with exocyclic amino groups. Adapted from T. Lindahl, 1993.

1.1.4.1. Hydrolytic DNA deamination

In the course of the hydrolytic deamination, purines adenine and guanine are converted into the hypoxanthine and xanthine residues, respectively. Xanthine is unable to pair stably with either cytosine or thymine and thus may result in arrested DNA synthesis, whereas hypoxanthine generates a pre-mutagenic lesion as it preferentially base pairs with cytosine (Friedberg, 2006). But as rates of purines deamination are low (for instance, conversion of adenine into hypoxanthine in single-stranded DNA occurs at about 2% of the rate of the conversion of cytosine to uracil (Lindahl, 1979)) and the resulting products are repaired efficiently, no real threat to the integrity of the genetic information is considered.

Hydrolytic deamination occurs most rapidly at 5-methylcytosine (5-meC) sites (Lindahl, 1993). 5-meC is produced by site-specific DNA (cytosine-5)-methyltransferase which transfer methyl group from S-adenosylmethionine to the C-5 position of cytosine in double-stranded DNA (Chen *et al.* 1994). Cytosine methylation has important functions such as modification of DNA as a defense against the invasion of the foreign DNA species in prokaryotes (Palmer and Marinus, 1994) and involvement in the regulation of gene expression, embryogenesis, genomic imprinting, aging, and some other processes in eukaryotic cells (Jaenisch and Bird, 2003). Deamination of 5-meC in DNA results in the formation of thymine and hence of T/G mismatch. The subsequent replication rounds will generate a GC→AT transition mutation. Base excision repair initiated by several highly specialized enzymes, and a specific repair process in some bacteria termed *very short patch repair* (VSP) mechanism are responsible for the repair of T/G mismatches (Bhagwat and Lieb, 2002).

Hydrolytic cytosine deamination occurs about 50 times quicker than deamination of the purines (Lindahl and Nyberg, 1972). Resulting uracil is formed at high rates especially in the single stranded DNA during transcription, replication or recombination (Lindahl and Barnes, 2000). Although uracil is normally confined to RNA, the formation of uracil in DNA is mutagenic due to its preferential pairing with adenine residue. If not repaired, this will lead to GC→AT transition mutation in 50% of progeny when replication proceeds. *E. coli* strains that are defective in the removal of uracil from DNA have an increased spontaneous mutation rate, and GC→AT base pair transitions are observed at selected sites in such mutants (Duncan and Miller, 1980). Deamination of cytosine can be enhanced by a number of chemical alterations and steric factors, by the formation of UV-radiation induced cyclobutane pyrimidine dimers, by certain intercalating agents or by the positioning of a mismatched or alkylated base

opposite cytosine. Deamination can also be promoted by reaction with nitrous acid or sodium bisulfate (Friedberg *et al.*, 2006). Generation of uracil by gamma radiation-induced deamination of cytosine and sensitivity of *E. coli* cells deficient in Ung and Smug1 DNA glycosylases to gamma-radiation was reported (An *et al.*, 2005). In eukaryotic cells, uracil can arise in DNA due to the enzymatic deamination of cytosine (Harris *et al.*, 2002), by drug treatment or folate deficiency (Kavil *et al.*, 2007). In addition, uracil can be incorporated into DNA during semiconservative replication and the extent of this incorporation is directly related to the size of intracellular dUTP pool. Presence of U/A base pairs rather than T/A base pairs, in general, does not change the coding information, but uracil-containing DNA possesses the altered binding affinities for the transcription factors or other regulatory proteins (Verri *et al.*, 1990).

Uracil residues in DNA exist transiently since they are subject to removal by the multi-step uracil initiated DNA base excision repair (BER) process in most organisms and by nucleotide incision repair pathway (NIR) described to date only in *M. thermautotrophicus* (Georg *et al.*, 2006; Schomacher *et al.*, 2009).

1.1.5. Repair of uracil in DNA

1.1.5.1. Uracil-initiated base excision repair

Base excision repair (BER), which is the primary defence mechanism against major forms of DNA base damage, occurs in two stages: an initial, damage specific stage carried out by individual DNA glycosylases targeted to distinct base lesions, and a damage-general stage that restores the correct DNA base sequence (Mol *et al.*, 1999). Figure 1.2 illustrates how damage-general stage of BER after removal of uracil by uracil-DNA glycosylase proceeds.

Uracil-DNA Glycosylases

The first UDG was discovered in *E. coli* by T. Lindahl in 1974 in a search for activities that would repair uracil in DNA. This also represented the discovery of BER (Krokan *et al.*, 2002). Ung from *E. coli* later proved to be a representative of widespread and highly conserved family of UDGs - family 1. At present, UDGs are classified into 5 families comprising the UDG-superfamily. Distribution of UDG family representatives in certain eubacteria, eukaryotes and archaea are summarized in Table 1.1.

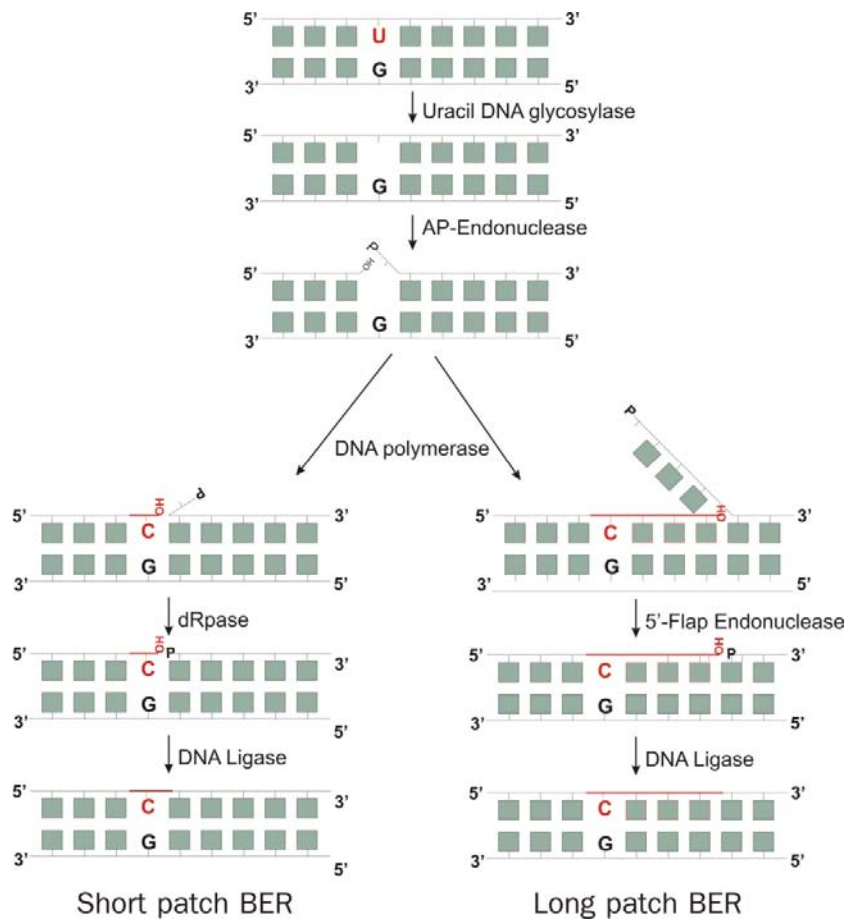


Figure 1.2: Schematic outline of uracil-initiated BER showing the separate steps. Uracil-DNA glycosylase recognises uracil base and cleaves the N-C1' glycosidic bond between uracil base and deoxyribose sugar. Generated AP-site (apurinic/aprimidinic site) is processed by an AP-Endonuclease by catalyzing the hydrolysis of sugar-phosphate backbone at the 5' side of AP-site and leaving 3'-OH and 5'-deoxyribose-phosphate (dRp) termini. In the *short patch* BER pathway 3'-OH serves as primer terminus for a DNA polymerase which replaces the AP-site by repair synthesis. dRp moiety is then removed by dRpase and the nick is ligated by a DNA ligase. In the *long patch* BER pathway strand displacement synthesis by DNA polymerase creates a 5' flap that is cleaved by 5'-flap endonuclease to create a ligatable nick. Adapted from Friedberg *et al.*, 2006 and Smolorz, 2009.

	Eubacteria		Eukaryotes		Archaea	
	<i>E. coli</i>	<i>T. thermophilus</i>	<i>S. cerevisiae</i>	<i>H. sapiens</i>	<i>A. fulgidus</i>	<i>M. thermautotrophicus</i>
Family 1 (Ung)	+	+	+	+	-	-
Family 2 (MUG/TDG)	+	+	-	+	-	+
Family 3 (SMUG)	-	-	-	+	-	-
Family 4 (tUDGa)	-	+	-	-	+	-
Family 5 (tUDGb)	-	+	-	-	-	-

Table 1.1: Phylogenetic distribution of uracil-DNA glycosylases. +: encoded in genome; -: not detected; **Ung** - Uracil N-Glycosylase, **Mug/TDG** - Mismatch specific Uracil-DNA-Glycosylase/Mismatch-specific Thymine-DNA-Glycosylase, **SMUG** - Single-strand-specific Monofunctional Uracil-DNA-Glycosylase, **tUDGa** and **tUDGb** - Thermostable Uracil-DNA Glycosylases. Adapted from Friedberg *et al.*, 2006.

Aside from enzymes from these 5 families, uracil in DNA is processed by DNA glycosylases which belong to structurally distinct “helix-hairpin-helix” (HhH) superfamily. Mig.MthI from *M. thermautotrophicus* (Horst and Fritz, 1996), Pa-Mig from *P. aerophilum* (Yang *et al.*, 2000), MBD4 from *H. sapiens* (Hendrich *et al.*, 1999) belong to this class of enzymes. These enzymes remove uracil from U/G and thymine from T/G mismatches, and do not act on single-stranded DNA. However, uracil appears to be a minor substrate for these enzymes, since the uracil-excising activity is not robust in crude extracts (Sartori *et al.*, 2001) and uracil can be removed only from certain sequence contexts (Horst and Fritz, 1996).

UDG activities corresponding to one family or other have been identified in organisms from all kingdoms, including the viruses, and many organisms have multiple examples. This distribution specifies the important role of uracil repair in the maintenance of genome integrity. The lack of UDGs which can be responsible for general uracil repair in some organisms, such as *M. thermautotrophicus*, can only stand for existence of alternative pathways to counteract the threat of uracil in DNA.

1.1.5.2. Uracil-initiated nucleotide incision repair

Nucleotide incision repair (NIR) is initiated through direct strand incision by an endonuclease resulting in 3'OH termini for DNA repair synthesis; the dangling damaged nucleotide is then a good substrate for flap endonuclease, DNA polymerase I or exonuclease (Ischenko and Saparbaev, 2002). Until Georg *et al.* (2006) identified Mth212 from *M. thermautotrophicus* to initiate the DNA uracil repair via NIR, *E. coli* Vsr-endonuclease was the only described enzyme to possess DNA uridine endonuclease activity. Vsr, however, incises the DNA strand only in the proper sequence context and processes only U/G mismatches, therefore does not qualify as an initiator of general DNA uracil repair (Gläsner *et al.*, 1995; Gabbara *et al.*, 1994; Schomacher *et al.*, 2009).

Initiation of NIR by Mth212

M. thermautotrophicus, as mentioned above, is devoid of genes encoding uracil-DNA glycosylases that can serve as initiators of general DNA uracil repair. Mismatch-specific glycosylase Mig.MthII and HhH glycosylase Mig.MthI from this organism were found to be unable to initiate general DNA uracil repair as these enzymes excise uracil only within certain

sequence contexts (Horst and Fritz, 1996; Starkuviene, 2001). To address the question to the DNA uracil repair in *M. thermoautotrophicus*ΔH members of our laboratory fractionated the cell extract and searched for relevant activity. As result of their work Mth212, exonuclease III homolog, was discovered and characterized biochemically. Mth212, in addition to the numerous enzymatic activities inherent to exonuclease III homologs, recognises uridine in DNA and cleaves the phosphodiester backbone direct to the 5' side of the 2'deoxyuridine residue independently of the sequence context and the nucleotide juxtaposed to the uridine residue in the complementary strand (Georg *et al.*, 2006).

Repair studies *in vitro* employing whole cell extracts demonstrated that in *M. thermoautotrophicus* ΔH general repair of DNA uracil residues is initiated by this direct strand incision catalyzed solely by Mth212 and this organism is completely dependent of this pathway (Schomacher *et al.*, 2009). The presence of Mth212, DNA polymerase B (mthPolB), 5'-flap endonuclease (mthFEN) and DNA ligase (mthDNA_ligase), purified to apparent homogeneity, was sufficient for complete repair of DNA uracil residues *in vitro* (Schomacher *et al.*, 2010).

If compared to BER (Figure 1.2), in this pathway Mth212 substitutes the two-step reaction achieved by consecutive action of UDG and AP-endonuclease in a single-step reaction by directly incising the DNA strand on 5' side of uridine residue. Following steps correspond to the *long patch* BER pathway: strand displacement synthesis by DNA polymerase (mthPolB) creates a 5' flap that is cleaved by 5'-flap endonuclease (mthFEN) to create a ligatable nick which is processed by DNA ligase (mthDNA_ligase).

Besides direct damage reversal, this constitutes the simplest DNA repair pathway characterized so far. This simplicity naturally suggests that this mechanism should be widely spread phylogenetically. However, in most organisms BER is the “quarterback” to withstand the threat of uracil in DNA. This suggests that the evolution of DNA uracil repair had at least two alternative ways: (1) evolution of uracil specific DNA glycosylase activity in some protein, resulting in the foundation of the UDG-superfamily and (2) expanding the substrate spectrum of an AP-endonuclease such that it accepts, in addition, uracil as substrate, as is the case with Mth212. The possibility of another alternative is still open as there are organisms,

such as *M. kandleri* AV19 and *M. stadtmanae*, devoid of both UDG genes and exonuclease III homolog genes (Schomacher *et al.*, 2009).

1.2. Objective and methodology of the study

1.2.1. Objective of the study

What is the structural basis of the unique activity of Mth212? The finding of a new pathway of uracil repair for archaeal DNA raised this question along with a query regarding the molecular mechanism of uracil recognition, in particular how Mth212 discriminates against cytosine and thymine residues. Within all identified and characterized exonuclease III homologs Mth212 is the only known (to date) representative that recognizes uridine in the DNA and initiates the repair. However, multiple sequence alignment of exonuclease III homologs with Mth212 revealed no remarkable divergence from the conserved sequence that can be in charge of the unique activity. In X-ray crystallography studies of the enzyme, co-crystallised with DNA (in cooperation with the department of Prof. Dr. R. Ficner), enzyme invariably bound to the ends of substrate DNA duplexes thus precluding insight into its interaction with DNA uridine residue. To begin of this study, attempts to clarify the mechanism of uracil recognition by means of directed mutagenesis were met with little success.

In this study, it is attempted to elucidate the mechanism of uridine recognition of Mth212. As above mentioned conventional methods were insufficient in shedding light on this mechanism, another approach was employed. New route taken employs genetics, the idea being to take an exonuclease III homolog without DNA uridine endonuclease activity and to provide it with this activity by means of directed evolution.

1.2.2. Methodology of the study

Directed evolution of proteins is known to be a powerful tool for generating enzymes with properties such as improved catalytic activities, increased thermostability or new substrate specificities. At the same time, modifying protein function precedes understanding the molecular mechanisms underlying those modifications (Arnold, 1998). This means that a transformation of a protein, homologous to Mth212 but with no activity against uracil, into DNA uridine endonuclease will bring about the knowledge of which amino acid residues

participate in the uridine recognition. Projecting these amino acids onto 3D structure of Mth212 will lead to the elucidation of structural peculiarities of Mth212 that lie underneath the unique activity and, at the same time, it is possible to shed light on the pathway taken by natural evolution that resulted on this activity. In addition, this knowledge can facilitate the discovery of other organisms, whose genomes are sequenced, that employ the same mechanism as *M. thermautotrophicus* for general DNA uracil repair.

When converting an enzyme into DNA uridine endonuclease, it is rational to remodel a protein scaffold which at most resembles Mth212. ExoA, exonuclease III homolog from *B. subtilis*, was chosen as an object for randomization. This protein, which shares 46% identity and 64% similarity with Mth212, was described as a multifunctional DNA-repair enzyme with AP-endonuclease, 3'-5' exonuclease, ribonuclease H, and 3'-monoesterase activities (Shida *et al.*, 1999). Crystal structure of this protein has not been solved yet. In addition, *B. subtilis* being host for PBS1 bacteriophage was decisive for choosing exonuclease III homolog from this organism for directed evolution (Results and Discussion, Section 3.2.1).

Directed evolution of enzymes involved in DNA repair and synthesis

The enzymes responsible for DNA repair and replication are in general highly conserved across diverse domains of life. And the question arising is whether such enzymes can tolerate changes in their amino acid sequence.

The nucleotide sequence of DNA polymerases is highly conserved within families and these enzymes demonstrate a remarkable conservation of structure, even in particularly divergent organisms. However, extensive studies on directed evolution carried out with *T.aquaticus* Pol I (*Taq* Pol I) revealed high mutability of the polymerase active site *in vivo* (Patel and Loeb, 2000). Moreover, *Taq* polymerase mutants that were able to efficiently synthesize long stretches of RNA from a DNA template were isolated. (Xia *et al.*, 2002). In other study HSV-1 TK gene encoding thymidine kinase was mutagenized and the enzymes with altered substrate specificities were reported (Black *et al.*, 1996). O⁶-Alkylguanine-DNA Alkyltransferase variants were evolved that show enhanced function, have altered substrate specificities or more resistant to inhibitors (Davidson *et al.*, 2002). In every case the creation of large altered proteins has

been achieved and the emerging picture is that even highly conserved proteins can tolerate wide-spread amino acid changes at the active site without substantial loss of activity.

1.2.2.1 Necessity of screening or selection methodology in directed evolution of enzymes

Directed evolution experiments consist of two major steps: first, the creation of genetic diversity in the target gene in the form of gene libraries; and second, an effective selection of the library for the desired catalytic activity. An array of methods has been developed to generate diversity: depending on the experiment, mutagenesis might entail degenerate oligonucleotide-directed or error-prone DNA synthesis, shuffling of mutant DNA fragments, combinatorial synthesis and other methods (for overview refer to Results and Discussion, Section 3.2.2 – 3.2.3). The bottleneck for most directed enzyme evolution endeavors is the availability of a genuinely high-throughput screen or selection for the target activity (Aharoni *et al.*, 2005). The difference between screening and selection lies in screening being an active search performed on individual clones and requires some spatial organization of the screened variants on agar plates, microtiter plates, arrays or chips, whereas selection act simultaneously on the entire pool of genes. Thus, the main advantage of genetic selection over screening is that many more library members can be analyzed at once. In the best screening protocols, which take advantage of fluorogenic or chromogenic substrates, the maximum number of library members that can be assayed is about 10^5 (Hilvert *et al.*, 2002). In contrast, up to 10^9 clones can be assessed using genetic selection in vivo in *E. coli* cells. The limit of the clones that can be surveyed is dependent, at least theoretically, on transformation efficiency. Therefore, genetic selection in bacteria other than *E. coli*, can be less efficient due to lower transformation efficiencies. It is challenging to develop suitable selection strategy for a particular catalytic activity. Coupling of the target reaction to survival in the selection step may require development of complex, non-trivial and intelligent assays (Hilvert *et al.*, 2002). In fact, most of the experimental effort of directed evolution is devoted to devising, validating and implementing a suitable methodology (Arnold, 1998).

1.2.2.2 Selection of a protein with acquired DNA uridine endonuclease activity

As described above, in protein evolution experiment the most demanding step is the development of a selection strategy. Since it is intended to provide an enzyme with DNA

uridine endonuclease activity, selection approach should meet following demands: (1) DNA uridine, the substrate for the new activity, must present in assay and (2) desired enzymatic activity must ensure the isolation of cells carrying this particular mutant from other cells. During this study three selection approaches for selecting ExoA mutant carrying DNA uridine endonuclease activity from the library were designed and tested.

Further application of established methodology

Once established, the selection approach can be employed in identifying enzymes responsible for the initiation of DNA uracil repair. Genomic libraries of organisms such as *M. mazei*, *M. jannaschii*, *M. kandleri*, *M. maripaludis*, where no UDG gene is available, can be constructed and enzymes responsible for general DNA uracil repair can be identified.

2 Materials and Methods

2.1 Materials

2.1.1 Bacterial strains

2.1.1.1 *Escherichia coli*

BL21_UXX (Georg *et al.*, 2006)

E. coli B, F⁻, *ompT*, *hsdS* (rB-mB⁻), *dcm*⁺, Tet^R, *gal* ι (DE3), *endA*, Hte [*argU*, *ileY*, *leuW*, Cm^R], Δ *ung*

One Shot TOP10 (Invitrogen, Carlsbad, CA)

F⁻ *mcrA* Δ (*mrr-hsdRMS-mcrBC*) ϕ 80*lacZ* Δ M15 Δ *lacX74* *nupG* *recA1* *araD139* Δ (*ara-leu*)7697 *galE15* *galK16* *rpsL*(Str^R) *endA1* λ ⁻

DH5 α (Invitrogen, Carlsbad, CA)

F⁻, Φ 80*dlacZ* M15, *endA1*, *recA1*, *hsdR1* (rK-mK⁺), *supE44*, *thi-1*, *gyrA96* (Nal^R), *relA1*, (*lacZYA-argF*) U169

TOP10F^o (Invitrogen, Carlsbad, CA)

F^o[*lacI^q* Tn10(tet^R)] *mcrA* Δ (*mrr-hsdRMS-mcrBC*) ϕ 80*lacZ* Δ M15 Δ *lacX74* *deoR* *nupG* *recA1* *araD139* Δ (*ara-leu*)7697 *galU* *galK* *rpsL*(Str^R) *endA1* λ ⁻

XL1-Red (Stratagene, USA)

F⁻ *endA1* *gyrA96*(nal^R) *thi-1* *relA1* *lac* *glnV44* *hsdR17*(rK⁻ mK⁺) *mutS* *mutT* *mutD5* Tn10

CJ236 (New England Biolabs, Ipswich, MA)

F Δ (*HindIII*)::*cat* (Tra⁺ Pil⁺ Cam^R)/ *ung-1* *relA1* *dut-1* *thi-1* *spoT1* *mcrA*

XL10-Gold Kan^r ultracompetent cells (Stratagene, USA)

Tet^r Δ (*mcrA*)183 Δ (*mcrCB-hsdSMR-mrrr*)173 *endA1* *supE44* *thi-1* *recA1* *gyrA96* *relA1* *lac* The [F⁻ *proAB* *lacI^q*Z Δ M15 Tn10 (Tet^r) Tn5 (kan^r) Amy]

C1a (Prof. G. E. Christie, Virginia Commonwealth University, USA), (Sasaki and Bertani, 1965)

F⁻ prototrophic

C1a Δ ung (this study)

F⁻ Δ ung::*kan*

C520 (Prof. G. E. Christie, Virginia Commonwealth University, USA), (Sunshine *et al.*, 1971)

F⁻ *supD*

C520 Δ ung (this study)

F⁻ *supD* Δ ung::*kan*

NM522 (Promega, Madison, USA)

F' *proA*⁺*B*⁺ *lacI*^f Δ (*lacZ*)M15/ Δ (*lac-proAB*) *glnV thi-1* Δ (*hsdS-mcrB*)5

NM522 Δ ung (Ber, 2009)

F' *proA*⁺*B*⁺ *lacI*^f Δ (*lacZ*)M15/ Δ (*lac-proAB*) *glnV thi-1* Δ (*hsdS-mcrB*)5 *Δ ung::kan*

BW25113 Δ xthA (Ber, 2009)

RrnB3 Δ *lacZ*4787 *hsdR*514 Δ (*araBAD*)567 Δ (*rhaBAD*)568 *rph-1* Δ *xthA*

2.1.1.2 *Bacillus subtilis*

W168 (BGCS, The Ohio State University, USA)

trpC2

SB19E (BGCS, The Ohio State University, USA)

ctrA1, *ts-2*, *Erm*^R

IH6140 (Dr. V. Kontinen collection of strains, National Institute for Health and Welfare, Helsinki, Finland), (Palva *et al.*, 1983)

Low exoprotease activity strain derived from strain IH6040: *amyE aroI906 metB5 sacA321*; obtained after multiple mutagenesis steps with NNG

IG-20 (BGSC, The Ohio State University, USA), (Bron *et al.*, 1975)

trpC2, *r(-)*, *m(-)*

ISW1214 (Dr. J-H. Kim collection of strains, Gyeongsang National University, Korea), (Ishiwa and Shibahara-Sone, 1986)

Tetracycline sensitive strain derived from strain 1012: *trpC2*, *hsrM1*, *leuA8*, *metB5*; obtained after mutagenesis with introsoguanidine

2.1.2 Bacteriophage strains

PBS1 (BGSC, The Ohio State University, USA), (Takahashi, 1963)

P2 vir1 (Prof. G. E. Christie, Virginia Commonwealth University, USA), (Bertani, 1957)

P2 vir1 Ram3 (Prof. G. E. Christie, Virginia Commonwealth University, USA), (Lindahl, 1971)

M13K07 helper phage (New England Biolabs, Ipswich, MA)

P1 (house collection)

2.1.3 Plasmid vectors

Below are the schematic representations of vectors used in this study. Gene reading frames are colored blue and replication origins are colored grey. Arrows indicate transcription or replication directions. Restriction endonuclease recognition sites used for the cloning of DNA fragments are shown. All schemes are created using Vector NTI 11.5 Software (Invitrogen, Carlsbad, CA).

2.1.3.1 pET_{28a} (Novagen, San Diego, CA)

For the nucleotide sequence of the pET28a vector refer to Appendix 7.1.1.

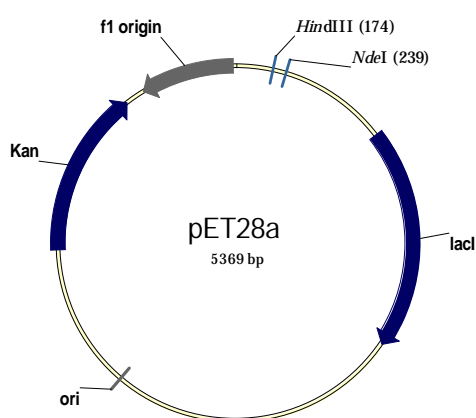


Figure 2.1: Schematic representation of pET_{28a} vector

Kan: neomycine phosphotransferase gene, provides kanamycine resistance. *lacI*: gene for Lac repressor.

2.1.3.2 pJET 1.2 (Fermentas, Burlington, Ontario)

For the nucleotide sequence of pJET1.2 vector refer to Appendix 7.1.2.

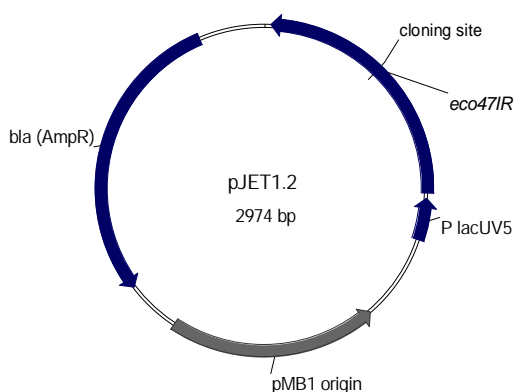


Figure 2.2: Schematic representation of pJET1.2 vector

bla: gene for β -lactamase, provides ampicilline resistance. *Eco47IR*: gene for a restriction endonuclease, lethal for *E. coli* when expressed

2.1.3.3 pBQ200_{BpiI} (Prof. Dr. J. Stülke, Institute of Microbiology and Genetics, Göttingen) (Martin-Verstraete *et al.*, 1994)

pBQ200_{BpiI} vector was obtained by introducing 2 *BpiI* (*BbsI*) restriction endonuclease sites via Site directed Quick-change[®] mutagenesis into pBQ200 vector DNA. For the nucleotide sequence of pBQ200_{BpiI} vector refer to Appendix 7.1.3.

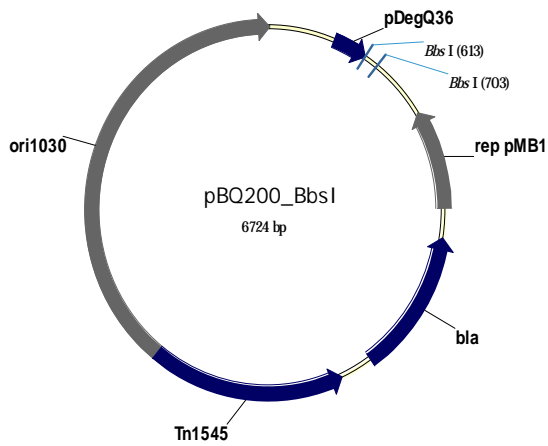


Figure 2.3: Schematic representation of pBQ200_ *Bpi*I vector

bla: gene for β -lactamase, provides ampicilline resistance. *Tn1545*: transposon *Tn1545* from *Streptococcus pneumoniae* carrying rRNA methylase gene, provides erythromycin resistance. Ori1030: *B. subtilis* replication origin. pDegQ36: mutagenized promoter of *B. subtilis degQ* gene (Msadek *et al.*, 1991).

2.1.3.4 pASK-08 (IBA GmbH, Göttingen, Germany)

pASK-08 vector was obtained from pASK_IBA3plus vector (B. Popova, unpublished). For the nucleotide sequence of pASK-08 vector refer to Appendix 7.1.4.

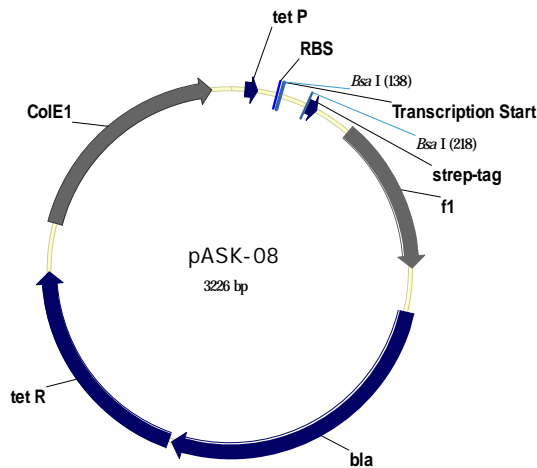


Figure 2.4: Schematic representation of pASK-08 vector

bla: gene for β -lactamase, provides ampicilline resistance. *tetR*: gene for repressor of *tet* promoter. *tetP*: *tet* promoter. RBS: ribosome binding site

2.1.3.5 pTNA (Prof. Dr. R. Sterner, Biophysik und biophysikalische Chemie, Universität Regensburg)

pTNA vector was obtained from pDS56/RBSII/*Sph*I (Qiagen, Hilden, Germany) vector, by exchanging the promoter region with *E. coli* Tryptophanase promoter (Henn-Sax, Disseration, 2001). For the nucleotide sequence of pTNA vector refer to Appendix 7.1.5.

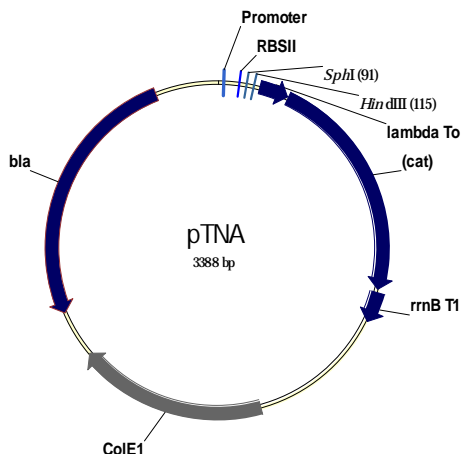


Figure 2.5: Schematic representation of pTNA vector

bla: gene for β -lactamase, provides ampicilline resistance. (cat): chloramphenicol acetyl transferase gene, protein is not expressed due to the lack of promoter. RBS II: synthetic ribosome binding site. lambda To, rrnB T1: terminator sequences.

2.1.3.6 pACYC177 (Chang and Cohen, 1978)

For the nucleotide sequence of pACYC177 vector refer to Appendix 7.1.6.

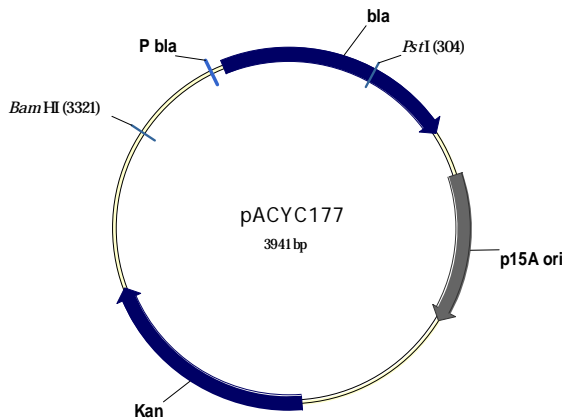


Figure 2.6: Schematic representation of pACYC177 vector

bla: gene for β -lactamase, provides ampicillin resistance. Kan: neomycin phosphotransferase gene, provides kanamycin resistance. P *bla*: promoter of *bla* gene

2.1.3.7 pBluescript II SK (+) (Fermentas, Burlington, Ontario)

For the nucleotide sequence of pBluescript II SK (+) vector refer to Appendix 7.1.7.

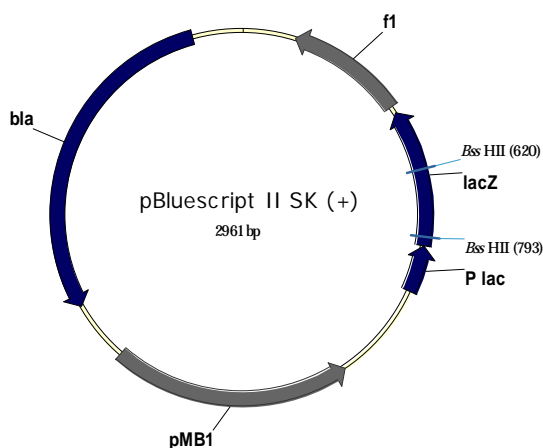


Figure 2.7: Schematic representation of pBluescript II SK (+) vector

bla: gene for β -lactamase, provides ampicillin resistance. *lacZ*: gene for N-terminal fragment of β -galactosidase. P lac: promoter of *lacZ* gene. f1: bacteriophage f1 intergenic (IG) region carrying the sequences required in cis for initiation and termination of phage f1 DNA synthesis and for packaging of DNA into bacteriophage particles. pBluescript II SK (+) is replicated such that the sense strand of *lacZ* gene is secreted within the phage particles.

2.1.4 2' Desoxyriboseoligonucleotides

All oligonucleotides were purchased from either Sigma (München) or PURIMEX (Gebenstein).

2.1.4.1 Primers for polymerase chain reaction

Primers for cloning of *exoA* into pET28a vector:

ExoA_For 5' AACATATGAAGTTGATTCATGGAATG 3'

ExoA_Rev 5' CGAAGCTTTCATATATTGATGATAAGTTC 3'

Primers for cloning of *exoA* into pBQ200 vector:

ExoA_XbaI_F 5'TCTAGACTCACTTATTTAAAGGAGGAAA
CAATCATGAAGTTGATTTTCATGGAATG 3'
ExoA_HindIII_R 5'AAGCTTCTAAGCATGATGATGATGATGA
TGTATATTGATGATAAGTTCAACCAC 3'

Primers for cloning of *mth212* into pBQ200 vector:

Mth212pbq200xbaIF 5' TCTAGACTCACTTATTTAAAGGAGGAAACAA
TCATGACCGTGCTAAAAATAATA 3'
Mth212pbq200pstIR 5' CTGCAGCTAATGATGATGATGATGATGTAGTT
CTATTTCCAGTCCTATGG 3'

Primers for cloning *exoA* into pASK vector:

pASK_BsaI_exoA_F 5' GTGTGGTCTCAAATGAAGTTGATTTTCATGGAA 3'
exoA_pASK_6His_2R 5' GTGGTCTCAGCTACTAATGATGATGATGATGA
TGTATATTGATGATAAGTTC 3'

Primers for cloning *exoA* into pTNA vector:

exoA_pTNA_F 5'GTGCATGCTAAAGTTGATTTTCATGGAATGTAAAC 3'
ExoA_HindIII_3R 5' GTAAGCTTCTAAGCATGATGATGATGATGATGT
ATATTGATGATAAGTTCAACAGG 3'

Primers for verification of *ung* deletion:

KAN_SEN 5' CGGTGCCCTGAATGAACTGC 3'
KAN_ANT 5' CGGCCACAGTCGATGAATCC 3'
UNG_AUS_SEN 5' CATCAACTTATGCGGGTGTG 3'
UNG_AUS_ANT 5' GCTGAATATCTCTGTGCGCAA 3'

Primers for cloning of *serU132* into pACYC177 vector:

serU_EcoRI_F 5' TGGAATTCGTTTTGCTCGCAAACCTCGTCAC 3'
serU_PstI_R 5' TGCTGCAGGTGTAAATCGTACAATGGTAAG 3'

Primers for cloning *ccdB* into pBluescript II SK (+):

ccdB_BssHII_2F 5' GTGCGCGCAGTTTAAGGTTTACACC 3'
ccdB_BssHII_R 5' GTGCGCGCTTATATTCCCCAGAACATCAGG 3'

2.1.4.2 Primers for Error-Prone PCR

Cloning into pBQ200 vector:

Exoa_ep_bpII_F 5' TGTGCGTCTCAGTTCCTCACTTATTTAAAGG 3'
Ep_exoa_esp3i_newR 5' TGTGCGTCTCTAGCGCTAAGCATGATGATGATG 3'

Cloning into pASK-08 vector:

pASK_EP-PCR_F 5' GTGTGGTCTCAAATGAAG 3'

pASK_EP-PCR_2R 5'GTGGTCTCAGCTACTAATGATGATGATGATGATG 3'

Cloning into pTNA vector:

exoA_pTNA_EP-PCR_F 5' GAGGAGAAATTAAGCATGC 3'

ExoA_ep_pbq200_R 5' AAGCTTCTAAGCATGATGATGATGATGATG 3'

2.1.4.3 Primers for Site-Directed Mutagenesis

Introduction of 2 *Bpi*I restriction sites into pBQ200 vector:

0512before1 5' GTAACAGATCAAATACCGAAGACTCGTTCACCCGGGATC 3'

0512before2 5' GATCCCCGGGTGAACGAGTCTTCGGTATTTGATCTGTTAC 3'

0512after1 5' GTGAAATTGTTATCCGCTCAGTCTTCCACACAACAT
ACGAGCC 3'

0512after2 5' GGCTCGTATGTTGTGTGGAAGACTGAGCGGATAACA
ATTCAC 3'

Removal of *Sph*I restriction site from *exoA*:

exoA_QC_F 5' GATTAGAGCGGATTGATTACCGTATGCAATGGGAAGA
GGCTTTAC 3'

exoA_QC_R 5' GTAAAGCCTCTTCCCATTGCATACGGTAATCAATCCG
CTCTAATC 3'

Overlap Extension Mutagenesis of *ccdB*:

ccdB_overlapextension_1

5' GATCCCCCTGGCTAGCGCACGTCTGCTGTCAGATTAAGTCT
CCCGTGAGCTCTACCCGGTGG 3'

ccdB_overlapextension_2

5'CCACCGGGTAGAGCTCACGGGAGACTTAATCTGACAGCAG
ACGTGCGCTAGCCAGGGGGATC 3'

ExoA R120K mutagenesis:

exoA_R120K_F 5'GATTAGAGCGGATTGATTACA
AGATGCAATGGGAAGAGG 3'

exoA_R120K_R 5' CCTCTTCCCATTGCATCTTGT
AATCAATCCGCTCTAATC 3'

ExoA S110_R111K_R120K mutagenesis:

exoA_3exchanges_F

5' GTTTACACGCCCAATGGCAAAGGGGATTAGAGCGGAT
TGATTACAAGATGCAATGGGAAGAGG 3'

exoA_3exchanges_R

5'CCTCTTCCCATTGCATCTTGTAAATCAATCCGCTCTAATCC
CCTTTTGCCATTGGGCGTGTAAC 3'

ExoA_D145N mutagenesis:

ExoA_D145N_1 5' CAGTGATTTTATGCGGTAATTTGAATGTAGCCCATC 3'
 ExoA_D145N_2 5' GATGGGCTACATTCAAATTACCGCATAAAAATCACTG 3'

2.1.4.4 Primers for DNA sequencing analysis

pJET1.2 vector sequencing primers:

pJET1.2 Forward 5' CGACTCACTATAGGGAGAGCGGC 3'
 pJET1.2 Reverse 5' AAGAACATCGATTTTCCATGGCAG 3'

pASK vector sequencing primers:

pASK_seq_F 5' CCACTCCCTATCAGTGATAG 3'
 pASK_seq_R 5' GTCGCACAATGTGCGCC 3'

pTNA vector sequencing primers:

pTNA_seq_2F 5' AATAAACAAATAGGGGTTCC 3'
 pTNA_seq_2R 5' TATCCAGTGATTTTTTCTC 3'

pBluescript II SK (+) sequencing primers

pBluescript_seq1 5' GAATAGACCGAGATAGGGTTG 3'
 pBluescript_seq2 5' CTGCAAGGCGATTAAGTTGGG 3'
 pBluescript_seq3 5' GGCACGACAGGTTTCCCGACTGG 3'

Primers for sequencing gpR region of P2 bacteriophage:

P2_gpR_seq_F 5' GCAGACGAACGGCGATTTAAG 3'
 P2_gpR_seq_R 5' CTGCCGCAGACGTTTCGCCAG 3'

2.1.4.5 Oligonucleotides for Endonuclease Assay

40_Prince_AP: 5'(F) GGGTACTTGGCTTACCTGCCCTGAPGCAGCTGTGGGGCGCAG3'
 40_Prince_U: 5'(F) GGGTACTTGGCTTACCTGCCCTGUGCAGCTGTGGGGCGCAG3'
 40_Prince_C: 5'(F) GGGTACTTGGCTTACCTGCCCTGCGCAGCTGTGGGGCGCAG3'
 40_Prince_T: 5'(F) GGGTACTTGGCTTACCTGCCCTGTGCAGCTGTGGGGCGCAG3'
 40_Prince_G: 5'CCCACAGCTGCCAGGGCAGGTAAGCCAAGTACCCTACGT3'
 40_Prince_C: 5'CCCACAGCTGCCAGGGCAGGTAAGCCAAGTACCCTAGCT3'
 40_Prince_A: 5'CCCACAGCTGCAAGGGCAGGTAAGCCAAGTACCCTAGCT3'
 40_Prince_T: 5'CCCACAGCTGCTAGGGCAGGTAAGCCAAGTACCCTAGCT3'
 35_Prince_G: 5' CTGCGCCACAGCTGCCAGGGCAGGTAAGCCAAG 3'
 23-M (23mer): 5'(F)GGGTACTTGGCTTACCTGCCCTG 3'

Underlined nucleotides build a mismatch pair in substrate oligonucleotides used in enzymatic tests. F: fluorescein (6-isomer); AP: model of a stable AP site

2.1.5 Molecular Ladders and Markers

2.1.5.1 DNA size marker

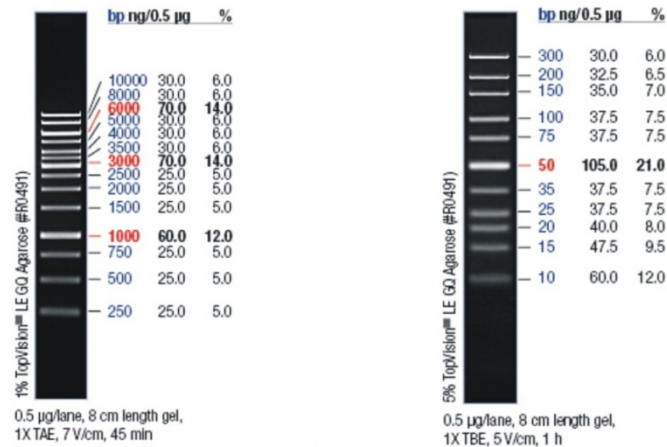


Figure 2.8: GeneRuler™ 1kb DNA Ladder (left) and GeneRuler™ Ultra Low Range DNA Ladder (right) (Fermentas, Burlington, Ontario).

The DNA molecular length standards were adjusted with TE buffer (2.1.9) and 6x loading dye solution (Fermentas) to the DNA concentration of 0.1 µg/ µl and stored at 4°C. Lengths are indicated in base pairs (bp).

2.1.5.2 Protein size marker

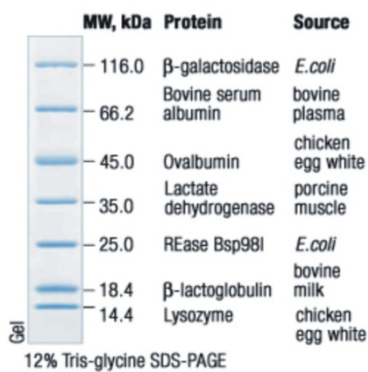


Figure 2.9: Unstained protein molecular weight marker (Fermentas, Burlington, Ontario). This marker was used in all SDS-PAGE analyses.

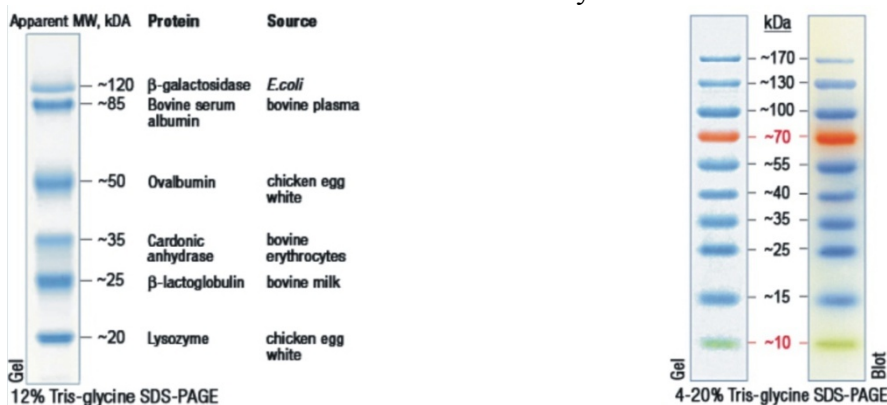


Figure 2.10: Prestained Protein Molecular Weight Marker (left) and PageRuler™ Prestained Protein Ladder (right) (Fermentas, Burlington, Ontario). These markers were used for Western blot analyses (2.2.3.2).

2.1.6 Enzymes und Proteins

Boehringer (Mannheim)	Ribonuclease A (Rnase A).
Fermentas (Burlington, Ontario)	Restriction endonucleases
	<i>Pfu</i> -DNA-Polymerase (recombinant)
	T4-DNA-Ligase
	Calf Intestine Alkaline Phosphatase (CAP)
New England Biolabs Inc. (Ipswich, MA)	Restriction endonucleases
	<i>Taq</i> -DNA-Polymerase
Own laboratory	<i>M. mazei</i> tUDGa – produced in <i>E. coli</i> and purified (by S. Ber)
	Ugi from PBS2 bacteriophage, produced in <i>E. coli</i> and purified (by L. Schomacher)
	Mth212 from <i>M. thermotrophicus</i> , produced in <i>E. coli</i> and purified (by E. Ciirdaeva)
Qiagen (Hilden, Germany)	Anti-Penta-His mouse monoclonal IgG1 antibody (BSA free)
Sigma (Steinheim)	Proteinase K
	Lysozyme
	Anti-mouse IgG (whole molecule)-Alkaline phosphatase conjugated, produced in goat

2.1.7 Chemicals and reagents

AGS GmbH, Heidelberg:

Qualex Gold Agarose

AppliChem, Darmstadt:

Acrylamid 4k – 30% solution; Ampicillin (Sodium salt); Bisacrylamid 4K–2% solution; Chloramphenicol; Erythromycin; Coomassie Brilliant Blue G250 und R250; Dithiothreitol (DTT); Methanol; Nickel (II)-Chloride;

Fermentas:

Isopropyl- β -D-Thio-Galactopyranosid (IPTG)

Fluka, Neu-Ulm:

Bromphenol blue; Dimethylsulfoxyd (DMSO); Glycerol, 87%; Formamide; Polyethylene glycol (PEG) 6000;

GE Healthcare, Uppsala, Sweden:

Chelating Sepharose™ Fast Flow

Invitex, Berlin:

dNTP (2'-Desoxyribosenucleosidtriphosphate)

Merck, Darmstadt:

2-Mercaptoethanol; Calcium chloride dehydrate; Formaldehyde; Magnesium chloride hexahydrat

MJ Research, Waltham, MA:

Chill-out™ liquid wax

Oxoid, Cambridge, UK:

Yeast extract; Tryptone; Bacteriological agar

Pharmacia LKB, Uppsala, Sweden:

Blue Dextran 2000

Roche Diagnostics, Mannheim:

“Complete, EDTA-free” Protease Inhibitor Cocktail Tablets

Roth GmbH, Kalsruhe:

Ammonium acetate, Ammonium chloride, Ammonium sulphate, Ampicillin sodium salt, Chloramphenicol, Citric acid monohydrate, Disodium phosphate, Ethanol, Ethidium bromide, Acetic acid, Urea, (4-(2-hydroxyethyl)-1-piperazineethanesulfonic acid (HEPES), 2-Propanol, Kanamycin, Potassium chloride, Potassium hydroxide, Methanol, Sodium acetate, Sodium chloride, Monosodium phosphate, Sodium hydroxide, Sodium thiosulfate, Phenol, Phosphoric acid, Rotiphorese® Gel30 (Acrylamide:Bisacrylamide 37.5:1), Sucrose, Hydrochloric acid (smoking), Tris (hydroxymethyl) aminomethane

Scharlau Chemie, Barcelona, Spain:

Ammonium persulfate, Chloroform, Boric acid, Imidazole

Serva, Heidelberg:

Ethylenediaminetetraacetic acid (EDTA), Glycine, Sodiumlaurylsulphate (SDS), N,N,N',N'- Tetramethylethylenediamine(TEMED)

Sigma, Steinheim:

Lincomycin, Tetrasodium pyrophosphate, Triethanolamine, Triton X-100 (Octylphenol-Polyethylenglycol), Polyethylenglycol-Sorbitan-Monolaurat (TWEEN® 20), Xylencyanol FF

2.1.8 Molecular biology Kits

Fermentas, Burlington, Ontario
 Genomed, Bad Oeyenhausen
 Macherey-Nagel, Düren
 Roche Diagnostics, Mannheim

CloneJET™ PCR Cloning Kit
 JETSTAR Plasmid Purification Kit
 NucleoTrap® and NucleoSpin® Gel extraction
 High Pure PCR Cleanup Micro Kit

2.1.9 Buffers and solutions

Common used buffers:

ALF-marker	95% Formamide, 20mM EDTA pH 8.0, 5 mg/ml Dextran-Blue, stored at 4°C
APS stock solution, 10%	Ammonium persulfate in H ₂ O, stored in aliquots at -20 °C
dNTP stock solution	10 mM of each dNTP in H ₂ O, stored at -20°C
EDTA stock solution	500 mM EDTA dissolved in H ₂ O with addition of solid NaOH
DTT stock solution	1M DTT in H ₂ O, sterilised (0.45 µm pore size filter) and stored at -20°C
Ethidium bromide stock solution	10 mg/ml Ethidium bromide
Isopropyl-β-D-thiogalactopyranosid (IPTG) stock solution	1M IPTG in H ₂ O, sterilised (0.45 µm pore size filter) and stored at -20°C
PBS-Buffer (1x)	10 mM Na ₂ HPO ₄ , 1.8 mM KH ₂ PO ₄ pH 7.3, 140 mM NaCl, 2.7 mM KCl
Phenol/Chloroform	25 vol. of phenol/TE, 24 vol. of Chloroform, 1 vol. of Isoamyl alcohol
Phenol/TE	Phenol, saturated with TE-Buffer, 0.1% (w/v) 8-Hydroxychinolin
SDS-PAGE Loading buffer (Hoechst)	98% Formamide, 10 mM EDTA pH 8.0, 0.025% Xylencyanol FF, 0.025% Bromphenol blue
RNase A stock solution	10 mg RNaseA in 1 ml of 10 mM Tris/HCl pH 7.5, 15 mM NaCl. The mixture was preheated for 15 min at 100°C and cooled down at RT

SSC-Buffer	50 mM NaCl, 15 mM Sodium citrate
Sucrose marker (DNA loading buffer)	60% (w/v) Sucrose, 0.05% (w/v) Bromphenol blue, 0.05% (w/v) Xylencyanol FF in TAE-Buffer
50x TAE buffer	2M Tris/Acetate, 50 mM EDTA
10x TBE buffer	0.89M Tris/Borate pH 7.9, 25 mM EDTA
T4-DNA-Ligase buffer	400 mM Tris/HCl pH 7.8, 100 mM MgCl ₂ , 100 mM DTT, 5 mM ATP
TE-buffer	10 mM Tris/HCl pH 8.0, 0.5 mM EDTA
Polymerase Buffers:	
ThermoPol Reaction Buffer (10x)	200 mM Tris/HCl, 100 mM KCl, 20mM MgSO ₄ , 100 mM (NH ₄) ₂ SO ₄ , 1% (v/v) Triton X-100, pH 8.8 at 25°C
<i>Pfu</i> -Polymerase Buffer (10x) with MgSO ₄	200mM Tris/HCl pH 8.8, 100mM (NH ₄) ₂ SO ₄ , 100mM KCl, 1% (v/v) Triton X-100, 1mg/ml BSA, 20mM MgSO ₄

Antibiotic stock solutions:

All stock solutions are sterilized by filtering (0.45µm pore size) and stored at -20°C.

Ampicillin stock solution	100 mg/ml in H ₂ O
Chloramphenicol stock solution	25 mg/ml in Ethanol
Erythromycin stock solution	2 mg/ml in H ₂ O
Kanamycin stock solution	50 mg/ml in H ₂ O,
Lincomycin stock solution	25 mg/ml in H ₂ O
Tetracycline stock solution	25 mg/ml in H ₂ O

Buffers for chromatography:

IMAC wash buffer	25 mM HEPES /KOH pH 7.6, 0.5M NaCl
IMAC-elution buffer	30 mM, 60 mM, 70 mM, 80 mM, 90 mM, 100 mM, 300 mM, and 500 mM Imidazole in IMAC wash buffer
Heparin column wash buffer	20 mM HEPES/KOH pH 7.6, 5 mM 2-Mercaptoethanol (sterile filtrated)
Wash buffer for making salt gradient	3M NaCl, sterile filtrated

JETSTAR buffers (Genomed, Bad Oeynhausen):

E1	50 mM Tris/HCl pH 8.0, 10 mM EDTA
E2	200 mM NaOH, 1% (w/v) SDS
E3	3.1M Potassium acetate pH 5.5
E4	100 mM Sodium acetate pH 5.0, 600 mM NaCl, 0.15% Triton X-100
E5	100 mM Sodium acetate pH 5.0, 800 mM NaCl,
E6	100 mM Tris/HCl pH 8.5, 1.25 M NaCl

Buffers for restriction endonucleases (1x, Fermentas, Burlington, Ontario):

B+ buffer	10 mM Tris/HCl pH 7.5, 10 mM MgCl ₂ , 0.1 mg/ml BSA
G+ buffer	10 mM Tris/HCl pH 7.5, 10 mM MgCl ₂ , 50 mM NaCl, 0.1 mg/ml BSA
O+ buffer	50 mM Tris-HCl pH 7.5, 10 mM MgCl ₂ , 100 mM NaCl, 1 mg/ml BSA
R+ buffer	10 mM Tris/HCl pH 8.5, 10 mM MgCl ₂ , 100 mM KCl, 0.1 mg/ml BSA
Buffer Y+/Tango™	33 mM Tris/Acetate pH 7.9, 10 mM magnesium acetate, 66 mM potassium acetate, 0.1 mg/ml BSA
<i>Bam</i> HI-buffer	10 mM Tris/HCl pH 8.0, 5 mM MgCl ₂ , 100 mM KCl,
<i>Eco</i> RI-buffer	50 mM Tris/HCl pH 7.5, 10 mM MgCl ₂ , 100 mM NaCl, 0.02% Triton X-100, 0.1 mg/ml BSA

Buffers for restriction endonucleases (1x, New England Biolabs, Ipswich, MA):

NEB 1	10 mM Bis-Tris Propane/HCl pH 7.0, 10 mM MgCl ₂ , 1mM DTT
NEB 2	10 mM Tris/HCl pH 7.9, 10 mM MgCl ₂ , 50 mM NaCl, 1 mM DTT
NEB 3	50 mM Tris/HCl pH 7.9, 10 mM MgCl ₂ , 100 mM NaCl, 1 mM DTT

NEB 4	20 mM Tris/Acetate pH 7.9, 10mM Magnesium acetate, 50 mM Potassium acetate, 1 mM DTT
Activity assay buffer:	
Endonuclease buffer (1x)	20 mM H ₂ KPO ₄ /HK ₂ PO ₄ buffer pH 6.2, 50 mM KCl, 1 mM MgCl ₂ , 0.1 mg/ml BSA
Sucrose Gradient Buffers:	
10% Sucrose Buffer	100mM Tris/HCl pH 8.0, 10mM EDTA, 10mM NaCl, 10% (w/v) Sucrose, autoclaved
30% Sucrose Buffer	100mM Tris/HCl pH 8.0, 10mM EDTA, 10mM NaCl, 30% (w/v) Sucrose, autoclaved
40% Sucrose Buffer	100mM Tris/HCl pH 8.0, 10mM EDTA, 10mM NaCl, 40% (w/v) Sucrose, autoclaved
SDS-PAGE buffers:	
Coomassie R250 dye solution	0.7% (w/v) Coomassie R-250 in Methanol, 20% Acetic acid, mixed at 1:1 before use
Loading dye (or sample buffer)	200 mM Tris/HCl, 8M Urea, 200 mM DTT, 2% (w/v) SDS, 0.05% Bromphenol blue
Laemmli buffer (1x)	25 mM Tris/HCl pH 8.4, 200 mM Glycin, 0,1% (w/v) SDS
SDS	10% (w/v) SDS in H ₂ O
Stacking gel buffer	1.25M Tris/HCl pH 6.8
Separating gel	1.875M Tris/HCl pH 8.8
Buffers for Western Blot analysis	
AP detection buffer	100mM Tris pH 9.5, 5mM MgCl ₂ , 100mM NaCl
BCIP stock solution	50µg/ml in 100% DMF
Blocking Buffer	5% BSA in TBS-Tween Buffer
NBT stock solution	75µg/ml in 70% DMF
Semi-dry Transfer Buffer	25mM Tris, 150mM Glycine, 10% Methanol
TBS-Tween Buffer	20mM Tris/HCl pH 7.5, 500mM NaCl, 0.05% Tween 20
Buffers for preparation of <i>E. coli</i> competent cells	
TFBI	30mM KOAc, 100mM RbCl, 10mM CaCl ₂ , 50mM MnCl ₂ , 15% Glycerin, pH 8.5 with Acidic acid, sterile filtrated

TFBII 10mM MOPS, 75mM CaCl₂, 10mM RbCl, 15% Glycerin pH 6 with KOH, sterile filtrated

Buffers and solutions for *B. subtilis* transformation

1mM HEPES, pH 7

PEB-Buffer 272mM Sucrose, 1mM MgCl₂, 7mM Potassium phosphate, pH 7.4

2xSMM 342g sucrose, 4.72g Sodium maleate, 8.12g MgCl₂·6H₂O, adjust pH to 6.5 with NaOH, add H₂O to 1L, autoclaved 10min at 109°C

SMMP equal volume of 2xSMM and 4XPAB-Medium

PEG 10g of Polyethylene glycol 8000 in 2ml of 1xSMM, autoclaved 10 min at 109°C

G-P. Xue growth medium LB medium containing 0.5M Sorbitol

G-P. Xue recovery medium LB containing 0.5M Sorbitol, 0.38M Mannitol,

G-P. Xue electroporation medium 0.5M Sorbitol, 0.5M Mannitol, 10% Glycerol

Buffers and solutions for working with bacteriophages

PBS1 bacteriophage

Y-medium 10mM K₂HPO₄, 20mM NaH₂PO₄, 0.1% (w/v) yeast extract, 100mM NaCl, 30mM K₂SO₄, 0.5mM MgSO₄, 0,1mM CaCl₂, 0.04mM FeCl₃·6H₂O in H₂O, autoclaved

PBS1-Buffer 100mM NaCl, 30mM K₂HPO₄, 20mM NaH₂PO₄, 0.5mM MgSO₄, 0,1mM CaCl₂, 0.04mM FeCl₃·6H₂O, 0.1% (w/v) yeast extract in H₂O, autoclaved

P2 bacteriophage

P2 bacteriophage growth medium LB containing 0.1% Glucose, 2mM MgCl₂

P2 Buffer 10mM Tris, pH 7.5, 10mM MgCl₂, 1% (w/v) Ammonium acetate

P1 bacteriophage

MC-Buffer 100mM MgSO₄, 5mM CaCl₂

1M Sodium Citrate

1M MgSO₄

1M CaCl₂

2.1.10 Bacterial Growth Media

dYT- (double Yeast Tryptone)	1.6% (w/v) Trypton, 1% (w/v) yeast extract, 0.5% (w/v) NaCl in H ₂ O, autoclaved
LB (Luria Bertani) medium	1% (w/v) Trypton, 0.5% (w/v) yeast extract, 1% (w/v) NaCl in H ₂ O, autoclaved
LB-Agar	1% (w/v) Trypton, 1.5% (w/v) Agar, 0.5% (w/v) yeast extract, 1% (w/v) NaCl in H ₂ O, autoclaved
LB-Topagar	1% (w/v) Trypton, 0.7% (w/v) Agar, 0.5% (w/v) yeast extract, 1% (w/v) NaCl in H ₂ O, autoclaved
SP-Agar	0.8% (w/v) Nutrient Broth, 0.02% (w/v) MgSO ₄ x7H ₂ O, 1% (w/v) KCl; autoclaved, then 1ml CaCl ₂ (100mM), 1ml MnCl ₂ (10mM), 2ml Ammonium iron(II)citrate (2.2mg/ml) into 1L of medium added
SOC-Medium	2% (w/v) Tryptone, 0.5% (w/v) yeast extract, 10mM NaCl, 2.5mM KCl, 10mM MgCl ₂ , 10mM MgSO ₄ , 20mM Glucose, autoclaved
PAB (Pennassay Broth) Medium	1.75% (w/v) Difco Antibiotic Medium No. 3
DM3 Medium	250ml 1M Sodium succinate (adjusted to pH 7.3 with NaOH), 50ml 5% (w/v) Casamino acids, 25ml 10% (w/v) yeast extract, 50ml Phosphate buffer, 15ml 20% (w/v) Glucose, 10ml 1M MgCl ₂ , 2.5ml 2% (w/v) BSA, 100ml 4% (w/v) molten agar. All solutions were sterilized either by autoclaving or sterile filtering.

Antibiotics were added after media were autoclaved and cooled to below 60°C.

2.1.11 Equipment and hardware

Automated Laser Fluorescence	
DNA Sequencer (A.L.F.-sequencer)	GE Healthcare, Uppsala, Sweden
Incubator	W. C. Heraeus GmbH, Hanau

Constant Cell Disruption System	Constant Systems Ltd, Northants, England
Electrophoresis unit	model 2050
Midget	GE Healthcare, Uppsala, Sweden
Gel Jet Imager	Intas, Göttingen
Gene Pulsar [®] and Pulse Controller	BioRad, Munich
Metal block thermostat	Institute of Microbiology and Genetics, University of Göttingen
NovaBlot 2117-250	Pharmacia LKB, Bromma
Milli-Q [®] Water Purification System	MILLIPORE, Eschborn
Pipetman [®] Model P1000, P200, P20	Gilson, Bad Camberg
pH-Meter-526	Schütt Labortechnik, Göttingen
Rotary shaker	Infors AG, Bottmingen, Switzerland
Thermocycler Primus 96plus	MWG Biotech, Ebersberg
Branson Sonifier W-250	Heinemann, Schwáb. Gmünd
UV-VIS Spectrophotometer	UV-1601 SHIMADZU Corporation, Kyoto, Japan
UVT2035 <u>UV transilluminators</u>	Herolab, Wiesloch
UV-Lamp 254 nm	Schütt Laborthechnik, Göttingen
Envico sterile hood	CEAG Slurp Reinraumtechnik
Precision Balances L 420 P	Sartorius, Göttingen
Precision Balances U 4800 P	Sartorius, Göttingen
Vision Workstation, BioCad [®] Family	Applied Biosystems, Foster City, CA
Vortex Genie 2 [™]	Bender & Hobein AG, Zurich, Switzerland

Electrophoresis power supplies:

ECPS 3000/150	GE Healthcare, Uppsala, Sweden
LNGs 350-06	Heinzinger, Rosenheim

Centrifuges:

Centrikon T-1055	Kendro, Langenselbold
Mikroliter	Hettich, Tuttlingen
Mikro Rapid/K	Hettich, Tuttlingen
Rotanta/RPC	Hettich, Tuttlingen
Roto Silenta/RP	Hettich, Tuttlingen
Sorvall [®] RC5C (Rotor SS34)	Kendro, Langenselbold

2.1.12 Other materials

Baktolin 5.5 (Disinfection solution)	Bode Chemie, Hamburg
Dialysis tubes VISKING®	SERVA, Heidelberg
Disposable Syringes	Perumo®Syringe, Leuven, Belgium
Glass flasks and test tubes	Schott, Mainz
Glass pipettes	Brand, Wertheim
Glass plates for SDS gels	GE Healthcare, Uppsala, Sweden
Heparin column, Poros® HE 20	Applied Biosystems, Foster City, CA
Meliseptol (disinfection solution)	Braun Melsungen AG, Melsungen
Parafilm	American National Can., Chicago, USA
pH-Indicator stick	Merck, Darmstadt
PCR cups	Biozym, Hess.-Oldendorf
Petri dishes	Greiner, Nürtingen
Pipette tips	Sarstedt, Nümbrecht
Protran BA85 Nitrocellulose	Whatman® GmbH, Dassel
Precision Cells-Quartz glass cuvettes	Hellma, Mühlheim/Baden
Reaction Vessels (1,5 ml, 2 ml, 50 ml)	Sarstedt, Nümbrecht
Scalpel blades	Bayha GmbH, Tuttlingen
Ultrafiltration tubes	Vivaspin Vivascience®, Hannover

2.1.13 Software

ALF-Manager	Version 3.02 (1995), GE Healthcare, Uppsala, Sweden
BOXSHADE	Version 3.21, K. Hofmann and M. Baron (www.ch.embnet.org/software/BOX_form.html)
Chromas [©]	Version 1.45 (32 bit), Version 2.01 and Version 2.31 Technelysium Pty. Ltd.
CLUSTAL W	Service of European Bioinformatics Institute (EBI) http://www.ebi.ac.uk/Tools/clustalw/
CorelDRAW® Graphic Suite 12	Corel Corporations, Ottawa, Canada
Fragment Manager	Version 1.2 (1995), GE Healthcare, Uppsala, Sweden
MultAlin (by Florence Corpet)	http://bioinfo.genotoul.fr/multalin/multalin.html
PyMOL™	Version 0.98 (2005), DeLano Scientific LLC, San Carlos, CA
ProtParam	ExPaSy Proteomics Server (http://expasy.org) , Swiss

	Institute of Bioinformatics, Lausanne, Switzerland
Vision Workstation Perfusion Chromatography	Version 2.0, Applied Biosystems, Foster City, CA
Microsoft® Office Word	Version 2007, Microsoft GmbH, Unterschleißheim
Vector NTI	Version 11.5, Invitrogen, Carlsbad, CA

2.1.14 Databanks

NCBI-Databank for protein, nucleotide, and genomic sequences:

<http://www.ncbi.nlm.nih.gov/>

RCSB Protein Data Bank (PDB) archive

<http://www.rcsb.org/pdb/home/home.do>

2.2 Methods

2.2.1 Microbiological methods

2.2.1.1 Bacterial growth

E. coli and *B. subtilis* cell cultures were grown in LB-Medium or dYT-Medium at 37°C and 200 rpm, if not stated otherwise. *E. coli* inoculations were made from either fresh overnight cultures or -20°C glycerin stock. *E. coli* glycerine culture stocks were made by re-suspending of 1 ml over night culture in glycerine at 1:1 ratio (v/v) and stored at -20°C. Alternatively, 9% DMSO culture stock was made and stored at -80°C. *B. subtilis* inoculations were made from bacterial spores, stored on SP-Agar (sporulating) plates. Bacterial growth was monitored by determining optical density of the culture at 600 nm (OD₆₀₀).

2.2.1.2 Bacteriophage growth

2.2.1.2.1 PBS1 bacteriophage

Preparation of PBS1 bacteriophage lysate (plate lysate method)

100µl of bacteriophage lysate obtained from BGSC (2.1.2) was diluted 1:10, 1:100 and 1:1000 in 1 ml of Y-Medium and transferred to glass tubes containing 3ml of Y-medium. 500µl of mid-log phase *B. subtilis* W168 cells were added to phage suspensions and incubated for 15 min at RT. 4 ml of melted LB-topagar was given to each glass tube, mixed and the suspension was immediately poured onto two fresh LB-agar plates. Plates

were incubated overnight at 30°C. On the next day top-agar layer was scraped off the plates and passed several times through syringe (without needle) to crush the agar. 20 ml of Y-Medium and few drops of chloroform were then added to this suspension and incubated overnight at 4°C. Lysate was centrifuged 3 times for 15 min at 4000 rpm at RT to pellet the agar and rest of bacterial cells and the supernatant was stored at 4°C.

Determination of the bacteriophage lysate titer

100µl of bacteriophage lysate was serially diluted (10^{-1} to 10^{-10}) in 1ml of Y-Medium and transferred to glass tubes containing 2ml of Y-Medium. 500µl of 500µl of mid-log phase *B. subtilis* was added to each tube and incubated 15 min at RT. 2.5 ml of melted LB-topagar was given to each suspension, mixed and poured onto fresh LB-agar plates. Plates were incubated at 30°C overnight. Plaques on plates containing from 100-500 plaques were counted on the next day and the bacteriophage titer in 1ml was calculated. Titer of the lysate prepared according to above described method was $\sim 5 \times 10^9$ pfu/ml.

Mutagenesis of PBS1 bacteriophage

Approximately 1×10^8 pfu of PBS1 bacteriophage were suspended in 6ml of PBS1-Buffer and subjected to UV-irradiation for 2.5 min or 5min. UV-irradiation was achieved using UV-Lamp at 254nm and $0.5 \text{ J sec}^{-1} \text{ m}^{-2}$. Whole suspension was aliquoted in 200µl of irradiated phage suspension and transferred to glass tubes containing 2ml Y-Medium and mixed with 500µl of mid-log phase *B. subtilis* cells followed by incubation for 15 min at RT. 2.5 ml of melted LB-topagar was given to each suspension, mixed and poured onto fresh LB-agar plates. Plates were incubated over night at 30°C and clear plaques were sought.

2.2.1.2.2 P2vir1Ram3 bacteriophage

Preparation of P2vir1Ram3 bacteriophage lysate (Kahn *et al.*, 1991)

500µl of overnight culture of *E. coli* cells grown in P2 bacteriophage growth medium was inoculated in 50 ml of P2 bacteriophage growth medium supplemented with 2mM CaCl_2 and grown to mid-log phase ($\text{OD}_{600} \sim 0.6$). P2vir1Ram3 bacteriophage plaque was picked from the plate, given to *E. coli* culture and incubated for 7 min at 37°C without shaking. The culture was then incubated at 37°C with shaking for approximately 2 hours until cell lysis occurred. When lysis began 200µl of 0.5M EDTA, 500µl of 1M MgCl_2 were added to chelate calcium for preventing adsorption of bacteriophage particles into cellular debris

and to stabilize bacteriophage particles, respectively. 0.8g of NaCl was added and when dissolved 10g of PEG6000 was given. The suspension was incubated for 15 min at 4°C with shaking at 200rpm and 1 hour on ice. Afterwards the lysate was centrifuged for 10 min at 10000rpm and 4°C. The pellet was dissolved in 2ml of P2 Buffer, few drops of chloroform were added and the bacteriophage stock solution was stored at 4°C.

Determination of the P2vir1Ram3 bacteriophage lysate titer

100µl of a standing overnight culture of *E. coli* strain that will permit growth of bacteriophage was mixed with 100µl of serial dilutions (1:10 to 1:10⁻⁸) of the bacteriophage lysate incubated for 7 min at RT and 2.5ml of melted LB-topagar was given. Suspension was plated out on LB-agar plates and incubated overnight at 37°C. Plaques on plates containing from 100-500 plaques were counted on the next day and the bacteriophage titer in 1ml was calculated. Titer of the lysate prepared according to above described method was ~10⁹ pfu/ml.

2.2.1.2.3 Preparation of P1 bacteriophage lysate and P1 transduction

E. coli bacteriophage P1 was used for transduction of kanamycine cassette for disruption of *ung* gene. Therefore the donor strain for lysate of P1 preparation was *E. coli* BL21_UXX (2.1.1.1). *E. coli* cells were grown to mid-log phase in LB Medium containing 5mM CaCl₂, 0.2% glucose. 100µl of P1 bacteriophage lysate (own laboratory collection, propagated on *E. coli* K12) was added and incubation was continued at 37°C with shaking. After ~3 hours lysis of the culture was completed. Several drops of chloroform was added and vortexed followed by centrifugation for 30 min at 4000 rpm and RT. Few drops of chloroform was added and the lysate was stored at 4°C.

For transduction, 2 ml of overnight culture of the recipient strain grown in LB medium was centrifuged (6000rpm, 2 min, RT) and the pellet was resuspended in 2 ml of LB medium containing 100mM MgSO₄, 5mM CaCl₂. 100µl of (1) undiluted, (2)1:10 diluted, (3)1:100 diluted, (4) 1:1000 diluted in MC-Buffer P1 lysate was given to 100µl of bacterial cells and incubated for 30 min at 37°C (cells without P1 lysate and P1 lysate without cells were taken for control). 200µl of 1M sodium citrate, pH 5.5 was added followed by 1ml of LB Medium and the mixture was incubated at 37°C for 1 hour. Cells were pelleted at 7000 rpm for 3 min and resuspended in 100 µl of LB Medium containing 100mM sodium citrate, pH5.5. Finally, cells were plated onto LB-agar plates with kanamycin. On next day bacterial colonies were re-streaked on LB-agar plates with kanamycine spreaded with

100µl of 100mM sodium citrate, pH 5.5. Next, colony-PCR was performed to test the transduction effectiveness.

2.2.1.3 Transformation of bacteria

2.2.1.3.1 Transformation of *E. coli*

Transformation of *E. coli* cells made competent by RbCl method (Hanahan, 1985)

500µl of overnight culture was inoculated into 50ml LB-Medium and was grown to mid-log phase ($OD_{600} \sim 0.6$) at 37°C with agitation. Culture was then incubated 10 min on ice followed by 10 min centrifugation at 4.000 r.p.m. and 4°C (Rotanta/RPK, Hettich). Cells were resuspended in 10ml of ice-cold TFBI Buffer, incubated 10 min on ice and centrifuged again. Thereafter, cells were resuspended in 2 ml ice-cold TFBII Buffer and incubated 10 min on ice. Cells were then aliquoted (100µl) and frozen at -80°C. For transformation, plasmid DNA was incubated with cells 30 min on ice. Transformation mixture was subjected to heat shock at 42°C for 1 min followed by incubation on ice for 2 min. 1ml of SOC-Medium was added and cells were incubated at 37°C for 1 hour with gentle rolling. Cells were then diluted and plated on LB-agar plates containing antibiotic.

Transformation of competent *E. coli* by electroporation (Dower *et al.*, 1988)

500 µl of overnight *E. coli* culture was inoculated into 50 ml of dYT medium (2.1.10) and grown to mid-log phase ($OD_{600} \sim 0.6$) at 37°C on a shaker. Cells were harvested by centrifugation in 50 ml falcon tubes for 10 min at 4.000 rpm. and 4°C (Rotanta/RPK, Hettich), resuspended in 50 ml of ice-cold H₂O and incubated on ice for 20 min. Then cell suspension was centrifuged and cell pellet was washed 4 times by resuspension in ice-cold H₂O (40 ml, 30 ml, 20 ml and 10 ml), followed by centrifugation after each wash. Finally, pellet was dissolved in 1-2 ml of H₂O and left on ice. For the transformation, 1-2 µl of DNA solution (2µg) were mixed with 75 µl of electrocompetent cells and incubated on ice for 5 min. DNA-cell mixture was transferred into a chilled electroporation cuvette and subjected to the pulse at 2.5kV, 200Ω and 25µF. Transformants were immediately resuspended in 1ml of SOC medium, incubated for 1h at 37°C on a roller and 100 µl aliquots (with or without dilution) were plated on LB agar plates containing appropriate antibiotics. Competent cells were plated on antibiotic containing agar plates as negative control.

2.2.1.3.2 Transformation of *B. subtilis*

Transformation of *B. subtilis* cells by electroporation (Brigidi *et al.*, 1990)

500µl of overnight culture of *B. subtilis* was inoculated in 50ml LB-Medium and grown to an OD₆₀₀ of ~0.6 corresponding to mid.log phase. Cells were chilled on ice for 30 min, harvested by centrifugation (10 min at 4.000 rpm. and 4°C (Rotanta/RPK, Hettich)), rinsed once in 1mM HEPES pH 7, twice in PEB-Buffer and resuspended in 800µl of PEB-Buffer. For electroporation, plasmid DNA diluted in 10µl of PEB-Buffer was added to cells and followed by incubation on ice for 30 min. Cells were then transferred to a cold 0.1cm electroporation cuvette and subjected to a high-voltage electric pulse (2.5kV, 200Ω and 25µF). Immediately after pulse 1 ml of SOC-Medium was added and the cell suspension was incubated at 37°C for one before plating onto selective media.

***B. subtilis* protoplast transformation (Chang and Cohen, 1979)**

200µl of *B. subtilis* overnight culture grown in PAB-Medium was inoculated in 10ml warm PAB-Medium and incubated at 37°C with shaking (200rpm). When the culture reached an OD₆₀₀ of ~0.5, cells were pelleted (10 min at 4000 rpm at RT) and resuspended in 5ml of warm SMMP. 5mg of lysozyme were added and mixed by gentle inverting of the tube several times. After 2 hours of incubation at 37°C in a roller drum conversion of cells into protoplasts was checked under microscope (protoplasts have a spherical appearance). Protoplasts were harvested by centrifugation (10 min at 4000 rpm at RT) and the pellet was resuspended in 5ml of SMMP. For transformation, plasmid DNA was gently mixed with 150µl of protoplasts and the mixture was added to the tube containing 450µl of PEG and gently mixed. Mixture was incubated at RT for 2 min and 1.5ml of SMMP was then added, mixed and centrifuged (7min at 8000rpm at RT). Whole supernatant was removed and the 300µl of SMMP was added to the pellet without mixing. Mixture was incubated 90 min at 37°C with gentle rolling and dilutions were then plated on DM3 plates without antibiotics. Plates were incubated at 37°C for 2 days. After regeneration, transformants were identified by replica-plating onto selective media. As a control protoplasts were plated onto LB-agar plates: only cells that were not converted to protoplasts will grow.

***B. subtilis* electroporation in high osmolarity solutions (Xue *et al.*, 1999)**

Overnight culture of *B. subtilis* was diluted 16-fold in growth medium and was grown at 37°C to OD₆₀₀ of ~0.85-0.95. The cells were chilled on ice for 10 min and harvested by

centrifugation for 5 min at 4000 rpm and 4°C). Following 4 washes in ice-cold electroporation medium, the cells were suspended in 1.25 ml of the electroporation medium with a cell concentration of $\sim 10^{10}$ cfu/ml. Competent cells can be stored at -80°C. For transformation, 60µl of competent cells were mixed with 1µl DNA and then transferred to an ice-cold electroporation cuvette (1mm electrode gap). After incubation for 1 min cells were exposed to a single electrical pulse using a Gene Pulser (BioRad Laboratories, Richmond, CA) set at 25µF and 200Ω, resulting in time constants of 4.5-5.0ms. Immediately following electrical discharge, 1ml of recovery medium was added to the cells. After incubation at 37°C for 3h cells were plated on LB-agar plates containing antibiotic. Plates were incubated at 37°C overnight.

2.2.2 Molecular biological methods

2.2.2.1 DNA extraction

Bacterial genomic DNA extraction

Overnight culture of bacterial cells (2ml) was pelleted and resuspended in 300µl 250mM Tris (pH 8.0) containing 10mg/ml lysozyme and incubated 30 min at 37°C. Afterwards 300µl of 0.5% SDS, 50mM Tris (pH 7.5), 0.4M EDTA, 1mg/ml proteinase K was added and incubated at 50°C for 30 min. The suspension was mixed with 600 µl of tris-equilibrated phenol, centrifuged 10 min at 13000 rpm and RT; supernatant was mixed with 300µl phenol and 300µl chloroform and centrifuged; supernatant was mixed with 600µl chloroform and centrifuged. Finally, genomic DNA was precipitated with ethanol.

Ethanol precipitation of DNA

1/10 vol. of 7M ammonium acetate and 3 vol. of 96% ethanol were added to DNA samples followed by incubation at -20°C for 1 hour. DNA was pelleted by centrifugation for 30 min at 15000 rpm and 4°C (Mikro Rapid/K Hettich). DNA pellets were washed with 70% ethanol, centrifuged for 15 min at 4°C, and dried at 37°C. Finally, dried DNA pellets were dissolved in double distilled water (ddH₂O) and stored at -20 °C.

Bacteriophage DNA extraction

50ml of bacterial culture grown to mid-log phase was infected with $\sim 10^9$ bacteriophage particles and incubated for 3 hours at 37°C with shaking. 1 ml of chloroform was added to complete the lysis. Suspension was incubated overnight at 4°C without shaking and on the

next day DNaseI and RNaseA were added (1µg/ml) and incubated for 30 min at RT. Cell debris were pelleted by centrifugation for 20 min at 4000 rpm and RT. 1M NaCl, 10% (w/v) PEG6000 were added to the supernatant, dissolved by slow stirring and incubated on ice for 1 hour. Bacteriophage particles were precipitated by centrifugation for 30 min at 10000 rpm and 4°C. The pellet was dissolved in 500µl of PBS buffer and 500µl of chloroform was then added. Suspension was thoroughly vortexed and then centrifuged for 15 min at 8000 rpm and 4°C. The aqueous phase was subjected to phenol/chloroform extraction followed by ethanol precipitation of DNA as described above.

Small scale plasmid DNA extraction (mini-prep) by alkaline lysis

2 ml of bacterial culture grown over night at 37°C were used to prepare plasmid DNA by modified alkaline/SDS lysis method using JetStar E1, E2, E3-solutions (Birnboim and Doly, 1979). *E.coli* cells were pelleted by centrifugation for 1 min at 13000 rpm and RT. Pellet was resuspended in 150 µl of E1 solution by vortexing and 150 µl of E2 lysis solution was added followed by incubation for 5 min at RT. After neutralization with 150 µl of E3 solution, samples were incubated for 10 min on ice, and centrifuged for 15 min at 15000 rpm and 4°C. RNase A solution (10 µg/ml final concentration) was added to the supernatant followed by incubation for 30 min at 37°C. Finally, plasmid DNA was phenol/chlorophorm extracted and precipitated with ethanol as described above.

Large scale plasmid DNA extraction (midi-prep)

JETstar[®] Kit was used for plasmid DNA preparation from 50 ml of overnight *E.coli* culture. Cells were pelleted by centrifugation (4000 rpm, 10 min, 4°C) and resuspended in 4 ml of E1 solution until homogeneity. Then E2 solution was added with gentle mixing and samples were incubated for 5 min at RT. After addition of E3 solution, samples were mixed by multiple inversions and cell debris were removed by centrifugation for 10 min at 4000 rpm and RT. Cleared supernatant was applied to a JETstar column equilibrated with E4 solution followed by washing twice with 10 ml of E5 solution. DNA was eluted with 5 ml of E6 solution, precipitated with 0.7 volume of isopropanol and pelleted by centrifugation for 15 min at 15000 rpm and 4°C. Finally, DNA pellet was washed with 70% ethanol, dried at 37°C, and redissolved in 10 µl of double distilled water (ddH₂O).

2.2.2.2 Polymerase Chain Reaction (PCR)

2.2.2.2.1 Standard PCR

Reaction mix		Step	Temperature	Time
Template DNA	100ng	1	95°C	5 min
Primer, forward	10pmoles	2	94°C	1 min
Primer, reverse	10pmoles	3	TA*	1 min
<i>Pfu</i> -Polymerase	1U	4	72°C	1 min
10x <i>Pfu</i> - Polymerase buffer	2.5 µl	5	72°C	10 min
dNTPs	0.2mM each	Step 2-4: 25x repeat cycles		
dd H ₂ O	up to 25 µl			

Table 2.1: (Left) Common PCR mixture used for amplification of DNA fragments from plasmid and genomic DNA templates. (Right) Thermocycler program used with modifications of annealing temperature, elongation time, and/or elongation temperature depending on the primer pair used and on the length of PCR fragment. * T_A: Optimal primer annealing temperature calculated by following equation:

$T_A = (T_{m1} + T_{m2}) / 2 - 3^\circ\text{C}$, where T_{m1} and T_{m2} are melting temperatures of Primer 1 and Primer 2, accordingly; T_m of PCR primers were calculated using the following equation: $T_m [^\circ\text{C}] = 69.3 + 0.41(\%G+C) - 650/N$ (Chester and Marshak, 1993)

2.2.2.2.2 Error-Prone PCR (Cadwell and Joyce, 1992)

Mutagenic PCR protocols employ several modifications relative to standard PCR that might be considered mutagenic, including: (1) increased concentration of *Taq* polymerase; (2) increased extension time; (3) increased concentration of MgCl₂; (4) addition of MnCl₂; (5) dNTP concentration bias. Several error-prone PCR conditions were tested (refer to Results and Discussion 3.2.3 Section) and Table 2.2 shows conditions of error-prone PCR that were used after all optimizations.

Reaction mix		Step	Temperature	Time
Template DNA	100 ng	1	95°C	5 min
Primer, forward	50pmoles	2	94°C	1 min
Primer, reverse	50pmoles	3	TA*	1 min
dATP, dGTP	0.2mM each	4	72°C	2 min
dTTP, dCTP	0.2mM each	5	72°C	10 min
MgCl ₂	6.5mM	Step 2-4: 25x repeat cycles		
ThermoPol Reaction Buffer (10x)	10 µl			
<i>Taq</i> -Polymerase	5 U			
dd H ₂ O	up to 100 µl			

Table 2.2: (Left) error-prone PCR mixture employed for mutagenesis of *exoA*. (Right) Thermocycler program used with modifications of annealing temperature depending on the primer pair used. *T_A: Optimal primer annealing temperature was calculated as described above in the description of Table 2.1.

Error-prone PCR product was purified by extraction from agarose gel (2.2.2.6), cloned into

pJET1.2 cloning vector (2.2.2.8) and transformed into *E. coli* cells (2.2.1.3.1). Plasmid DNA was extracted (2.2.2.1) from randomly picked clones and subjected to DNA sequencing analysis (2.2.2.10). All clones were washed-out from the plates and the plasmid DNA was extracted using large-scale plasmid DNA preparation method (2.2.2.1) and stored at -20°C. Randomized *exoA* was digested out from pJET1.2 vector and re-cloned into appropriate expression vector (2.2.2.8). Detailed description of the library construction is in Results and Discussion Section 3.2.2.

2.2.2.2.3 Colony-PCR

This protocol is used to quickly screen for right clones carrying desired DNA fragment directly on bacterial cells. For this bacterial colony was picked from the plate and cells were suspended in 25µl of 1x ThermoPol Reaction Buffer (in case of *B. subtilis* cells 0.05mg/ml of lysozyme was added as well) in the PCR reaction tube. 30 µl of Chill-out™ Wax was added on top of each suspension to prevent evaporation. Cell suspension was then incubated for 5 min at 98°C. Finally, standard PCR mixture (described above) was added to the cell suspension and the PCR was carried out under conditions of the standard PCR (see above).

2.2.2.2.4 Introduction of mutations into plasmid DNA using Quick-Change® site-directed mutagenesis (protocol from Stratagene)

This PCR based mutagenesis allows introducing of site-specific mutations in double-stranded plasmid DNA. This procedure utilizes plasmid vector carrying the site of interest and a pair of complementary oligonucleotide primers containing a desired mutation. During the “cycling reaction” *Pfu* DNA polymerase extends primers annealed to the template plasmid DNA. As the result linear mutated plasmid DNA is generated. Template plasmid DNA must be isolated from Dam-methylase expressing *E. coli dam*⁺ strain. In these cells template plasmid DNA is methylated at 5'-G^(m-6)ATC-3' sites and this methylated or hemimethylated DNA is the target of *DpnI* restriction enzyme. By this means one can get rid of the parental template DNA after the “cycling reaction” and only synthetic plasmid DNA that carries desired mutations will be left. When the reaction product is introduced into *E. coli* XL10-Gold Kan (2.1.1.1) cells by transformation (2.2.1.3.1), newly synthesized mutated plasmid DNA is circulated via illegitimate recombination by endogenous bacterial machinery.

“Cycling reaction” was performed under conditions depicted in the Table 2.3.

Reaction mix		Step	Temperature	Time
Template DNA	50ng	1	95°C	5 min
Primer 1	125ng	2	94°C	1 min
Primer 2	125ng	3	TA*	1 min
<i>Pfu</i> -Polymerase	2.5U	4	72°C	8 min
10x <i>Pfu</i> - Polymerase buffer	5 μ l	5	72°C	20 min
dNTPs	0.2mM each	Step 2-4: 18x repeat cycles		
dd H ₂ O	up to 25 μ l			

Table 2.3: (Left) “Cycling reaction” mixture used for Quick-change® site-directed mutagenesis (Right) Thermocycler program used for the “cycling reaction”. T_A^* indicates an annealing temperature for mutagenic primer estimated using following formula:

$$T_A = T_m - 10$$

$T_m = 81.5 + 0.41(\%G+C) - 675/N - \% \text{ mismatch}$, where N is the primer length in bases and values for %G+C and % mismatch are the whole numbers.

After the “cycling reaction” 1 μ l of *DpnI* was added to the reaction and incubated for 1 hour at 37°C. Finally, 2.5 μ l of the reaction was used for the transformation of *E. coli* XL10 Gold Kan (2.1.1.1) cells.

10-20 single colonies were used for plasmid DNA preparation (2.2.2.1) and the DNA was verified for desired mutations by DNA sequencing analysis (2.2.2.10).

2.2.2.2.5 Site-directed mutagenesis by overlap-extension using PCR (Jansohn, 2006)

Site-directed mutagenesis by overlap-extension was used when two sites within a DNA fragment in relative distance from each other were to be mutated. Specific alterations in the nucleotide sequence are introduced by incorporating nucleotide changes into two overlapping primers. Complementary oligonucleotide primers (overlap primer 1 and 2), 5' and 3' flanking primers (“forward” and “reverse” respectively) and the PCR are used to generate two DNA fragments having overlapping ends. These fragments are combined in a subsequent “fusion” reaction in which the overlapping ends anneal, allowing the 3' overlap of each strand to serve as a primer for the 3' extension of the complementary strand. The resulting fusion product is amplified further by PCR using “forward” and “reverse” primers.

Preliminary two fragments were amplified following conditions depicted in Table 2.4.

Reaction mix 1		Reaction mix 2	
Template DNA	100ng	Template DNA	100ng
Primer overlap 1	25pmoles	Primer overlap 2	25pmoles
Primer reverse	25pmoles	Primer forward	25pmoles
<i>Pfu</i> -Polymerase	2U	<i>Pfu</i> -Polymerase	2U
10x <i>Pfu</i> - Polymerase buffer	5 μ l	10x <i>Pfu</i> - Polymerase buffer	5 μ l
dNTPs	0.2mM each	dNTPs	0.2mM each
dd H ₂ O	up to 50 μ l	dd H ₂ O	up to 50 μ l

Step	Temperature	Time
1	95°C	5 min
2	94°C	40 sec
3	60°C	40 sec
4	72°C	50 sec
5	72°C	10 min

Step 2-4: 28x repeat cycles

Table 2.4: PCR conditions used for amplification of 2 preliminary fragments of overlap extension. (Left) PCR 1, (Right) PCR 2, (Below) Thermocycler program used for both PCRs.

Next, both PCR products were purified by extraction from agarose gel (2.2.2.6) and the overlap extension PCR was carried out under conditions depicted in Table 2.5.

Reaction mix		Step		
PCR product 1	50ng	1	95°C	5 min
PCR product 2	50ng	2	94°C	45 sec
Primer reverse	25pmoles	3	55°C	45 sec
Primer forward	25pmoles	4	72°C	1 min
<i>Pfu</i> -Polymerase	2U	5	72°C	10 min
10x <i>Pfu</i> - Polymerase buffer	5 μ l	Step 2-4: 30x repeat cycles		
dNTPs	0.2mM each			
dd H ₂ O	up to 50 μ l			

Table 2.5: (Left) Overlap extension PCR conditions; (Right) Thermocycler program used for PCR

Final PCR product was purified by extraction from agarose gel (2.2.2.6) and cloned into cloning pJET1.2 vector (2.2.2.8). Once the DNA sequencing analysis (2.2.2.10) confirmed the presence of mutations, DNA fragment was re-cloned into appropriate expression vector (2.2.2.8).

2.2.2.3 Spectrophotometric determination of DNA concentration

Absorption of ultraviolet (UV) light by the ring structure of purines and pyrimidines is the basis of the spectrophotometric DNA analysis. DNA samples were diluted in ddH₂O (1:10 or 1:100) depending on estimated concentrations. DNA concentration were determined by measuring the absorbance at $\lambda=260$ nm (A_{260}) using a spectrophotometer and a quartz

cuvette. The concentration was calculated based on the assumption that $A_{260} = 1.0$ is equal to 50 $\mu\text{g/ml}$ of double-stranded DNA, to 40 $\mu\text{g/ml}$ of single-stranded DNA and RNA and to 20 $\mu\text{g/ml}$ of oligonucleotides. The purity of DNA was assessed by the A_{260}/A_{280} ratio. Ratios between 1.8 and 2.0 are indicative of pure, protein-free DNA.

2.2.2.4 Agarose gel electrophoresis

DNA molecules can be separated according to their size by electrophoretic migration. For preparative and analytical DNA analysis 1% agarose gel electrophoresis was used. The agarose was dissolved in 1xTAE buffer in a microwave. Then 0.5 $\mu\text{g/ml}$ of ethidium bromide was added and the gel was poured into a horizontal gel-forming chamber. DNA samples were mixed with 0.5 vol. of loading buffer and loaded onto gel. Gels were run in 1xTAE buffer at the constant electric field power of 5-10 V/cm. DNA in the gel was visualized under UV light at 305 nm using UV transilluminator.

2.2.2.5 Denaturing polyacrylamide gel electrophoresis (A.L.F.-PAGE)

Automated Laser Fluorescence DNA Sequencer (A.L.F.-DNA sequencer) allows direct detection of fluorescently labeled DNA. During electrophoresis DNA fragments migrate downwards through the gel. The laser beam excites fluorescently labeled DNA and the emitted light is detected by fluorescent detection system. Collected photo-detector signals are then digitized and sent to a computer for further processing. Results are represented in the form of intensity peaks plotted against the running time scale. Reaction products of activity assays performed with DNA modifying enzymes were analyzed by A.L.F.-sequencer. DNA samples were mixed with A.L.F.-marker (2.1.9) and applied onto 11% denaturing polyacrylamide/urea gel (30 x 28 x 0.5 cm). Gels were prepared as described below.

11% A.L.F.-PAGE gel recipe:

Reagent	Amount
Urea	29.43 g (7M)
Acrylamide (30%)	24.84 ml (10.65%)
Bisacrylamide (2%)	12.42 ml (0.35%)
10XTBE	8.40 ml
APS (10%)	700 μl
TEMED	70 μl
ddH ₂ O	up to 70 ml

Sterile filtered A.L.F.-PAGE gel was poured in between two cleaned (in succession with water, ethanol and isopropanol) thermostable glass plates and a plastic comb was

inserted to form wells. Gel was polymerized for approximately 30 min at RT. The comb was then removed, wells were rinsed with water, gel was placed into electrophoresis chamber, and buffer reservoirs were filled with 1XTBE buffer. Before applying samples, the gel was preheated for 20 min. DNA samples were mixed with A.L.F. marker ($\frac{1}{2}$ sample volume), preheated for 5 min at 95°C, and applied onto the gel loading up to 15 μ l into each well. The gel was run for 250 min at a constant power of 52W, 52°C, a laser power of 4mW, and a sampling power of 2s. Electrophoresis data were processed using Fragment Manager (GE Healthcare, 2.1.13).

2.2.2.6 Purification of DNA fragments

DNA extraction from agarose gel

To extract DNA from agarose gel, the desired DNA fragment was excised from the gel with a sterile scalpel under UV light (305 nm). DNA was eluted from the gel using either NucleoTrap® (Macherey & Nagel, Düren) or High Pure PCR Cleanup Micro Kit (Roche Diagnostics, Mannheim) purification kits according to „*Protocol for DNA extraction from agarose gels using the NucleoTrap® kit*” or „*Purification of DNA fragments from Agarose Gel*“ from manuals of the each kit.

Sucrose gradient purification of DNA fragments

In order to achieve better cloning efficiencies linear plasmid DNA required for the construction of mutant gene library was subjected to sucrose gradient purification after digestion with restriction endonucleases (2.2.2.7). DNA fragments migrate through a sucrose gradient at a rate that is dependent on their size.

500 μ l of 40% Sucrose solution was pipetted into ultra-centrifuge tube. This solution was carefully overlaid with 9.5 ml of mixture of 30%- and 10%- Sucrose solutions which was prior to that prepared in the gradient mixer. Digested DNA sample was pipetted onto the gradient and the whole was overlaid with paraffin. Centrifugation of the gradient was achieved at 30000 rpm and 15°C for 21 hours. Afterwards, bottom of the centrifuge tube was stabbed with a needle and ~500 μ l aliquots of the solution were made. 10 μ l from each aliquot was analyzed by agarose gel electrophoresis. Desired DNA fragment was isolated from the solution by ethanol precipitation (2.2.2.1).

2.2.2.7 DNA cleavage by restriction endonucleases

For effective DNA cleavage optimal temperatures and buffers recommended by

manufacturer were used (2.1.6). 50 U of enzyme was used for preparative DNA cleavage (minimum 5 μg) in 100 μl assay volume for 1h or maximal 16h. For analytical DNA cleavage (300-500 ng), 5 U of restriction enzyme in 20 μl assay volume were used. In case of double digestion, if no united buffer could be found where both enzymes would show 50-100% activity, two subsequent digestion reactions were performed. After first digestion, DNA was precipitated with ethanol (2.2.2.1).

2.2.2.8 Cloning of DNA fragment into vector DNA

Cloning of DNA fragment into pJET1.2 cloning vector

Cloning of the PCR products into pJET1.2 cloning vector (2.1.3.2) was achieved using CloneJET™ PCR Cloning Kit (2.1.8) according to the *BluntEnd Cloning Protocol* and *StickyEnd Cloning Protocol* provided with manual of the kit. pJET1.2/blunt is a linearized cloning vector. The 5'-ends of the vector contain phosphoryl groups. Recirculized pJET1.2/blunt vector expresses a lethal *eco47IR* restriction enzyme after transformation and is not propagated. As a result, only recombinant clones containing the insert appear on culture plates.

PCR-products were purified by extraction from agarose gel (2.2.2.6) and subjected to ligation reactions according to following protocols.

BluntEnd Cloning Protocol:

For cloning blunt-end PCR products generated by proofreading DNA polymerases such as *Pfu* DNA polymerase.

First, ligation reaction was set up on ice according to following recipe:

Component	Volume
2XReaction Buffer *	10 μl
blunt-end PCR product, purified	2 μl (~0.15 μmol ends)
pJET1.2/blunt cloning vector (50ng/ μl)	1 μl (~0.05 μmol ends)
Water, nuclease-free	up to 19 μl
T4 DNA Ligase	1 μl
Total volume	20 μl

* 2xReaction Buffer component description is not supplied with the kit

Ligation mixture was incubated for 30 min at RT. 2 μl of the ligation reaction was used directly for transformation of *E. coli* (2.2.1.3.1).

StickyEnd Cloning Protocol:

For cloning PCR products with 3'-dA overhangs generated by *Taq* DNA Polymerase.

First, ligation reaction was set up on ice according to following recipe.

Component	Volume
2XReaction Buffer	10 μ l
PCR product, purified	2 μ l (~0.15pmol ends)
Water, nuclease-free	up to 19 μ l
DNA Blunting Enzyme*	1 μ l
Total volume	18 μ l

* The DNA Blunting Enzyme is a proprietary thermostable DNA polymerase with proofreading activity. It removes 3'-overhangs and fill-in 5'-overhangs. Nucleotides for the blunting reaction are included in the 2xReaction Buffer.

The mixture was incubated for 10 min at 70°C, chilled on ice and subjected to following reaction.

Component	Volume
PCR-product after blunting reaction	18 μ l
pJET1.2/blunt Cloning vector (50ng/ μ l)	1 μ l
T4 DNA Ligase	1 μ l
Total volume	20 μ l

Ligation mixture was incubated for 30 min at RT. 2 μ l of the ligation reaction was used directly for transformation of *E. coli* (2.2.1.3.1).

Cloning of DNA fragment into expression vector

Linear DNA fragments obtained after digestion with restriction endonucleases (2.2.2.7) were purified prior to ligation either by extraction from agarose gel or via sucrose gradient (2.2.2.6). To prevent the re-circulization of the majority of vector DNA during the ligation, linearized vector was subjected to dephosphorylation of DNA ends by treating with Calf Intestine Alkaline Phosphatase (CAP) directly after digestion with restriction endonucleases. For this, 2 μ l of CAP was given to 20 μ l of digestion reaction and the mixture was incubated for 1 hour at 37°C. Afterwards CAP was heat-deactivated by incubating at 80°C for 20 min.

Ligation mixture contained purified linear vector and insert DNA in 1:3 molar ratio, T4 DNA ligase and 1x T4 Ligase Buffer. T4 DNA ligase catalyzes the formation of a phosphodiester bond between juxtaposed 5' phosphate and 3' hydroxyl termini in duplex DNA. Amounts of DNA in the reaction were calculated according to formula:

$$\text{Insert Mass in ng} = 3 \times \frac{\text{Insert Length in bp}}{\text{Vector Length in bp}} \times \text{Vector Mass in ng}$$

Ligation mixture was incubated overnight at 37°C and on the next day transformed into *E. coli* (2.2.1.3.1). As a control, self-ligation of the vector DNA was tested each time when

ligation reaction was performed.

2.2.2.9 Preparation of oligonucleotide substrates for activity assays

For endonuclease assays, 0.01 pmol/ μ l substrate stocks were prepared by hybridization of 5 pmol of a fluorescein-labelled oligonucleotide with 25 pmol of an opposite strand oligonucleotide in 100 μ l of 1XSSC buffer (2.1.9) using an automated thermocycler (Program: 90°C, 15 sec; 80°C, 3 min; 50°C, 15 min; 20°C, 15 min), followed by a 1:5 dilution with water. In case of a single-stranded (ss) substrate preparation, 5 pmol of fluorescein-labelled oligonucleotides were mixed with 100 μ l of 1XSSC buffer and 400 μ l of water subsequently.

2.2.2.10 DNA sequencing analysis

DNA sequencing analysis was made by Goettingen Genomics Laboratory (G2L) using chain termination method by Sanger (Sanger et al., 1977). DNA samples were prepared by mixing a template DNA, a sequencing primer (2.1.4.4) and ddH₂O to a final volume and concentrations recommended by G2L. Sequence data were analyzed using Chromas[©].

2.2.3 Protein biochemical methods

2.2.3.1 Sodium dodecyl sulphate polyacrylamide gel electrophoresis (SDS-PAGE)

Gel electrophoresis provides a means of separating molecules that migrate through a porous matrix in response to an electric field. In denaturing sodium dodecyl sulphate polyacrylamide gel electrophoresis (SDS-PAGE) (Laemmli, 1970), sodium dodecyl sulphate (SDS) - an anionic detergent - confers a negative charge to polypeptides in proportion to their length and β -mercaptoethanol - a reducing agent - reduces disulfide bridges in proteins. Consequently, proteins are separated based on their molecular mass. Laemmli gels are composed of two different gels (stacker and running gel). SDS-PAGE gels (7.5 cm x 8 cm x 0.75 cm) were prepared as shown below.

15% SDS-PAGE recipe:

Components	15% Resolving gel (60 ml)	5% Stacking gel (35 ml)
Acrylamid/Bisacrylamid 30% (37.5:1)	30 ml	5.9 ml
1.875 M Tris-HCl, pH 8.8	12 ml	-
1.25 M Tris-HCl, pH 6.8	-	3.5 ml
10% sodium dodecyl sulphate (SDS)	600 μ l (1% final)	350 μ l (1% final)
dH ₂ O	17.2 ml	-
10% ammonium persulfate (APS)*	200 μ l	120 μ l
TEMED*	30 μ l	35 μ l

* Added just before pouring the gel

15% resolving gels were poured between two glass plates, overlaid with isopropanol to compose the flat gel surface and polymerized for 30 min at room temperature (RT). Then 5% stacking gel mix was made, poured onto top of the resolving gel, a comb was inserted and gel was polymerized for 30 min at RT. Protein samples were mixed with 1/5 volume of loading buffer (2.1.9) and denatured by heating for 5 min at 95°C just before loading onto the gel. Gels were run in 1x Laemmli buffer (2.1.9) at 20 mA constant current. For staining, the gel was removed from glass plate and put into Coomassie staining solution (equal volumes of Coomassie brilliant blue R-250 in methanol (0,7 %) and 20% Acetic acid) and incubated at RT for 30 min with slow shaking. For de-staining, the gel was cooked in water in the microwave.

2.2.3.2 Western Blot Analysis

Following electrophoresis, proteins in a polyacrylamide gel can be transferred to a positively charged nitrocellulose membrane by semi-dry electroblotting, where the gel and membrane are sandwiched between two stacks of filter paper that have been pre-wet with transfer buffer. The membrane is placed near the anode, and the gel is placed near the cathode. SDS-coated, negatively charged proteins are transferred to the membrane when an electric current is applied. Once transferred to the membrane, the proteins can be probed with epitope-specific antibodies. In this study proteins that carry polyhistidine tag (6xHis) were investigated by Western Blot analysis and Anti-Penta-His antibody (Qiagen, Hilden (2.1.6.)) was used. The position of the anti-His antibody bound to immobilized 6xHis-tagged protein is visualized using secondary anti-mouse IgG antibody (Sigma, Steinheim (2.1.6.)) conjugated to alkaline phosphatase together with enzyme substrate BCIP in combination with NBT (chromogenic method). All Western blot analyses in this study were performed according to the protocols described in *QIAexpress Detection and Assay Handbook* provided together with Anti-Penta-His antibody.

2.2.3.3 Crude cell extract preparation

To test the expression of recombinant proteins, test expressions were performed in 50 ml of bacterial culture. Induced and non-induced *E.coli* cells or *B. subtilis* cells were harvested by centrifugation for 10min at 4000 rpm and 4°C, resuspended in 500µl of 1x Laemmli buffer (2.1.9) and sonicated on ice for 3x1 min using Branson Sonifier 250 (output level 5, duty cycle 50%). Cell debris was pelleted by centrifugation for 15 min at 8000 rpm and

4°C and 15µl of the supernatant was analyzed by 15% SDS-PAGE (2.2.3.1).

2.2.3.4 Whole protein extract preparation of *B. subtilis* cells

200ml of *B. subtilis* mid-log phase culture was centrifuged for 30 min at 4000rpm and 4°C, the pellet was resuspended in 2 ml of PBS-Buffer and sonicated on ice for 2X3 min using Branson Sonifier 250 (output level 5, duty cycle 50%). Cell debris was pelleted by centrifugation for 20 min at 8000 rpm and 4°C. Proteins in the supernatant were concentrated by ammonium sulphate precipitation (to 80% saturation; centrifugation for 15 min at 15000 rpm and 4°C). The protein pellet was re-suspended in 1 ml of PBS-Buffer followed by the dialysis against 3 L of PBS-Buffer. The molecular-weight cutoff (MWCO) of the dialysis membrane was 14000. Whole protein extract was used further for activity assays (2.2.3.11).

2.2.3.5 Heterologous protein expression

For overexpression and further purification of the protein *exoA* gene was cloned into expression vectors pET28a (2.1.3.1) and pASK-08 (2.1.3.4). In pET expression system (pET28a vector and *E. coli* BL21_UXX strain (2.1.1.1)) expression of the target gene is regulated by strong T7 promoter (of bacteriophage origin), which is selectively recognised only by T7 RNA polymerase. BL21 (DE3) expression host possesses T7 RNA polymerase gene, *lac* promoter and *lac* operator incorporated in its genome. Expression of T7 RNA polymerase and consequently of the target gene can be activated by addition of lactose or its analogue isopropyl-β-D-thiogalactopyranosid (IPTG) to a cell culture. In pASK-08 vector pASK-08 vector works with the tightly regulated *tet* promoter. The *tet* repressor is encoded on the pASK-08 vector and is constitutively expressed from the promoter of β-lactamase (*bla*) gene. Expression of the recombinant protein is stringently repressed until efficient chemical induction with a low concentration of anhydrotetracycline (AHT). Special *E. coli* strain is not required.

20 ml of overnight culture of *E. coli* expression strain carrying respective expression vector was used to inoculate 1L of dYT selective medium (2.1.10) in 3L Erlenmeyer flasks. Culture was grown at 37°C with shaking to an OD₆₀₀ of 0.6. Gene expression was induced by addition of IPTG to a final concentration of 1 mM or AHT (anhydrotetracycline) to final concentration of 200 ng/µl and cell culture was further incubated for 3h at 30°C if not indicated otherwise. Cells were harvested by centrifugation for 30 min at 4000 rpm and 4°, resuspended in 25 ml of IMAC-washing buffer (2.1.9) and centrifuged for 30 min at 9000

rpm and 4°C. Cell pellet was frozen and stored at -80°C. After thawing and resuspension in 20 ml of IMAC-washing buffer (2.1.9), cells were homogenized by sonication on ice for 2X3 min using Branson Sonifier 250 (output level 5, duty cycle 50%) and disrupted by passage through a Constant Systems Ltd (Daventry, England) cell disruptor at 180 MPa and 14°C. Cell debris was precipitated by centrifugation for 1h at 15.000 rpm and 4°C. Clear cell lysate was subjected to Immobilized Metal Ion Affinity Chromatography (IMAC) (2.2.3.6). Cell pellets were also analysed by SDS-PAGE (2.2.3.1) to check for possible aggregation of target protein.

2.2.3.6 Immobilized Metal Ion Affinity Chromatography

Immobilized Metal Ion Affinity Chromatography (IMAC) is based on highly specific coordinate binding of amino acids to immobilized metal ions. Recombinant proteins used in this study were fused with a polyhistidine-tag at their C- or N-terminus. Imidazole ring of histidine residue possess high affinity to Ni²⁺ ions that in case of IMAC are immobilized on a sepharose matrix. During IMAC purification, cell lysate is incubated with affinity matrix, washed with buffer and the target protein is then eluted with imidazole gradient.

IMAC column was prepared by pouring 5 ml of 50 % slurry of Chelating Sepharose™ Fast Flow (2.1.7), previously equilibrated in IMAC buffer, into 5 ml plastic syringe and let it settle down by gravity force. Then the column was equilibrated with 1 column volume (5ml) of 100 mM NiCl₂, washed with 5 column volumes of water, and equilibrated with 3 column volumes of IMAC washing buffer (2.1.9). Clear bacterial cell lysate, prepared as described in 2.2.3.5, was applied onto the IMAC column followed by 2x washing each time with two column volumes of IMAC-washing buffer (2.1.9). Target protein was eluted from the column by passing two column volumes of IMAC elution buffer (2.1.9), one at a time (imidazole concentration: 30, 40, 50, 60, 70, 80, 90, 100, 300 and 500 mM). Collected IMAC fractions were analyzed by 15% SDS-PAGE (2.2.3.1). Fractions containing protein of interest were combined and concentrated to a final volume of 5 ml.

2.2.3.7 Heparin affinity chromatography

Heparin affinity chromatography was performed on a pre-packed POROS® HE20 (Perfusion chromatography, PerSeptive Biosystems) column using Vision Workstation (BioCad® Family, Applied Biosystems, 2.1.11) designed for automated control of essential chromatographic parameters such as: flow-rate, pressure, pH, elution volume, fraction

volume *etc.*, and sophisticated computerized data analysis. Heparin coupled with a high number of anionic sulphate groups is a high-capacity cation exchanger that allows specific purification of positively charged DNA binding enzymes from protein mix. Specific proteins can be then selectively dissociated from heparin with a salt gradient. Heparin column was equilibrated with heparin washing buffer (2.1.9) at a flow rate of 4 ml/min. Then 5 ml of concentrated protein solution obtained after IMAC (2.2.3.6) was diluted 1:10 with heparin washing buffer (up to 50 ml final volume) and applied onto heparin column at same flow rate. The column was washed with 30 ml of heparin washing buffer. Proteins retained in the column were eluted with 15 column volumes of a continuous 0-1.5M NaCl salt gradient and collected in 1 ml fractions. Protein elution was monitored at 260 and 280nm by a computer-controlled spectrophotometer and results were displayed as a dual line chromatogram. Peak heparin fractions were analyzed by SDS-PAGE (2.2.3.1). Fractions containing protein of interest were pooled and concentrated (2.2.3.9).

2.2.3.8 Spectrophotometric determination of protein concentration

Concentration of purified proteins was determined by measuring the absorbance at 250-300nm (UV-Region). Aromatic amino acids (tyrosine, phenylalanine and tryptophan) exhibit a strong UV-light absorbance. Consequently, proteins absorb UV-light in proportion to their aromatic amino acids content and total concentration. The molar concentration of protein solutions were estimated using Lambert-Beer law and following equation:

$$A = \epsilon \cdot c \cdot d \quad \Leftrightarrow \quad c = \frac{A}{\epsilon \cdot d} \quad ; \text{Where}$$

A = Absorbance

C = molar concentration

d = light path (cm)

*The molar extinction coefficient (ϵ_{280}) was calculated for each particular protein from its amino acid sequence using following equation (Pace et al., 1995):

$$\epsilon_{280}(M^{-1}cm^{-1}) = \sum Trp \cdot 5500 + \sum Tyr \cdot 1490 + \sum Cystine \cdot 125$$

2.2.3.9 Protein samples concentration and storage

Purified proteins were concentrated up to 0.5 - 1 ml final volume using 20 ml centrifugal concentrators (Vivaspine, Vivascience[®]) with appropriate Molecular Weight Cut Off (MWCO) at 3000 rpm and 4°C (Rotanata/RPC, Hettich). The protein concentration was determined measuring absorbance at 280 nm using a spectrophotometer (2.2.3.8). Concentrated protein solutions were mixed with glycerol at a 1:1 ratio and stored at -20°C or -80°C.

2.2.3.10 Endonuclease assay

0.12 pmoles of appropriate substrate (2.2.2.9) was pre-incubated in Endonuclease Buffer (2.1.9) for 10 min 37°C. Then an appropriate amount of enzyme was added to a final volume of 50 µl and reaction mix was incubated for 20 min unless otherwise specified. To stop the reaction, 25µl of A.L.F.-marker (2.1.9) was added and the samples were heated for 5 min at 95°C. 7 µl of the assay was applied onto 11% A.L.F.-PAGE (2.2.2.5) which is ~17 fmol of fluorescein-labelled material.

2.2.3.11 Activity assay with *B. subtilis* protein extract

0.12 pmol of U/G mismatch containing substrate (2.2.2.9) was pre-incubated in Endonuclease Buffer (2.1.9) with or without UGI (100 pmoles) at 37°C or 65°C for 10 min. 10 µl of *B. subtilis* protein extract was added (final volume of the reaction: 50µl) and the assay was incubated for 20 min at 37°C or 65°C. 100 pmoles of purified Mth212 was added into some assays concomitantly with the protein extract. To stop the reaction, 25µl of A.L.F.-marker (2.1.9) was added and the samples were heated for 5 min at 95°C. 7 µl of the assay was applied onto 11% A.L.F.-PAGE (2.2.2.5) which is ~17 fmol of fluorescein-labelled material.

2.2.3.12 Treatment of PBS1 bacteriophage DNA with tUDGa

2.5µg of PBS1 DNA was pre-incubated in 20mM Phosphate Buffer with 50mM KCl at 37°C for 10 min. In reaction with uracil DNA glycosylase, 400 pmoles of tUDGa was added to final volume of 25µl and the reaction was incubated at 37°C 30 min. In all reactions NaOH was added (100mM final concentration) and incubated at 95°C for 5 min. Finally, HCl was added (100mM final concentration) and 10µl of assay was subjected to agarose gel electrophoresis (2.2.2.4). Untreated PBS1 DNA used as a control was suspended in 35µl of 20mM Phosphate Buffer with 50mM KCl and 10µl was taken for agarose gel electrophoresis as well.

2.2.3.13 Treatment of PBS1 bacteriophage DNA with Mth212

2.5µg of PBS1 DNA was pre-incubated in Endonuclease Buffer (2.1.9) at 37°C for 10 min. 1, 10, 100 or 1000 pmoles of Mth212 was added to the final volume of 25µl and the reaction was incubated at 37°C or 65°C for 20 min. 10µl of assay was subjected to agarose gel electrophoresis (2.2.2.4).

3 Results and Discussion

3.1 Production and characterization of ExoA from *Bacillus subtilis*

With the purpose of elucidation of structural roots lying underneath the unique uridine endonuclease activity of Mth212, directed evolution of an exonuclease III homolog without this specific activity into Mth212-like enzyme was attempted during this work. ExoA protein from *B. subtilis* was chosen as an object for randomization (Introduction, 1.2.2). As Mth212, ExoA is an exonuclease III homolog and these enzymes are most likely having similar tertiary structure. Crystal structure of ExoA was not solved to date; however, multiple sequence alignment of exonuclease III homologs showed that ExoA differs from Mth212 to the same extent as it differs from other exonuclease III homologs (Figure 3.1). Mth212 shares 46% identical and 64% similar amino acid residues with ExoA, whereas human HAP1 has 41% identity and 60% similarity with Mth212.

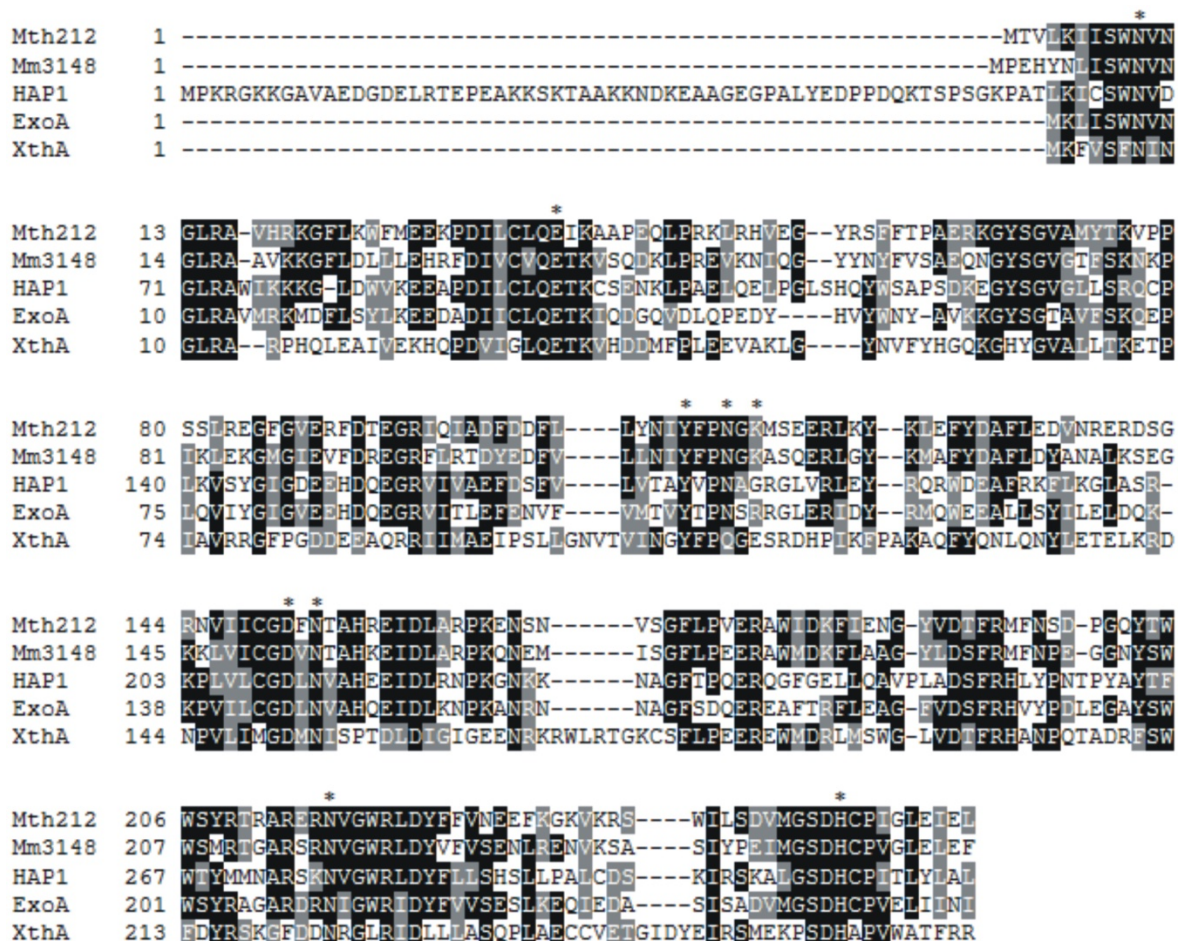


Figure 3.1: Multiple sequence alignment of *B. subtilis* ExoA with exonuclease III homologs such as Mm3148 (*M. mazei*), Mth212 (*M. thermoautotrophicus*), XthA (*E. coli*) and APE1 (HAPI (*H. sapiens*)). Identical and similar amino acid residues are highlighted in black and grey, respectively. Amino acid residues involved in the catalysis by APE1 according to (Mol *et al.*, 2000) and (Rothwell *et al.*, 2000) are marked with asterisks. Alignment was performed using the CLUSTAL W2.0.12 algorithm and arranged by BOXSHADE 3.21 software (2.1.13).

3.1.1 Production and purification of ExoA

In order to provide ExoA with DNA uridine endonuclease activity, the most essential step is to ensure that ExoA do not possess activity against uracil in DNA. ExoA has not been tested for this activity when it was characterized by Shida *et al.* (1999), and therefore biochemical characterization of ExoA, in particular the status of specific activity against uracil in DNA, was carried out. For this, ExoA was produced in an *E. coli* BL21_UXX *ung*-strain (2.1.1.1) as a N-terminal 6xHis-tagged recombinant protein using a pET_28a expression vector (2.1.3.1; cloning of *exoA* into pET_28a was performed by N. Krietenstein). Protein extract was prepared as described in 2.2.3.5 and the recombinant ExoA protein (ExoA henceforth) was purified using an immobilized-metal-ion affinity chromatography (IMAC, refer 2.2.3.6 for methods).

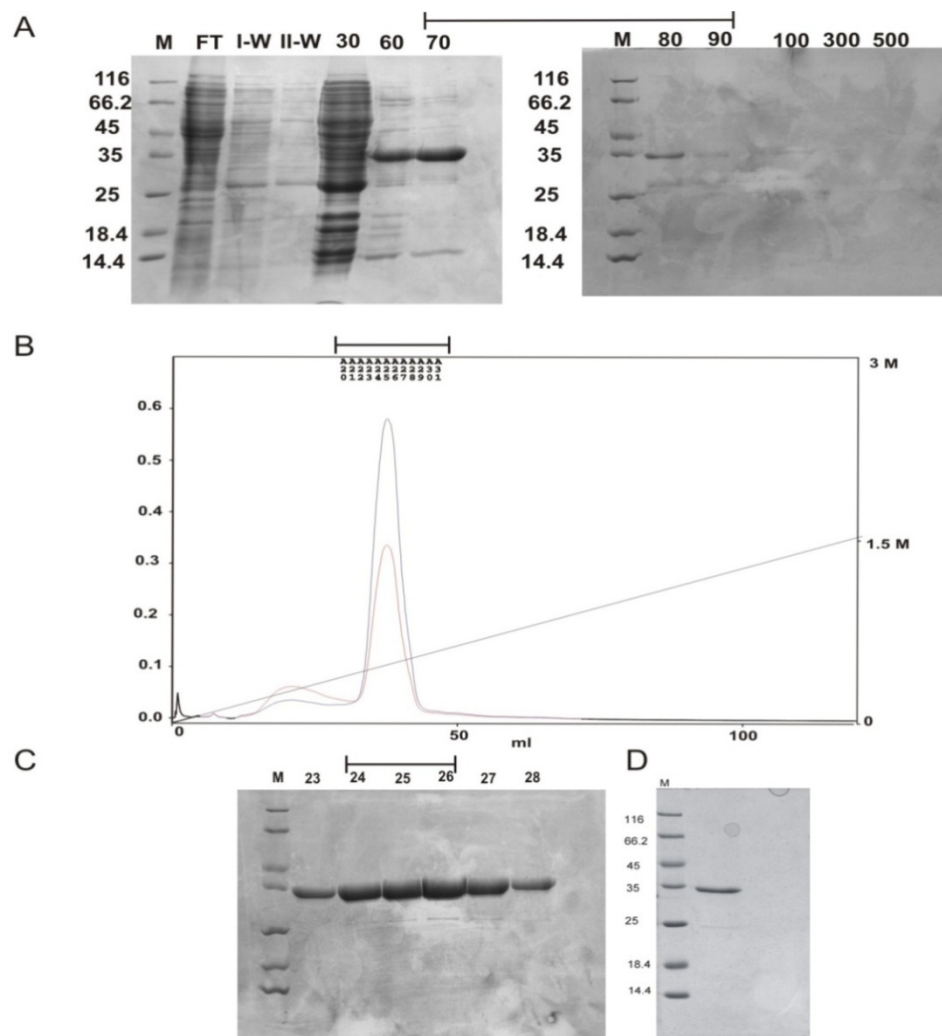
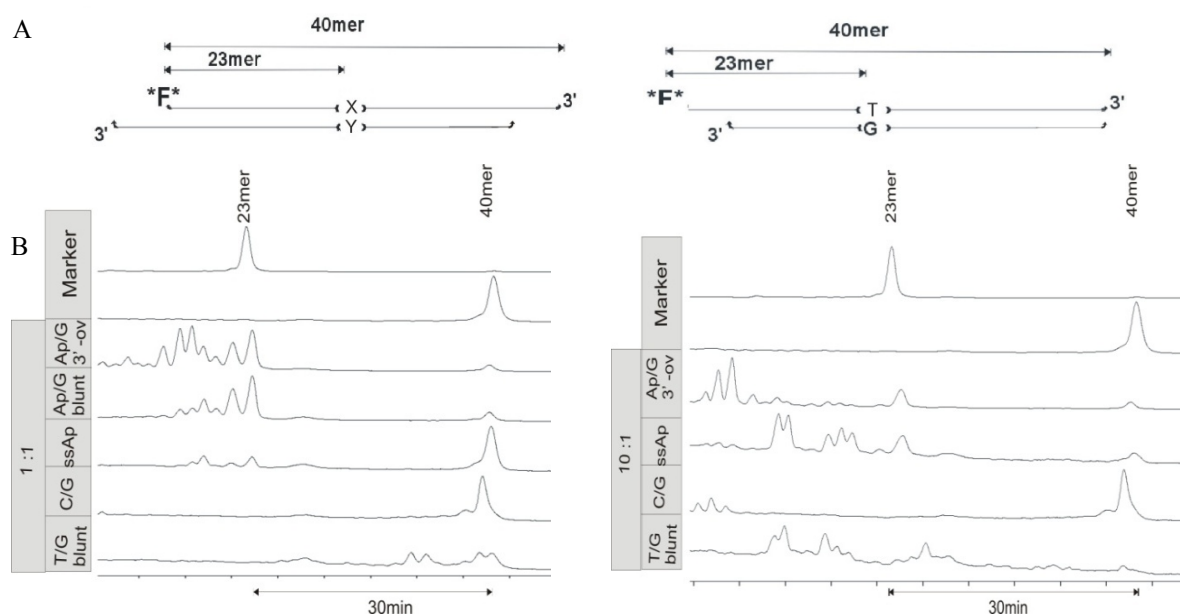


Figure 3.2: Purification of ExoA. **A:** Immobilized-metal-ion affinity chromatography (IMAC) fractions on 15% SDS-PAGE. (**M**) Molecular weight marker, (**FT**) Flow-through fraction (cell lysate eluted from IMAC column). (**I-W** and **II-W**) Column wash fractions. **30-500:** Protein fractions eluted with 30-500 mM imidazole in IMAC wash buffer. Brackets indicate fractions pooled for subsequent purification. **B:** Elution profile of the ExoA purification by Heparin affinity chromatography. Left ordinate: absorption at 260nm (red) and 280 nm (blue); right ordinate: concentration of NaCl in mol [M]; abscissa: elution volume in ml. Numbers above the chromatogram indicate fractions that were analysed by 15% SDS-PAGE shown in panel C. Brackets indicate fractions pooled and concentrated for subsequent enzymatic characterization. **D:** 15% SDS-PAGE of purified ExoA.

Analysis of protein fractions by SDS-PAGE revealed an enriched, partly purified protein with the expected molecular weight of ~34 kDa that was eluted by 70 – 90 mM imidazole containing buffer (Figure 3.2A). These fractions were further purified by a Heparin affinity chromatography (2.2.3.7). Proteins were eluted from the column using a linear gradient of NaCl (0 – 1.5 M) and the main peak of elution was analyzed by SDS PAGE (Figure 3.2B and C). Elution fractions containing the purified ExoA were then concentrated (2.2.3.9) to the final volume of 1 ml. The protein concentration was determined (2.2.3.8); the protein yield was approximately 3 mg (obtained from 1 L of culture medium). Eventually, protein was analyzed by SDS-PAGE for purity (Figure 3.2D).

3.1.2 Biochemical characterization of ExoA

ExoA was produced to test whether it is devoid of DNA uridine endonuclease activity. Activity assays were performed as described in 2.2.3.10 using 40-mer double-stranded DNA oligonucleotide substrates containing a mismatch at position 24. One of the DNA strands in substrate duplex was labelled with fluorescein on its 5' end. A schematic representation of assay substrate is shown in Figure 3.3A. Reaction products obtained during endonuclease assays were analysed under denaturing conditions by 11% A.L.F.-polyacrylamid gel electrophoresis (2.2.2.5) (Figure 3.3B).



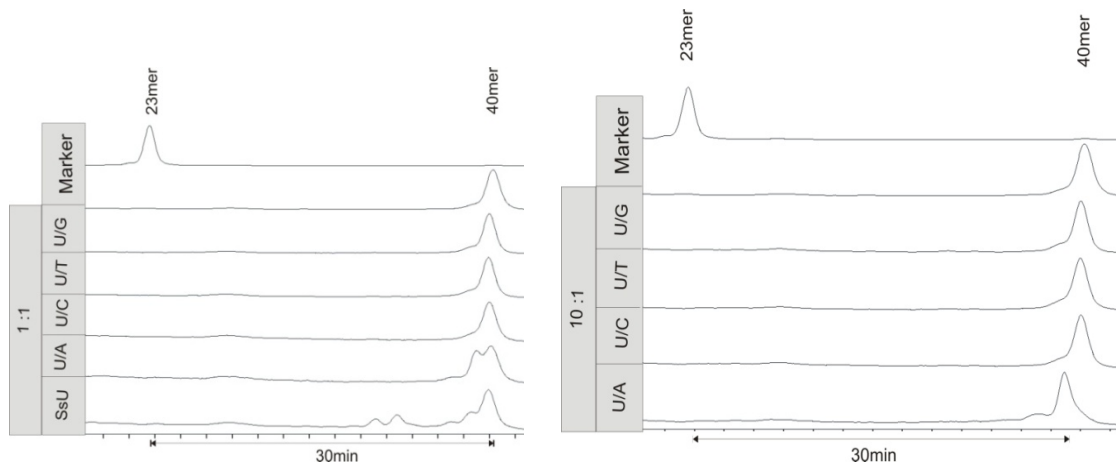


Figure 3.3: ExoA activity assay. **A:** schematic representation of substrate; X = AP, C, U; Y = G, T, C, A; F=fluorescein. Substrate containing T/G mismatch is blunt-ended. **B:** A.L.F.-PAGE analysis of ExoA activity assay with different substrates. 0.12pmol of substrate was used at enzyme:substrate ratio of 1:1 or 1:10 in Endonuclease Buffer (2.19), incubated 10 min at 37°C without enzyme prior to enzymatic reaction for 30 min at 37°C.

An AP-site containing substrate resulted in a product migrating with the same electrophoretic mobility as the 23-mer marker, confirming that ExoA is an AP-endonuclease. Series of shorter products were also generated as a result of further degradation of the main 23-mer product due to 3'→5' exonuclease activity of ExoA. Same products of 3'→5' exonuclease activity were also observed when blunt-ended T/G mismatch containing substrate was used for the assay. However, reaction with a substrate containing single stranded 3' overhang did not yield in degradation products, confirming the 3'→5' exonuclease activity of ExoA to be active only on double stranded DNA. These results are in agreement with findings of T. Shida *et al.* showing that ExoA exhibits same activities as members of the exonuclease III family, such as AP-endonuclease and 3'→5' exonuclease activities (Shida *et al.*, 1999). Activity assays (Figure 3.3) further demonstrated that ExoA, also when in excess, do not process uracil in U/G, U/C, U/T, U/A mismatches as well as uracil in ssDNA indicating that this protein does not possess DNA uridine endonuclease activity and therefore ExoA can be used in the directed evolution of an enzyme with DNA uridine endonuclease activity.

To conclude this sub-section, it was demonstrated that overproduced ExoA can be maintained in *E. coli* Δung strain. In connection with attempts to overproduce ExoA in *E. coli* $\Delta xthA$ strain (Section 3.5) these results are of considerable importance.

3.2 Attempted genetic selection of an ExoA mutant carrying DNA uridine endonuclease activity with the use of PBS1 bacteriophage

3.2.1 Design of a selection procedure

For genetic selection to work, an ExoA mutant must contribute to a growth advantage for the cell. The arising question in this study is how ExoA with acquired DNA uridine endonuclease activity can contribute to this? In this approach PBS1 bacteriophage from *B. subtilis* fulfilled the requirement. PBS1 bacteriophage contains uracil instead of thymine in its DNA (Takahashi, 1963) and, in order to protect its DNA from the attack of BER, it produces UGI, a small protein that inhibits the uracil-DNA glycosylase (family 1 UDG) of the host (Wang and Mosbaugh, 1989). UGI cannot inhibit exonuclease III homologs (Schomacher, 2007). Thus, any ExoA with acquired DNA uridine endonuclease activity should be able to initiate DNA uracil repair and, due to the exceedingly numerous uridine sites in PBS1 DNA, scores of single-strand breaks will be produced which will lead to consequent fragmentation of bacteriophage DNA. In any other cells that do not possess additional activity, PBS1 will successfully finish its reproduction and kill cells by lysis. This would provide a possibility to directly select cells resistant to bacteriophage infection due to acquired DNA U-Endo activity.

However, PBS1 belongs to the group of so called pseudolysogenic bacteriophages (Slepecky and Hemphill, 2006). Pseudolysogeny is a phenomenon in which an association between bacteriophage and its host mimics lysogeny in that host cell lysis is delayed or does not occur (Singleton and Sainsbury, 2006). Unlike true lysogeny, in this case bacteriophage genome does not integrate into the host chromosome (Abedon, 2008). The genome may be carried, but not expressed or replicated, within a cell in a susceptible population of bacteria, and the genome is passed to only one of the daughter cells at each cell division; a culture containing a proportion of such 'carrier cells' is known as a carrier culture. After several successive transits from cell to daughter cell, the bacteriophage genome enters the lytic cycle and progeny bacteriophages are released by cell lysis. These may infect other cells which may in turn become carrier cells (Singleton and Sainsbury, 2006). Presumably, PBS1 was included into this group of bacteriophages because of the instability of the lysogenic state (Takahashi, 1963). In any case, such interaction of PBS1 with its host interferes with its use in the selection approach. It will be impossible to select cells that survived bacteriophage infection due to the acquired DNA uridine endonuclease activity from those that survive due to established pseudolysogeny. Therefore, a clear

plaque mutant of PBS1 was required to select cells exhibiting DNA uridine endonuclease activity among other cells. This mutant, named PBS2, has been described in the literature by different groups (Takahashi, 1963; Katz *et al.*, 1976; Lauer and Klotz, 1976; Duncan and Warner, 1977), but it is no longer available in the scientific community. Since mutagenesis of a bacteriophage into a clear-plaque variant is well described for other bacteriophages (Dowding and Hopwood, 1973; Walker, 1978; Calsou *et al.*, 1987), it was decided to mutagenize PBS1 bacteriophage into its clear-plaque variant in our laboratory. Figure 3.4 gives an overview to this approach.

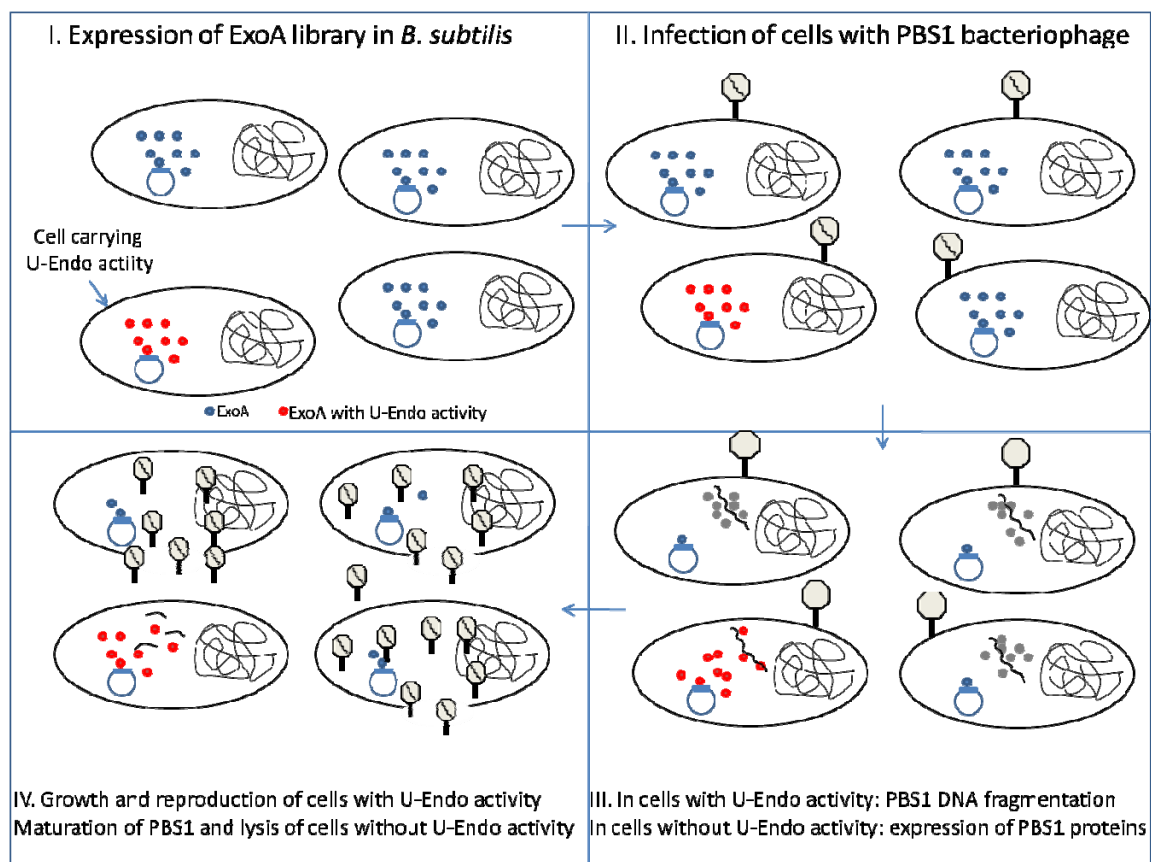


Figure 3.4: Schematic outline to the approach employing bacteriophage PBS1 and *B. subtilis*. U-Endo: DNA uridine endonuclease activity.

According to this design of selection procedure, experiments during this part of the work were grouped into two groups: construction of a mutant *exoA* library (Section 3.2.2) and investigations on PBS1 bacteriophage and attempts to obtain a clear-plaque mutant of PBS1 (Section 3.2.3) and were performed in parallel.

3.2.2 Construction of a mutant gene library

Series of experimental strategies have been developed to generate mutant gene libraries that differ significantly from each other. Random mutagenesis which targets whole genes

may be achieved by passing cloned genes through mutator strains, by treating DNA or whole bacteria with various chemical mutagens, or using error-prone PCR. There are also other random mutagenesis strategies which target single or few selected amino acids or regions of a protein that might be important for a certain function (Brakmann and Lindemann, 2004). Sequence diversity can also be generated by DNA shuffling (Suenaga *et al.*, 2004), hypermutagenesis (Vartanian *et al.*, 1996) or cassette mutagenesis (Black *et al.*, 1996).

The error-prone PCR method is one of the most popular approaches to generate libraries in directed evolution experiments because of its simplicity and versatility. In addition, the rate of mutation in error-prone PCR can be altered by modifying PCR conditions (Wang *et al.*, 2006). Variations in error rates can be obtained in a number of ways. One of the most straightforward methods is the combination of introducing small amount of Mn^{2+} (in place of the natural Mg^{2+} cofactor) to reduce the base pairing specificity (Beckman *et al.*, 1985) and including unbalanced dNTP stoichiometry to force misincorporation (Cadwell and Joyce, 1994; Cirino *et al.*, 2003). Mutagenic PCR conditions also include increased Mg^{2+} concentration to stabilize noncomplementary base pairs and increased polymerase concentration to enhance the probability of elongation of misprimed termini (Gelfand and White, 1990). Construction of mutant *exoA* library using error-prone PCR was performed according to the scheme shown in Figure 3.5.

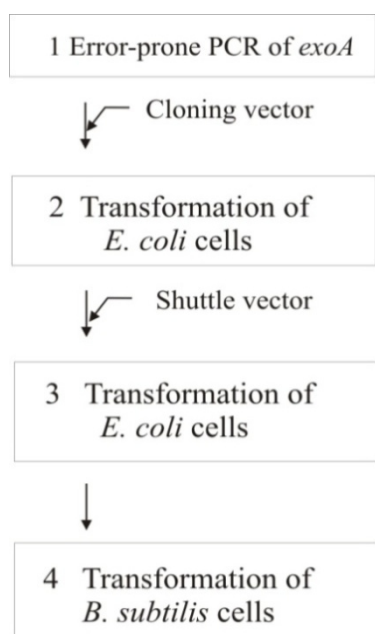


Figure 3.5: Scheme of library construction strategy. *exoA* served as a template for error-prone PCR (1), the PCR product was inserted into the cloning vector and transformed into *E. coli* cells (2). Thereafter, vector DNA containing the mutant gene library was isolated, the randomized *exoA* fragment was detached from the vector by restriction endonuclease digestion, re-cloned into shuttle vector and introduced into *E. coli* cells by transformation (3). Next, shuttle vector containing the mutant *exoA* library was isolated and the library was established in *B. subtilis* cells (4) by means of transformation.

Mutagenesis of *exoA* by passage through a mutator strain was abandoned due to unfavourable ratio of substitutions over frameshift mutations and considerably low mutation frequencies (data not shown).

3.2.2.1 Optimisation of error-prone PCR conditions

According to Cadwell and Joyce, error-prone PCR protocols employ several modifications relative to standard PCR that might be considered mutagenic, including: (1) increased concentration of *Taq* polymerase; (2) increased extension time; (3) increased concentration of $MgCl_2$; (4) addition of $MnCl_2$ and (5) dNTP concentration bias. The last two modifications are expected to have the greatest impact on the error-rate (Cadwell and Joyce, 1992). Different error-prone PCR (2.2.2.2) conditions were tested to find the optimal PCR condition suitable for the purpose of generating mutant *exoA* library. All reaction mixtures contained 100ng of template DNA, 50 pmoles of each primer, 6.5mM $MgCl_2$ and 5 Units of *Taq* polymerase. ThermoPol Reaction Buffer was used in all reactions. The mutagenic reaction mixtures contained varying concentrations of $MnCl_2$ and dNTPs; the effect of different sets of conditions on the number and type of mutations is summarized in Table 3.1.

MnCl ₂ concentration, dNTP bias	Number of sequenced clones	Number of deletions /insertions	Average mutation number per gene	Mutation frequency per position
0 mM dATP, dGTP 0.2mM each dTTP, dCTP 0.2mM each	12	-	0.25	$3.3 \cdot 10^{-4}$
0.5mM dATP, dGTP 0.2mM each dTTP, dCTP 1mM each	16	14 deletions	14.08	$1.9 \cdot 10^{-2}$
0.5mM dATP, dGTP 1mM each dTTP, dCTP 1mM each	14	6 deletions	5.1	$6.8 \cdot 10^{-3}$
0.25mM dATP, dGTP 1mM each dTTP, dCTP 0.2mM each	8	4 deletions	9.6	$1.2 \cdot 10^{-3}$
0.25mM dATP, dGTP 0.4mM each dTTP, dCTP 1mM each	18	8 deletions	5.8	$7.7 \cdot 10^{-3}$
0.1mM dATP, dGTP 1mM each dTTP, dCTP 0.2mM each	25	9 deletions	1.4	$1.8 \cdot 10^{-3}$
0mM dATP, dGTP 1mM each dTTP, dCTP 0.1mM each	15	8 deletions (1 trinucleotide)	3.26	$4.3 \cdot 10^{-3}$
0 mM dATP, dGTP 1mM each dTTP, dCTP 0.2mM each	21	2 deletions	1.2	$1.5 \cdot 10^{-3}$
0mM dATP, dGTP 0.2mM each dTTP, dCTP 1mM each	31	2 deletions	2	$2.6 \cdot 10^{-3}$

Table 3.1: Effects of various PCR conditions on mutation frequency and number of deletions or insertions. The average mutation number includes all mutation types. Mutation frequency was calculated as total number of mutations/total number of nucleotides sequenced (756 nucleotide positions between the two sequencing primers). For sequences refer to Appendix 7.2.1.

PCR with standard dNTP concentration (0.2mM each) and without $MnCl_2$ resulted in only 3 mutations within 9072 nucleotides that were sequenced (first row in Table 3.1). Including of $MnCl_2$ in the PCR reaction leads to higher number of mutations: average mutation

number per gene being 5.1 when 0.5mM MnCl₂ was added to reaction and no dNTP bias was implied. However, number of deletion mutations was also considerably high: 14 single nucleotide deletions in 16 clones were obtained when MnCl₂ was added to the PCR reaction compared to 2 deletions in 31 clones without MnCl₂ (sequences can be found in Appendix 7.2.1). Mutagenic role of Mn²⁺ is suggested to be due to its interaction with the enzyme-template complex, possibly altering the conformation at the active site of the polymerase (El-Deiry *et al.*, 1984). Frameshift mutations such as deletions and/or insertions of 1 or 2 nucleotides within the reading frame of a gene will lead to expression of novel and/or truncated polypeptides. Therefore this type of mutations should be avoided when a gene library is being constructed. The appropriate mutation frequency depends theoretically on the length of the gene, the average number of random mutations that the protein can accept without unfolding and the mutation bias. Error-prone PCR with dATP, dGTP (0.2mM each), dTTP, dCTP (1mM each) and without MnCl₂ yields 2 substitutions in average and 0.064 deletions per gene (highlighted in blue, Table 3.1). Due to this favourable ratio of substitutions over frameshift mutations this set of error-prone PCR condition was selected for further use. Mutation types and their frequencies obtained by error-prone PCR under this optimized condition are summarized in Table 3.2.

Total mutations in 31 clones		62 in 23405 nt
Transitions	A→G	26.6%
	G→A	3.3%
	T→C	30%
	C→T	10%
Transversion	A→T	8.3%
	T→A	15%
	G→C	-
	C→G	-
	A→C	1.66%
	C→A	1.66%
	G→T	-
Δ1 deletions	2	
Insertions	-	

Table 3.2: Sequence context of mutation types and their frequencies obtained by the optimized error-prone PCR.

As shown in Table 3.2, this PCR condition did not result in G→C and C→G transversion mutations, which is in agreement with the results of Shafikhani *et al* (Shafikhani *et al.*, 1997). Because of difference in experimental conditions employed in our study, a comparison of mutation frequencies during mutagenic PCRs with published data was difficult. For instance, some reaction buffers may be more mutagenic than the others (Eckert and Kunkel, 1990); different AT content of the template may introduce biases,

caused by the fact that the A→G and T→C transitions are the most frequent substitution under standard PCR conditions (Fromant *et al.*, 1995).

3.2.2.2 Cloning of the library and transformation of *E. coli*

The *exoA* randomized by means of error-prone PCR was inserted into different *E. coli* cloning vectors with considerably high cloning efficiencies (3.2.2., Figure 3.4). Direct cloning of the PCR product into shuttle vector was inefficient for the library construction (data not shown).

pJET1.2 (2.1.3.2) cloning vector was then chosen over pCR II-TOPO and pCR[®]-Blunt II-TOPO vectors because of (1) better cloning efficiency and (2) availability of a negative selection against non-recombinant clones. The latter was achieved due to expression of a lethal restriction enzyme when the vector is self-ligated. *E. coli* cells were transformed with the pJET1.2 cloning vector after insertion of randomized *exoA*. To achieve sufficient high transformation efficiency, different *E. coli* strains and two transformation techniques were used (2.2.1.3.1). Results are summarized in Table 3.3.

Transformation method	<i>E. coli</i> strain	Number of clones (pJET_ <i>exoA</i>)	Number of transformants / μ g pUC19
RbCl ₂ method	DH5 α	1600	5.6*10 ⁷
	TOP10	35000	7*10 ⁶
Electroporation	DH5 α	900	2*10 ⁷
	TOP10	1150	8.6*10 ⁶

Table 3.3: Transformation efficiency of *E. coli* with pJET1.2 vector containing mutant *exoA* library. Table shows results of single experiment for each transformation (method descriptions: 2.2.1.3.1). Covalently closed, circular, supercoiled DNA of pUC19 vector was used as a control.

Maximal number of clones was obtained with chemically (RbCl₂) competent One Shot TOP10 *E. coli* cells (2.1.1.2) and was used therefore for library generation.

Approximately 9*10⁵ colonies with randomized *exoA* in pJET1.2 vector were collected and used for plasmid DNA isolation (2.2.2.1). For protein expression in *B. subtilis*, the *exoA* library was then cut out from the pJET1.2 vector re-cloned into linearized and purified pBQ200 shuttle vector (2.2.2.8) that was modified previously into pBQ200_ *BpiI* (2.1.3.4) using site-directed Quick-change[®] mutagenesis (2.2.2.2.4) to introduce two *BpiI* recognition sites. *BpiI* cleaves downstream of its recognition site and generates any desired 4 base 5'-overhangs. This feature makes this enzyme more efficient in respect of library generation than other conventional restriction endonucleases that cleave palindrome sites. Routinely, 3*10⁵ clones were obtained from each transformation. Colonies were then collected and used for isolation of the mutant *exoA* library in pBQ200_ *BpiI* shuttle vector.

Expression of ExoA when cloned into pBQ200_ *BpiI* shuttle vector was under regulation of a strong DegQ36 promoter (Msadek *et al.*, 1991); ribosome binding site of the *B. subtilis gapA* gene was upstream of the translational start of *exoA* gene (Meinken *et al.*, 2003).

3.2.2.3 Investigation of transformation efficiencies of different *B. subtilis* strains

It is well known that *B. subtilis* cells exhibit transformation efficiencies few orders of magnitude lower than gram-negative *E. coli* cells (Trevors *et al.*, 1992). Nonetheless, three major options exist for the introduction of DNA into *B. subtilis* by transformation: (1) transformation of naturally competent bacteria, (2) polyethylene glycol (PEG)-mediated transformation of protoplasts and (3) electroporation. During DNA transfer into naturally competent *B. subtilis* cells, the DNA suffers double-strand cleavage at the cell surface and one of the two strands is stripped away during the actual entry into the cell (Cutting and Youngman, 1994). For that reason this method is inappropriate for establishing the mutant *exoA* library in *B. subtilis*. Therefore, the other two methods were used and transformation efficiencies were determined for several *B. subtilis* strains (Table 3.5).

Transformation method	Expected max. transformation efficiency (/μg DNA)	<i>B. subtilis</i> strain	Transformation efficiency /μg pBQ200_ <i>exoA</i>
Protoplast transformation	$2 \cdot 10^7$ (S. Chang and N. Cohen, 1979)	W168	28
		SB19E	18
		IG-20	35
Electroporation	10^4 (P. Brigidi <i>et al.</i> , 1990)	W168	$1.6 \cdot 10^2$
		SB19E	59
		IG-20	$5 \cdot 10^2$
		ISW1214	$8.9 \cdot 10^2$
Electroporation in high osmolarity solution	$1.4 \cdot 10^6$ (G-P. Xue <i>et al.</i> , 1999)	W168	$6 \cdot 10^3$
		SB19E	$1.2 \cdot 10^2$
		IH6140	$7 \cdot 10^4$
		ISW1214	$8 \cdot 10^2$

Table 3.5: Transformation efficiencies of *B. subtilis* strains. Second column of the table shows highest transformation efficiencies described in the literature to the time of study. For genotypes of *B. subtilis* strains and methods used, refer to Material and Methods section 2.1.1.2 and 2.2.1.3.2, respectively.

The protoplast transformation method in our study did not work as efficient as it was described in the literature. Poor regeneration of protoplasts on DM3 stabilizing agar medium (2.1.10) and incomplete conversion of intact cells into protoplasts were the main problems faced during the experiments (data not shown). Electroporation of *B. subtilis* cells also delivered low transformation efficiency, even with restriction and modification deficient strains ISW1214 and IG-20.

Maximal transformation efficiency reached during this study was $7 \cdot 10^4$ transformants/μg DNA with *B. subtilis* IH6140 strain (kindly provided by Dr. V. Kontinen, National Institute

for Health and Welfare, Finland) by means of “Electroporation in high osmolarity solutions” (2.2.1.3.2). This transformation efficiency was lower compared to that obtained by Xue *et al.* (1.4×10^6 transformants/ μg DNA) who used same *B. subtilis* strain as well as the same method (Xue *et al.*, 1999). This difference is likely due to the use of different plasmid DNA. pUBxynA vector used by Xue *et al.* is a 5.9 kb Gram-positive vector carrying kanamycine resistance gene and expresses xylanase at high levels upon establishment within the cell which may lead to increased cell survival. In contrast, pBQ200_exoA vector used in this study is a 7.5 kb shuttle vector carrying erythromycin resistance gene.

To conclude this sub-section: (1) mutant *exoA* library of approximately 9×10^5 variants was constructed after optimization; (2) methods for transformation of *B. subtilis* cells were tested and the most efficient method was selected for this study.

3.2.3 Investigation of PBS1 bacteriophage

3.2.3.1 Verification of presence of uridine residues in PBS1 bacteriophage genome

As previously described, due to its unique DNA, PBS1 bacteriophage (2.1.2) was to be used in the selection of the ExoA protein variant which has acquired the DNA uridine endonuclease activity. Uridine in the PBS1 DNA is the target for this novel activity and it was important to ensure the presence of uridine residues in the DNA of bacteriophage. PBS1 bacteriophage was obtained from Bacillus Genetic Stock Center (BGSC), The Ohio State University, USA (2.1.2).

DNA was extracted from PBS1 bacteriophage particles (2.2.2.1), treated with DNA uracil glycosylase (2.2.3.12) and analysed by agarose gel electrophoresis (Figure 3.6).

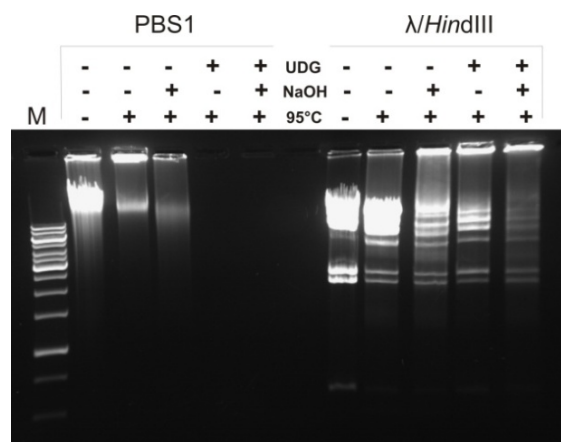


Figure 3.6: Analysis of PBS1 DNA processing by uracil-DNA glycosylase tUDGa by agarose gel electrophoresis. 2.5 μg PBS1 DNA was used for analysis. *Hind*III digested λ bacteriophage DNA was used as a control. Assay conditions (25 μl): 400pmol tUDGa in 20mM Phosphate Buffer with 50mM KCl, incubation at 37°C for 30 min; at 95°C for 5 min with NaOH (100mM end concentration). HCl was added to neutralize the reaction. 10 μl of assay was loaded onto gel. M: DNA size Marker GeneRuler™ 1kb (2.1.5.1)

The tUDGa homolog from *M. mazei* (Mm0486) that excises uracil base from U/G, U/C, U/T mismatches and U/A base pair was used for this assay (preparation by S. Ber, Ber 2009). Addition of NaOH to the reaction and incubation at 95°C drives strand cleavage at the base-free DNA site by β -elimination.

As shown in Figure 3.6, PBS1 DNA was completely degraded when tUDGa was added to the reaction; in contrast, *Hind*III digested λ DNA, which does not contain uracil residues, remains intact, indicating that PBS1 DNA is susceptible to the action of tUDGa due to the uracil presence.

To test the susceptibility of PBS1 DNA to the action of a DNA uridine endonuclease, bacteriophage DNA was treated with Mth212 (Figure 3.7, for method refer to section 2.2.3.13). Mth212 incises DNA strand 5' to the uridine residue and only when incisions are made on both DNA strands in near proximity it will lead to dsDNA break.

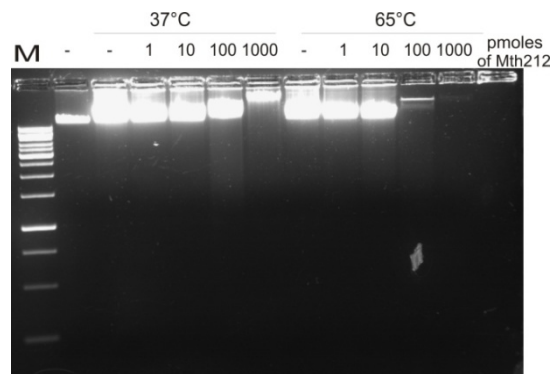


Figure 3.7: Agarose gel analysis of PBS1 DNA processing of by Mth212. Assay conditions (25 μ l): 2.5 μ g PBS1 DNA in Endonuclease Buffer (2.1.9), incubation at 37°C or 65°C for 20 min; amount of Mth212 in the reaction: upper bar of the figure. 10 μ l of assay was used for agarose gel electrophoresis. M: DNA size Marker GeneRuler™ 1kb (2.1.5.1)

Incubation of PBS1 DNA with Mth212 at 65°C, a temperature for maximal activity for Mth212, (Georg *et al.*, 2006, Schomacher *et al.*, 2009) resulted in PBS1 DNA degradation in an Mth212 concentration-dependent manner, with a maximum degradation at 1000 pmoles of Mth212, indicating that PBS1 DNA is susceptible to the action of DNA uridine endonuclease.

3.2.3.1.1 Processing of PBS1 DNA *in vivo*

Biochemical analysis of PBS1 DNA showed that it can be processed by Mth212 *in vitro*. To test whether PBS1 DNA will be attacked by Mth212 *in vivo*, Mth212 was expressed in *B. subtilis* after successful cloning of *mth212* gene into pBQ200 shuttle vector. As a control, inactive mutant of Mth212 *mth212_D151N* (Georg *et al.*, 2006) was used. Cells expressing the Mth212 or its inactive mutant were then infected with PBS1 bacteriophage and the plating efficiencies were measured (2.2.1.2.1) (Figure 3.8).

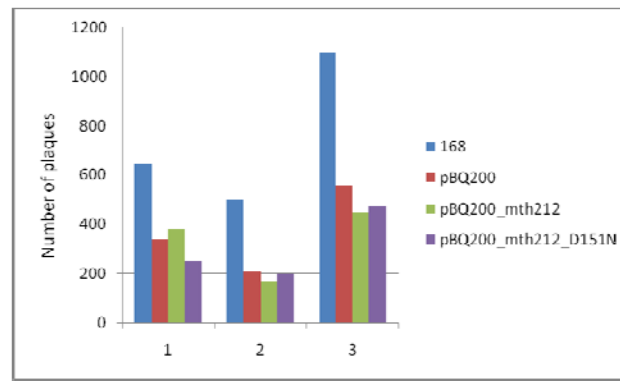


Figure 3.8: Number of PBS1 plaques when *B. subtilis* cells containing different vectors are infected. 168: wild-type (WT) strain of *B. subtilis*, pBQ200: empty vector, pBQ200_mth212: expression vector for WT Mth212, pBQ200_mth212_D151N: expression vector for inactive Mth212. 1, 2, and 3: ordinal number of experiments. For material and methods refer to Section 2.2.1.2.1..

It was expected that PBS1 DNA will be attacked by Mth212 soon after infection, leading to its degradation and thus bacteriophage death. However, no significant difference in plating efficiency was observed between cells harbouring pBQ200_mth212, pBQ200_mth212_D151N and the empty vector pBQ200 after infection with PBS1. The difference in plating efficiency between wild-type cells and cells carrying the shuttle vector is most probably due to the presence of antibiotics in the medium, since some antibiotics have been found to negatively affect bacteriophage growth (Santos *et al.*, 2009).

Observed lack of bacteriophage growth inhibition can be explained with following: (1) Mth212 is not expressed in *B. subtilis*; (2) Mth212 cannot properly fold in *B. subtilis*; (3) the temperature of 37 °C used for bacterial and bacteriophage growth is not optimal for Mth212 activity. The optimal temperature for Mth212 is 65°C (J. Georg *et al.*, 2006).

To address the question whether Mth212 is expressed and can properly fold in *B. subtilis*, a Western blot analysis was performed with the cytosolic fraction of crude cell extracts (2.2.3.2).

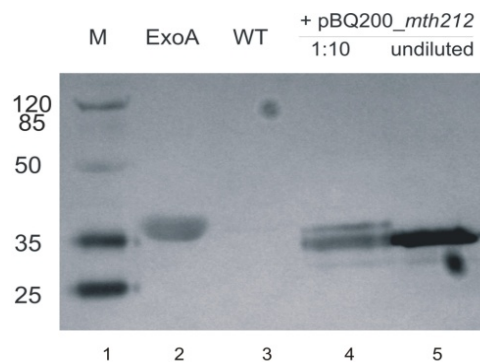


Figure 3.9: Western blot (2.2.3.2) analysis of the cytosolic fraction of crude cell extracts of *B. subtilis* using anti-Penta-His antibody (2.1.6) 1: (M) Protein Molecular Weight Marker (2.1.5.2); 2: Purified ExoA Protein, 100 pmoles, used as a positive control; 3: cell extract of *B. subtilis* strain W168; 4 and 5: cytosolic protein extract of *B. subtilis* strain W168 carrying pBQ200_mth212 vector, 1:10 diluted and undiluted, respectively.

A protein band of approximately 30 kDa size was detected in the cytosolic fraction of crude cell extract of *B. subtilis* carrying pBQ200_ *mth212* vector by (Figure 3.9). This was similar to the expected molecular weight of 6xHis-tagged Mth212 (31.17 kDa) indicating the expression of Mth212 and its proper folding in *B. subtilis*. Next, we analyzed enzymatic activity of this protein.

Because of the thermal instability of *B. subtilis* proteins at 65°C (optimal temperature for Mth212), it is impossible to infect *B. subtilis* cells with PBS1 bacteriophage at this temperature to see the influence of Mth212. Therefore, enzymatic activity tests were performed with the protein extracts of *B. subtilis* expressing Mth212 (Figure 3.10, for methods refer to section 2.2.3.11).

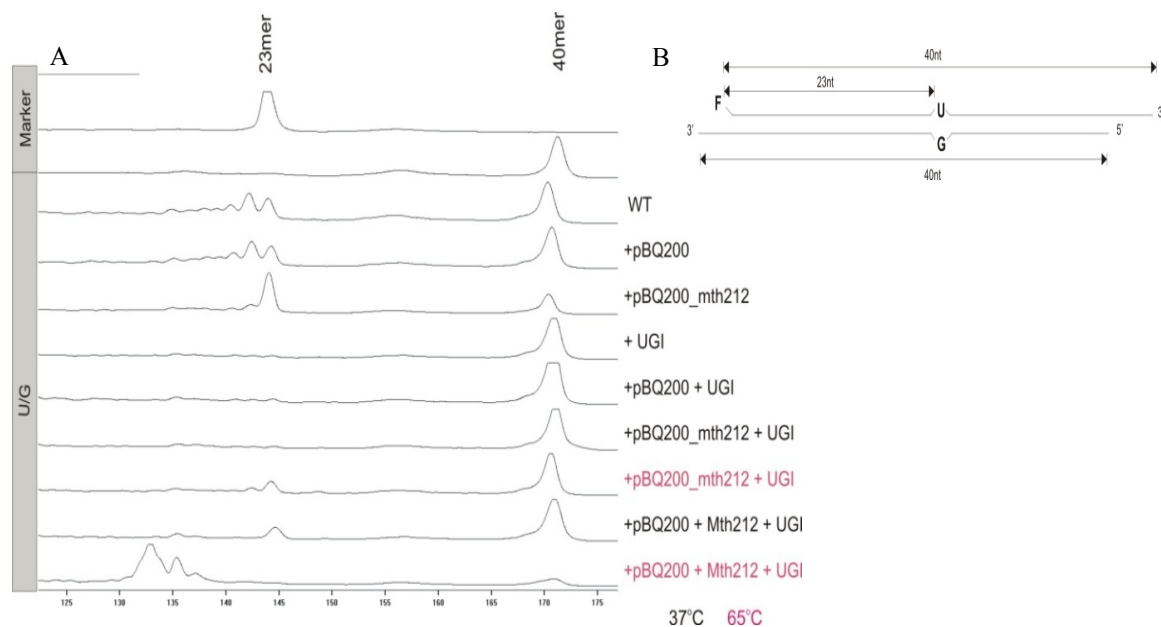


Figure 3.10: Activity assay of *B. subtilis* protein extracts. **A:** A.L.F. PAGE analysis of the assay. Assay conditions: 0.12 pmol substrate, 10 μ l protein extract in Endonuclease Buffer (2.1.9); incubation at 37°C or 65°C (labeled with red) for 20 min; WT: WT strain protein extract; protein extract from cells transformed with empty vector (pBQ200), or pBQ200_ *mth212* vector (2.2.3.4). UGI: uracil-DNA glycosylase Inhibitor (100 pmoles); for inhibition, UGI was added 10 min prior to substrate addition; 100 pmoles of purified Mth212 protein was used as positive control. **B:** Schematic representation of the substrate used in the assay.

As shown in Figure 3.10, all three types of cell extract; wild-type, cells containing pBQ200, and cells containing pBQ200_ *mth212*, produced a 23-mer and one or few shorter fragments from the oligonucleotide substrate with U/G mismatch. However, uracil-DNA glycosylase inhibitor protein, UGI, was able to completely inhibit this reaction, suggesting that (1) the 23-mer product is a result of activity of endogenous uracil-DNA glycosylases and AP-endonucleases of *B. subtilis*, (2) activity of Mth212 is too low at 37°C. In contrast, when the assay mixture was incubated at 65°C a 23-mer product peak was observed,

indicating the activation of Mth212, which cannot be inhibited by UGI. These results support the use of ExoA: since it is originated from *B. subtilis*, this protein will work at 37°C without any complication regarding the temperature optimum. Once it is converted to DNA uridine endonuclease, it would attack PBS1 bacteriophage DNA in *B. subtilis* cells.

3.2.3.2 Experiments to obtain clear-plaque mutant of PBS1 bacteriophage

As described in Section 3.2.1. a clear plaque mutant of PBS1, named PBS2, was required was for the genetic selection of cells exhibiting DNA uridine endonuclease activity. Since this mutant bacteriophage could not be found in the scientific community, it was decided to mutagenize PBS1 bacteriophage into its clear-plaque variant in our laboratory.

UV-irradiation was employed for mutagenesis of PBS1 to obtain a clear-plaque mutant. At first, a photokilling curve of PBS1 was made to optimize UV irradiation dose (Figure 3.11). Approximately 1×10^7 plaque forming units (pfu) of PBS1 bacteriophage were suspended in 6 ml of PBS1-Buffer (2.1.9) and subjected to UV-irradiation (254 nm, $0.5 \text{ J sec}^{-1} \text{ m}^{-2}$; 2.2.1.2.1). 100 μl of irradiated bacteriophage suspension was serially diluted and the dilutions were plated with 500 μl of log-phase *B. subtilis* cells as described in Materials and Methods (2.2.1.2.1). Cells were incubated overnight at 30°C and plaques were counted.

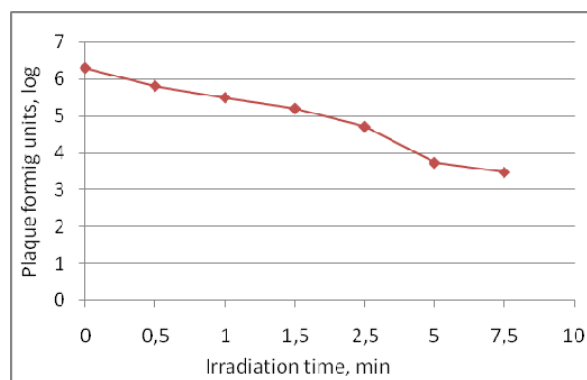


Figure 3.11: Semi-log curve of bacteriophage numbers after irradiation. UV irradiation dose: 254 nm, $0.5 \text{ J sec}^{-1} \text{ m}^{-2}$;

No plaque was detected after 10 minutes of irradiation of bacteriophage. However, after 2.5 and 5 minutes of UV irradiation bacteriophage number decreased by approximately 2 and 3 orders of magnitude, respectively and killed more than 99 % of the bacteriophage population. Higher dose of UV would decrease the number of viable bacteriophage particles drastically, whereas lower dose would induce insufficient damage to DNA. Therefore, UV irradiation dose of 2.5 - 5 min at 254 nm and $0.5 \text{ J sec}^{-1} \text{ m}^{-2}$ was established for consequent experiments to generate clear-plaque mutants (for detailed description of

PBS1 bacteriophage mutagenesis experiment refer to Material and Methods section 2.2.1.2.1). However, despite of high number of screened plaques, a bacteriophage with desired clear-plaque phenotype could not be obtained.

It is known that DNA damages caused by UV-irradiation induce SOS response in *E. coli* cells, resulting in error-prone translesion synthesis (Friedberg *et al.*, 2006). Jean Weigle was the first to observe that the UV-irradiation of the host cells (*i. e.* induction of SOS-response) lead to increased survival rate and number of mutant bacteriophages (Weigle, 1953). These phenomena were termed later as Weigle reactivation and Weigle mutagenesis, respectively. In this study, it was attempted to make use of Weigle mutagenesis phenomenon to increase the likelihood of clear-plaque mutation in PBS1 bacteriophage.

In order to determine whether Weigle reactivation of PBS1 bacteriophage occurs in *B. subtilis*, non-irradiated or irradiated (1 minute at 254nm and $0.5 \text{ J sec}^{-1} \text{ m}^{-2}$) *B. subtilis* cells were plated with irradiated PBS1 bacteriophage and plaques were counted (Figure 3.12).

A

$$\text{Weigle reactivation value (P. E. Love and R. E. Yasbin, 1984)} = \frac{\text{surviving fraction of irradiated bacteriophage incubated on irradiated cells}}{\text{surviving fraction of the irradiated bacteriophage incubated on non-irradiated cells}}$$

B

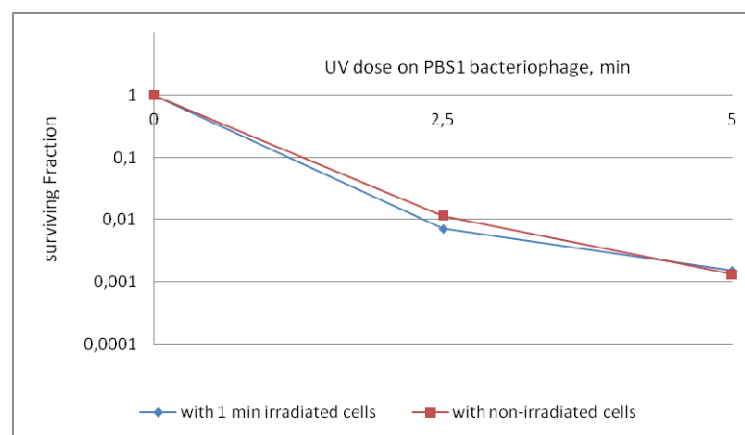


Figure 3.12: Determination of Weigle reactivation for PBS1 bacteriophage. **A:** Formula for calculating Weigle reactivation value. **B:** Semi-log plots of the surviving fraction of PBS1 bacteriophage plated with *B. subtilis* cells that were either non-irradiated or irradiated for 1min. Abscissa: UV-irradiation (at 254nm and $0.5 \text{ J sec}^{-1} \text{ m}^{-2}$) in minutes; ordinate: surviving fraction of bacteriophage.

Weigle reactivation value for PBS1 bacteriophage irradiated for 2.5 minutes was 0.592 ± 0.297 ($n = 3$). Weigle reactivation value for bacteriophage λ irradiated for 2.5 minutes, for instance, was approximately 100 (Weigle, 1953), leading to a conclusion that no Weigle reactivation occurred for PBS1. One can suggest that Weigle reactivation and mutagenesis effects might be bacteriophage specific. It is known that Weigle reactivation and mutagenesis are based on error-prone bypass of DNA lesions of SOS-induced cells

(Friedberg *et al.*, 2006). PBS1 bacteriophage utilizes its own virally encoded DNA polymerase which incorporates uracil instead of thymine during the viral DNA replication (Hitzeman and Price, 1978). If PBS1 DNA polymerase is not able to do translesion synthesis of bacteriophage DNA, it may explain the lack of Weigle reactivation for PBS1 bacteriophage. This result precluded the making use of Weigle mutagenesis to obtain a clear plaque mutant of PBS1.

To conclude this sub-section: in this study, UV mutagenesis was employed to generate lytic mutant of PBS1. However, no clear-plaque mutant was found even though approximately 2×10^6 plaques were screened. In the study of Takahashi, spontaneous clear-plaque mutant of PBS1, termed as PBS2, was found by plating of a large number of bacteriophage particles with *B. subtilis* (Takahashi, 1963), and, unfortunately, no quantitative data regarding this mutation was published. Spontaneous clear-plaque mutation frequency of *E. coli* λ h bacteriophage, for instance, is 0,025% which is 1 clear-plaque mutant in around 4000 and the clear-plaque mutation frequency increases when UV-irradiation is employed (Miura and Tomizawa, 1970).

Taken together, it can be suggested that mutations that lead to a clear-plaque phenotype in PBS1 occur extremely rare and the desired mutant cannot be obtained under experimental conditions employed in this study. Perhaps, complex lysis-lysogeny regulation mechanism exists for PBS1 and only several distinct mutations occurring simultaneously can result in a lytic mutant.

The employment of lytic mutant of PBS1 bacteriophage in the selection of ExoA with acquired DNA uridine endonuclease activity was the most straightforward way due to its intrinsic feature to contain uracil in the DNA. Given that this bacteriophage cannot be utilized for the selection another approach was designed.

3.3 Attempted genetic selection of an ExoA mutant carrying U-Endo activity with the use *E. coli* bacteriophage

3.3.1 Design of a selection procedure

This approach is similar to previous selection method that was envisioned for *B. subtilis*, but it utilizes *E. coli* as a host cell. Selection pressure is achieved here through the use of bacteriophage as well. However, since there are no known *E. coli* bacteriophages that have uracils in their DNA, like PBS1 bacteriophage does, this approach is not as straightforward as the approach implementing *B. subtilis* and PBS1.

In other words, uracils must be introduced into bacteriophage DNA. This can be achieved by growing bacteriophages on *E. coli* cells deficient of both uracil-DNA glycosylase and dUTPase activities (*dut⁻*, *ung⁻*). Thereby, up to 30% of all thymines in bacteriophage DNA can be replaced by uracil (Duncan and Weiss, 1982). On the other hand, once these bacteriophage particles infect cells that are not *dut⁻*, *ung⁻*, their DNA will not contain uracil anymore. This means that cells carrying DNA uridine endonuclease activity are not resistant to bacteriophage as soon as the first round of infection is completed. In order to protect the cells that survived the primary infection due to the acquired DNA uridine endonuclease activity from the second infection, secondary infection must be hindered. This can be achieved by using bacteriophages mutated in one of the genes expressed late in the bacteriophage development. This bacteriophage can be propagated in amber-suppressor *dut⁻*, *ung⁻* cells, where uracils will be introduced in its DNA. Subsequently, cells carrying the mutant gene library will be infected with these bacteriophages. In cells that carry DNA uridine endonuclease activity bacteriophage DNA will be fragmented due to uridine sites in DNA, whereas in other cells bacteriophage encoded proteins will be expressed. However, due to the mutation in late gene no mature bacteriophage will be released and at the same time the host cell will be overburden with production of defect bacteriophage particles which leads to the cell death. In this way, selection of cells expressing ExoA with desired activity can be achieved. Figure 3.13 gives an overview to this approach.

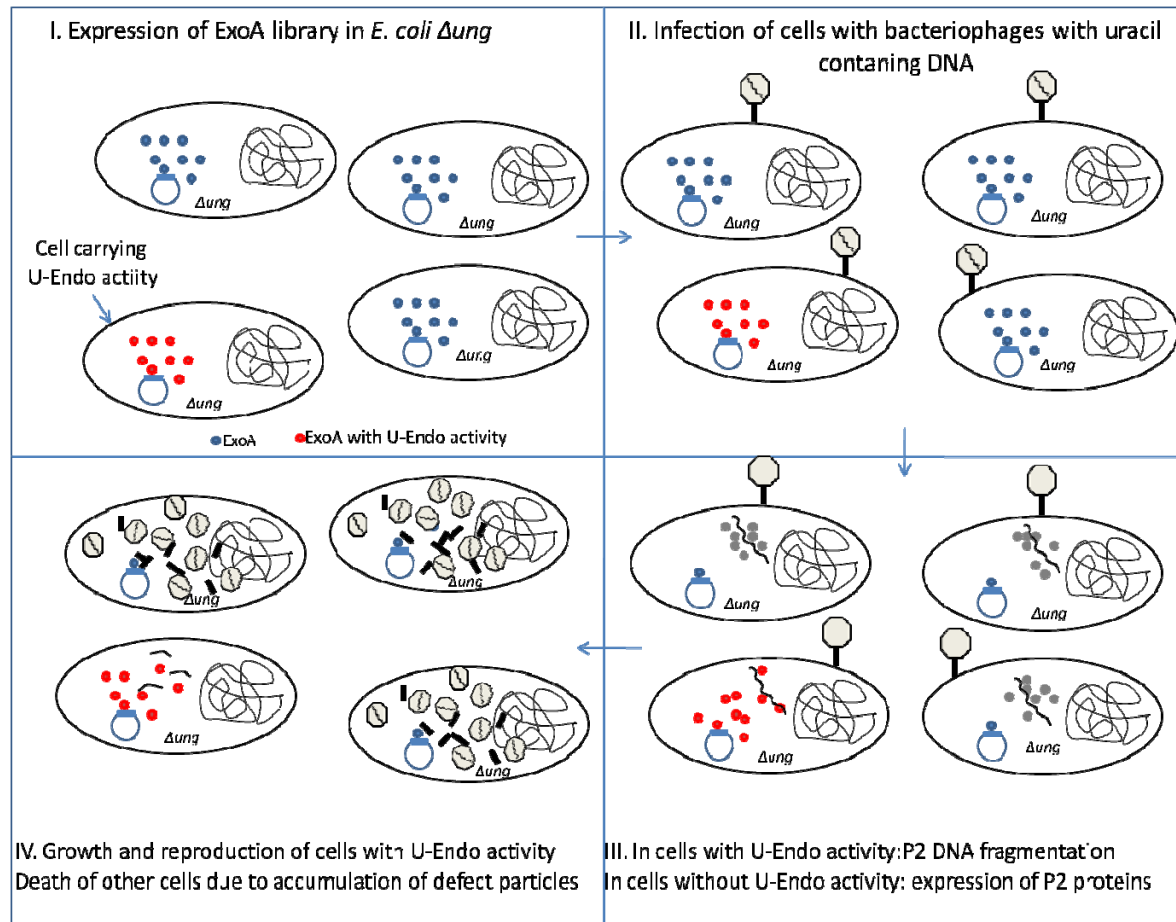


Figure 3.13: Schematic outline to the approach employing *E. coli* bacteriophage. U-Endo: DNA uridine endonuclease activity.

3.3.2 Construction of a mutant gene library

Error-prone PCR for randomization of *exoA* and cloning of *exoA* library into pJET1.2 vector were performed as before (Sections 3.2.2 and 3.2.4). Mutation frequencies, ratio of total mutation number to deletion and insertion number, as well as mutation types were determined after sequencing of clones. No significant differences were observed from results of previous library generation (3.2.3) (sequences can be found in Appendix 7.2.2). For protein expression in *E. coli*, mutant *exoA* library was re-cloned (2.2.2.8) into expression vectors pASK-08 (2.1.3.5) and pTNA (2.1.3.6). pASK-08 vector provides with inducible, high-level expression of protein, whereas pTNA vector provides with constitutive, low-level expression of protein. For cloning into pTNA vector *SphI* restriction endonuclease site was removed from *exoA* using site-directed Quick-change[®] mutagenesis (2.2.2.2.4) without affecting the protein sequence (for sequence refer to Appendix 7.3.1). Table 3.6 summarizes the construction of new mutant *exoA* libraries.

	<i>exoA</i> _pJET1.2 for pASK-08	<i>exoA</i> _pASK-08	<i>exoA</i> _pJET1.2 for pTNA	<i>exoA</i> _pTNA
Number of sequenced clones	48	48	48	48
Total number of transformants*	$8,1 \cdot 10^5$	$3 \cdot 10^6$	$4 \cdot 10^5$	$6,7 \cdot 10^5$

Table 3.6: Number of clones obtained during the generation of mutant libraries. *-clones from several transformations were pooled together.

3.3.3 Construction of *E. coli* mutant strains C1a Δ ung and C520 Δ ung

PBS1 bacteriophage expresses uracil-DNA glycosylase Inhibitor protein (UGI), which blocks the activity of uracil-DNA glycosylases of the host (Wang and Mosbaugh, 1989) to protect its DNA from the attack of BER. This gives “natural” possibility to select the protein with DNA uridine endonuclease activity. In this approach, however, gene of the uracil-DNA glycosylase (*ung*) must be knocked out in P2 bacteriophage indicator *E. coli* strains C1a (non-permissive strain, 2.1.1.1) and C520 (amber-suppressor strain, 2.1.1.1) to enable selection of DNA uridine endonuclease. The *ung* gene was knocked out by replacing it with a kanamycine cassette using P1 bacteriophage transduction (2.2.1.2.3). *E. coli* BL21_UX strain (Georg *et al.*, 2006) was used as a donor strain for transduction. Absence of complete ORF of *ung* was verified by PCR (2.2.2.2.1) (Figure 3.14).

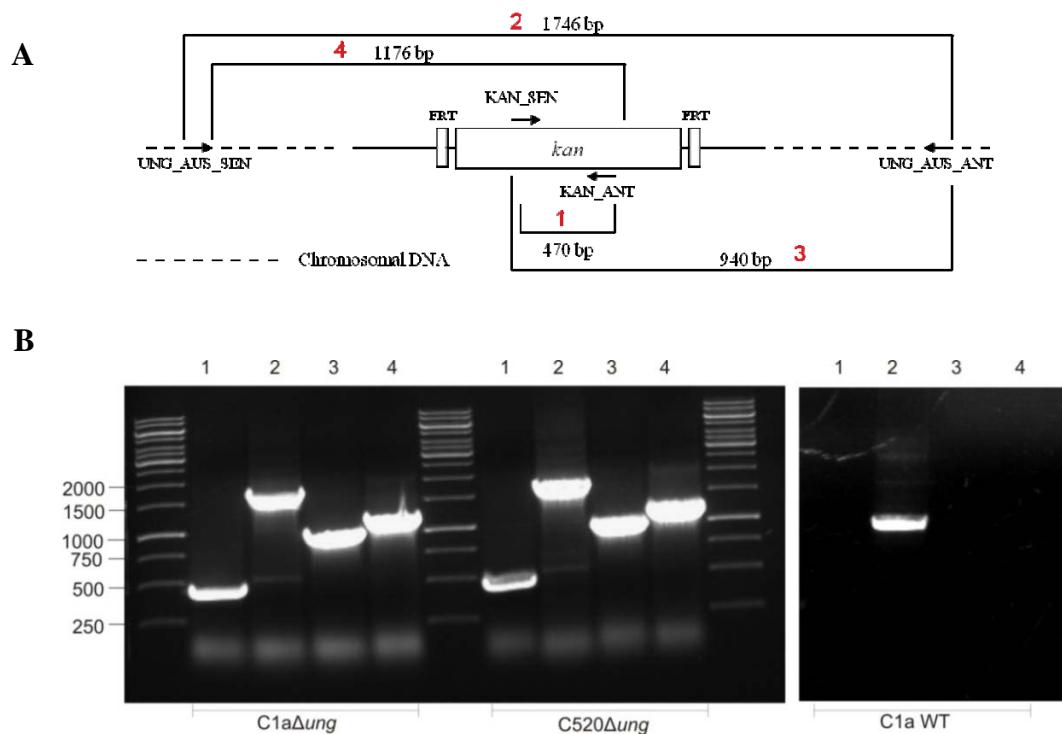


Figure 3.14: Deletion of *ung* gene in *E. coli* C1a and C520 strains. **A:** Scheme of Kanamycine cassette insertion into *E. coli* chromosome. Primer positions are shown by arrows, expected PCR-product (1, 2, 3, and 4) lengths are given in base pairs (bp). **B:** PCR-Analysis. 1, 2, 3, 4: PCR products using the primer combination shown on the scheme. DNA from *E. coli* C1a WT was used as a control, expected PCR product with the primer set 2 is 910 bp, and no product was expected with other primer sets.

3.3.4 Cloning of an amber-suppressor tRNA gene

For successful propagation of P2vir1Ram3 bacteriophage (2.1.2) on *E. coli* CJ236 *dut-*, *ung-* strain (2.1.1.1) presence of an amber-suppressor tRNA was necessary. Amber-suppressor tRNA gene *serU132* (Steege and Horabin, 1983) (Figure 3.15) was amplified by PCR (2.2.2.2.1) from *E. coli* C520 DNA, cloned into pBR322 vector using *EcoRI* and *PstI* and then re-cloned into pACYC177 vector using *BamHI* and *PstI* (2.2.2.8). The *serU132* insert was verified by sequencing (Appendix 7.3.2). pACYC177 is a low copy plasmid with a p15A origin of replication which makes it compatible with vectors containing ColE1 origin of replication such as expression vectors pASK-08 and pTNA.

```

GGGACTGTTAAATGCCAAATTCCTGGCATCATGGCAACCATCTGAACGGAGAGATGCCGGAGCGGCTGAACGGACCGG
TCTCTAAAACCGGAGTAGGGCAACTCTACCGGGGGTCAAATCCCCTCTCTCCGCCAATTATCAATG

```

Figure 3.15: Sequence of the *serU132* structural gene in pACYC177. The region corresponding to mature tRNA^{SerU132} is indicated by a regular line and nucleotides identical to the consensus sequence for the -10 and -35 regions of *E. coli* are indicated by dashed lines. The position of SerU132 mutation which corresponds to the middle nucleotide of the tRNA anticodon is shown in red (G→T). The adenine residue which serves as the tRNA start is indicated with an arrow (adapted from D. A. Steege and J. I. Horabin, 1983).

To test whether the presence of pACYC177_ *serU132* vector in *E. coli* enables the growth of P2vir1Ram3 in a non-permissive strain plating efficiencies of P2vir1Ram3 on different strains were measured. High-titer lysate of pure P2vir1Ram3 was made (2.2.1.1.2), bacteriophage DNA was isolated (2.2.2.1) and the presence of Ram3 mutation was confirmed by sequencing of the *R* gene (see Appendix 7.3.3 for the sequence; *R* gene sequence reference: Linderoth *et al.*, 1994). 100µl of the P2vir1Ram3 bacteriophage lysate was diluted and the dilutions were plated with 100µl of *E. coli* cells as described in section 2.2.1.1.2. Plaques were counted on the next day and the titer was determined.

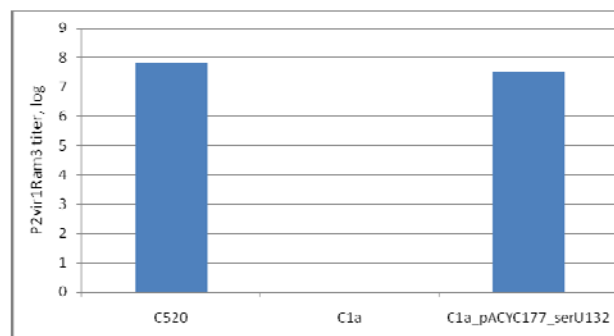


Figure 3.16: Titer of P2vir1Ram3 bacteriophage propagated on an amber-suppressor strain C520, non-permissive wild-type strain C1a (2.1.1.1) and C1a strain carrying pACY177_ *serU132*.

Wild-type cells lacking amber-suppressor tRNA did not support bacteriophage growth (Figure 3.16). In contrast, *E. coli* C1a strain transformed by pACYC177_serU132 vector permit the growth of P2vir1Ram3 bacteriophage, suggesting that tRNA^{SerU132} is synthesized in *E. coli* and the expression level is sufficient to suppress Ram3 amber mutation of the bacteriophage. Consequently, pACYC177_serU132 vector was employed in following experiments.

3.3.5 Cultivation of bacteriophage P2vir1Ram3 on *dut- ung-* strain

pACYC177_serU132 vector was introduced into *E. coli dut-, ung-* strain CJ236 cells by transformation (2.2.1.3.1) and cells were then infected with P2vir1Ram3 bacteriophage. Bacteriophage lysate was prepared (2.2.1.1.2) and, in order to see whether propagation on *dut, ung-* strain resulted on the incorporation of uracil into bacteriophage DNA, lysate titers on *E. coli* strains C520 and C520Δung (2.1.1.1) were determined (2.2.1.2.2).

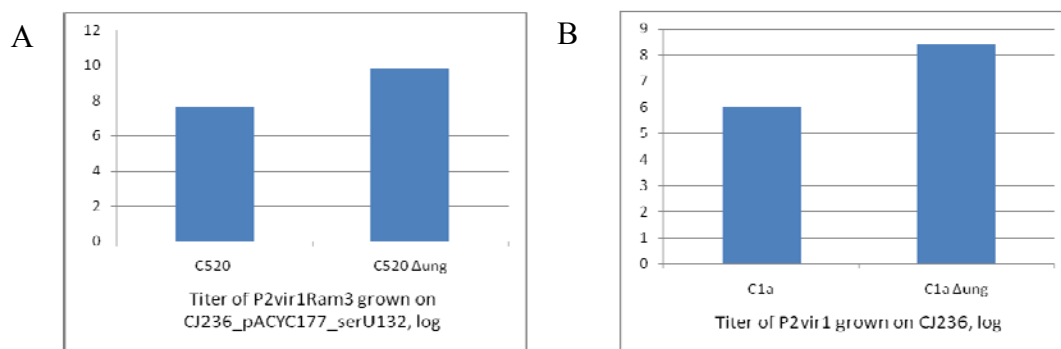


Figure 3.17: Titers of P2vir1Ram3 (A) and P2vir1 (B) bacteriophages propagated on *E. coli dut-, ung-* strain. C520: amber suppressor strain, C520Δung: C520 having *ung* deletion, C1a: *E. coli* WT strain, and C1aΔung: C1a having *ung* deletion.

The titer of P2vir1Ram3 passaged through CJ236/pACYC177_serU132 cells (designated as P2vir1Ram3-U henceforth) on C520 strain differs from the titer on C520Δung strain (Figure 3.17A). Approximately 99.3% of all bacteriophages did not grow in cells where DNA uracil glycosylase (Ung) was present. As a control, titer of P2vir1 bacteriophage lysate grown on *E. coli* CJ236 (designated as P2vir1-U henceforth) strain was determined (Figure 3.17B). P2 vir1 bacteriophage (2.1.2) was obtained after plating P2vir1Ram3 on *E. coli* C1a. Reversion of Ram3 mutation was verified by sequencing of *R* gene (see Appendix 7.3.4 for sequence). 1 % of the P2vir1-U bacteriophages was able to grow on C1a strain.

Taken together, these results suggest that uracil is incorporated into bacteriophage DNA upon propagating on *E. coli dut-, ung-* strain. The reduced ability of P2vir1Ram3 to grow

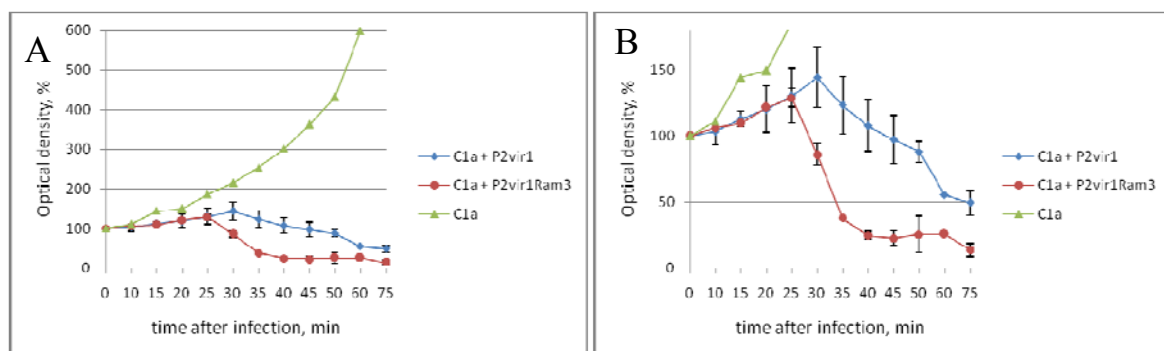
on *E. coli* C520 indicates that the genome of P2vir2Ram3-U is fragmented due to high number of DNA double-strand breaks. Double-strand breaks occur when uracil molecules incorporated nearly opposite each other in both DNA strands attract action of uracil-DNA glycosylase working together with AP-endonucleases.

Small percentage of P2vir1Ram3-U bacteriophages was able to grow on C520 cells. This may be due to the (1) low incorporation of uracil into DNA, in which case, uracils will be repaired without fragmentation of viral DNA, and (2) relatively low level of uracil-DNA glycosylase in wild-type cells (Olsen *et al.*, 1991). The latter will be overcome in our study by the use of pASK-08 expression vector which provides with the high level expression of the cloned gene.

3.3.6 Survey of inability of P2vir1Ram3 bacteriophage to finish infection

Inability to successfully finish infection with simultaneous inhibition of cell growth when bacteriophage is propagated on non-permissive strain was the major prerequisite of this approach. It was expected that when P2vir1Ram3 infects C1a cells overproduction of defective bacteriophage particles due to the lack of the *R* gene product takes place and as a consequence cell growth ceases because infected cells are not able to live as long or reproduce as fast as uninfected cells. This phenomenon was observed for P2vir1Kam12 bacteriophage infection in liquid culture; Kam12 is a lysis deficient mutant of P2vir1 and C1a cells stopped growing about 30 minutes post-infection but did not lyse (Zierman *et al.*, 1994) (Figure 3.18C).

To test whether infection of *E. coli* C1a with P2vir1Ram3 will trigger cell death, 10^8 of *E. coli* C1a cells in log-phase were suspended in dYT medium (10ml end volume), mixed with 10^9 of bacteriophage, incubated at 37°C with rotation and the optical density was measured over a time course (Figure 3.18A-B).



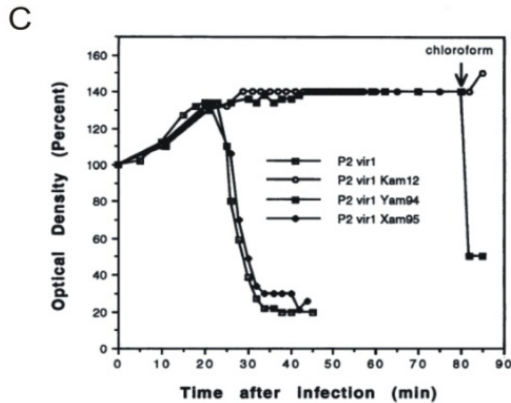


FIG. 5. Lysis of C-1a. Samples (9 ml) of cells in early-log phase (which is defined as 100%) were infected with the phage strains indicated at a multiplicity of infection of 10. (A) Infection with P2 *vir1* and P2 *vir1* amber mutants in genes *K*, *Y*, and *X*. Eighty minutes after infection, 300 μ l of chloroform was added to the cultures infected with the lysis-deficient *K* and *Y* mutants.

Figure 3.18: *E. coli* C1a cell growth upon bacteriophage infection. **A:** Measurements of the optical densities. **B:** Cell density plot (A) is magnified by decreasing y-axis maximum for a better interpretation. $N = 3$ for C1a+P2vir1 and C1a+P2vir1Ram3. **C:** Infection of C1a cells with Kam12 mutant of P2vir1 bacteriophage, adapted from Zierman *et al.*, 1994.

Optical densities of *E. coli* C1a cells decreased after 30 or 25 min when infected with P2vir1 or P2vir1Ram3 bacteriophage, respectively (Figure 3.18A-B). Normally, when cells stop to grow optical density remains unchanged. Infection of *E. coli* C1a cells by either P2vir1 or P2vir1Ram3 decreased optical density indicating cell lysis. However, in comparison to results of Zierman *et al.*, (1994) a delay of roughly 10 minutes was observed (Figure 3.18C).

Remarkably, infection with P2vir1Ram3 bacteriophage lead to lysis of non-suppressor cells. Mechanism of cell lysis regulation of P2 bacteriophage places it in the lambdoid group exemplified by λ , P22, Pa-2 and 21 bacteriophages (Ziermann *et al.*, 1994). The timing of lysis in these bacteriophages has been fine-tuned by involving a “holin” and an “endolysin” (a murein hydrolase) that are both necessary to induce precisely timed and rapid cell lysis (Rice and Bayles, 2008). It can be suggested that because functions involved in host cell lysis in P2vir1Ram3 bacteriophage are not affected (genes *K* and *Y*, endolysin and holin, respectively) cell lysis occurs despite of incomplete assembly of bacteriophage particles.

Next, *E. coli* C1a cell lysate obtained after infection of P2vir1Ram3 was tested whether it contains infectious bacteriophage particles (2.2.1.2.2). For this, 100 μ l of *E. coli* C1a cell lysate was diluted and dilutions were plated with 500 μ l *E. coli* C1a and C520 cells.

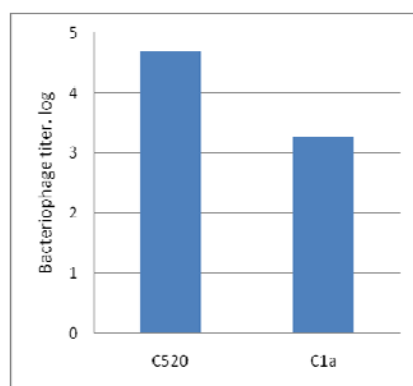


Figure 3.19: Bacteriophage titer of a lysate obtained after infecting *E. coli* C1a with P2vir1Ram3 on *E. coli* strains C1a and C520 (2.2.1.2.2).

The results from Figure 3.17 show that lysate obtained upon infection of *E. coli* C1a cells with P2vir1Ram3 contains bacteriophage particles of which some are capable of infecting C1a cells (180 plaques). These plaques are most likely arisen from bacteriophages that underwent reversion mutation of Ram3. Bacteriophage titer on *E. coli* C520 cells was 5×10^4 pfu/ml, these bacteriophages are probably P2vir1Ram3 that did not infect C1a cells. Considering that 10^9 pfu was used for infection in liquid culture, nearly 10^5 fold decrease in bacteriophage titer stands for the expected lack of bacteriophage reproduction in *E. coli* C1a cells.

Infection in liquid culture, however, brings along the major obstacle when the selection of a protein with uridine DNA endonuclease activity with the help of uracil containing bacteriophage DNA will be carried on. Small percentage of P2vir1Ram3 bacteriophage grown on *dut*⁻, *ung*⁻ strain was able to grow in C520 cells (3.3.5, Figure 3.17A). The progeny of these bacteriophages in liquid culture will rapidly spread and infect cells including those carrying desired activity. Therefore, after infection cells must be plated onto agar medium plates to provide with spatial separation of cells.

To test if the infection with P2vir1Ram3 bacteriophage will lead to *E. coli* C1a cell lysis on agar medium, the following experiment was done.

10^6 of *E. coli* C1a cells were infected with P2vir1Ram3 bacteriophage at MOI 1 (10^6 pfu added), MOI 0.1 (10^5 pfu added) and MOI 5 (5×10^6 pfu added) and the serial dilutions were plated and colonies were counted next day.

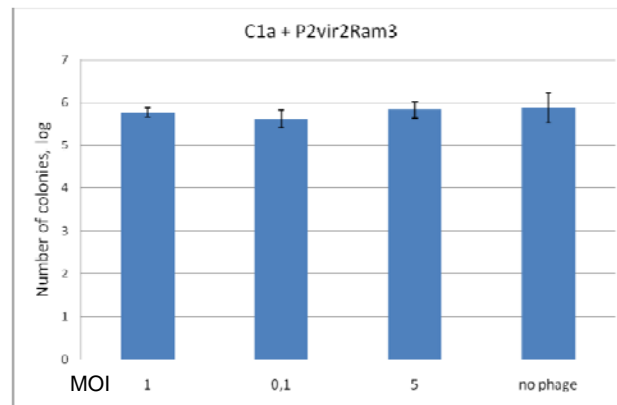


Figure 3.20: Plating efficiency of *E. coli* C1a cells when infected with P2vir1Ram3 bacteriophage at MOI 1, 0.1 and 5. n=3 (for method protocol: 2.2.1.2.2).

The number of *E. coli* C1a cells infected with P2vir1Ram3 at MOI 1, 0.1 and 5 was not significantly different from the number of uninfected cells (Figure 3.20), which suggests that C1a cells do not die upon infection with P2vir1Ram3. This result contradicts with results obtained with infection in liquid culture (Figure 3.18A-B) where *E. coli* C1a cells lysed upon infection with P2vir1Ram3. This means that accumulation of immature particles of P2vir1Ram3 bacteriophage in cells does not impair with the metabolism of infected cells, thus cells grow and reproduce relatively normal, however, when agitated these cells are prone to rapid lysis due to weakened cell wall caused by bacteriophage enzymes. At the same time, accumulation of defective bacteriophage particles in cells growing on agar medium has no influence on cell viability.

This result does not support the employment of P2vir1Ram3 bacteriophage in the selection of a protein with DNA uridine endonuclease activity. P2vir1Kam12 bacteriophage was the next candidate for this approach because of its ability to inhibit the cell growth without lysis as demonstrated by Zierman *et al.* (Figure 3.18C, Zierman *et al.*, 1994). Unfortunately, neither P2vir1Kam12 nor P2vir22Kam12 bacteriophages were available in the scientific community. Therefore, another approach for the selection of a protein with DNA uridine endonuclease activity was designed.

3.4 Attempted genetic selection based on heteroduplex DNA of phagemid pBluescriptII with uracil containing mismatch

This approach differs from above discussed strategies since it does not employ bacteriophages. Instead, ability of DNA uridine endonuclease to initiate repair of uracil containing mismatch is utilized. The principle underlying this approach is: a heteroduplex DNA with a mismatched uridine residue (U/T) introduced within *E. coli* lethal gene is generated. Thymine in this mismatch is a part of a stop codon, which is placed on purpose to truncate the lethal protein information, whereas uracil in complementary strand, if not repaired, will lead to restoration of the wild-type protein information when DNA replication proceeds. When cells carrying mutant *exoA* library will be transfected with this heteroduplex DNA, uracil-thymine mismatch within lethal gene will be repaired in cells with additional DNA uridine endonuclease activity, leading to expression of a truncated protein, which in turn enables the cell survival, and in all other cells with no DNA uracil repair lethal gene product will kill those, thus enabling the selection. *E. coli* host cells for this experiment must be devoid of both UDG and MutS that initiate BER and methyl-directed mismatch repair (MMR), respectively. For heteroduplex DNA construction pBluescript II SK (+) phagemid vector and *E. coli ccdB* gene, product of which is an inhibitor of DNA gyrase, were chosen. Figure 3.21 gives an overview to the use of heteroduplex DNA in selection.

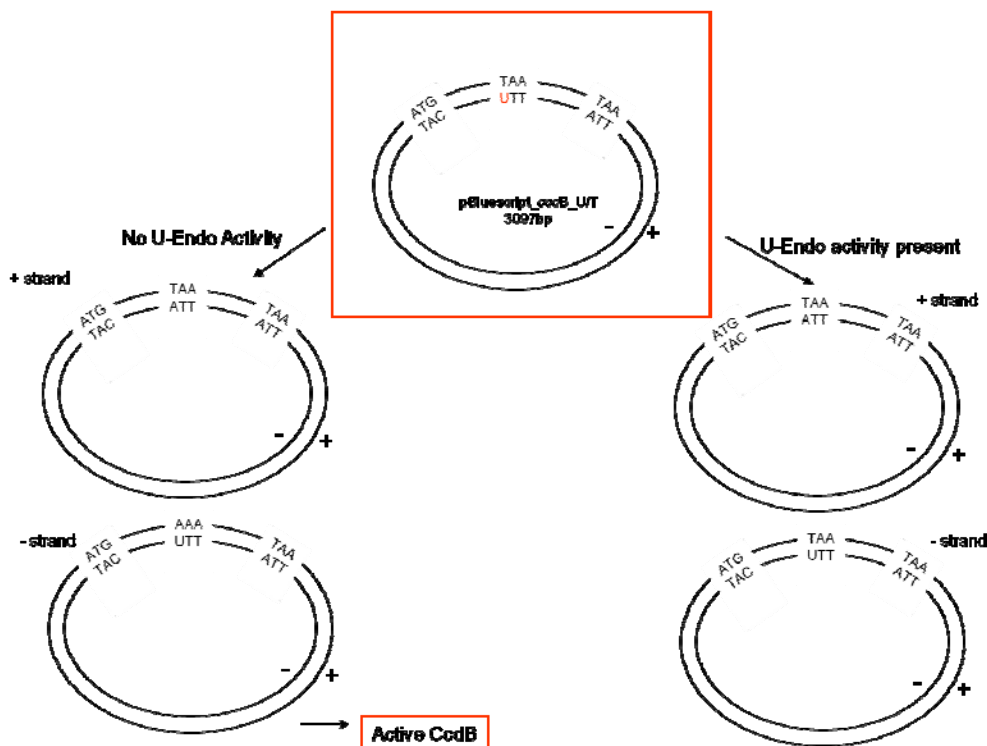


Figure 3.21: Schematic outline to the approach employing heteroduplex DNA. When *E. coli* Δung , $\Delta mutS$ cells are transformed with pBluescript_ *ccdB*_U/T construct there are 2 possible ways. (Left panel) If no DNA uridine endonuclease is present in the cell, U/T mismatch will not be repaired and after first round of replication information encoded on the –strand of pBluescript_ *ccdB*_U/T will lead to expression of active CcdB protein thus killing the host cell. (Right panel) If uridine DNA endonuclease is expressed in the cell U/T mismatch will be repaired and after first round of replication information encoded on both strands of pBluescript_ *ccdB*_U/T vector will lead to expression of truncated CcdB thus enabling the cell growth and reproduction

3.4.1 Construction of mutant gene library

Error-prone PCR for randomization of *exoA* and cloning of *exoA* library into pJET1.2 vector were performed as described before (Sections 3.2.2 and 3.2.4). Mutation frequencies, ratio of total mutation number to deletions and insertions, as well as number and mutation types were determined after sequencing of clones. No significant differences were observed from previous results of library generation (3.2.3) (sequences can be found in Appendix 7.2.3). For protein expression in *E. coli*, mutant *exoA* library was re-cloned into the expression vector pACYC177 (2.1.3.7) because of its compatibility with vectors containing ColE1 origin of replication. *SphI* restriction endonuclease site was introduced into the vector sequence by site-directed Quick-change[®] mutagenesis (2.2.2.2.4) to enable the cloning of randomised *exoA* with concomitant disruption of ampicillin resistance gene sequence.

3.4.2 Construction of heteroduplex DNA

Heteroduplex DNA containing base/base mismatches, ssDNA gaps or multibase loops have been extensively used for genetic analysis of DNA repair mechanisms *in vivo* (Kramer *et al.*, 1984, Shenoy *et al.*, 1987, Campbell *et al.*, 1989, Aprelikova and Jiricny, 1991). In this study, we used *E. coli* lethal gene *ccdB* to generate a heteroduplex DNA containing U/T mismatch for a selection of an enzyme capable of repairing this mismatch. Preparation of covalently closed circular heteroduplex DNA was intended to be done according to the scheme envisaged in Figure 3.22.

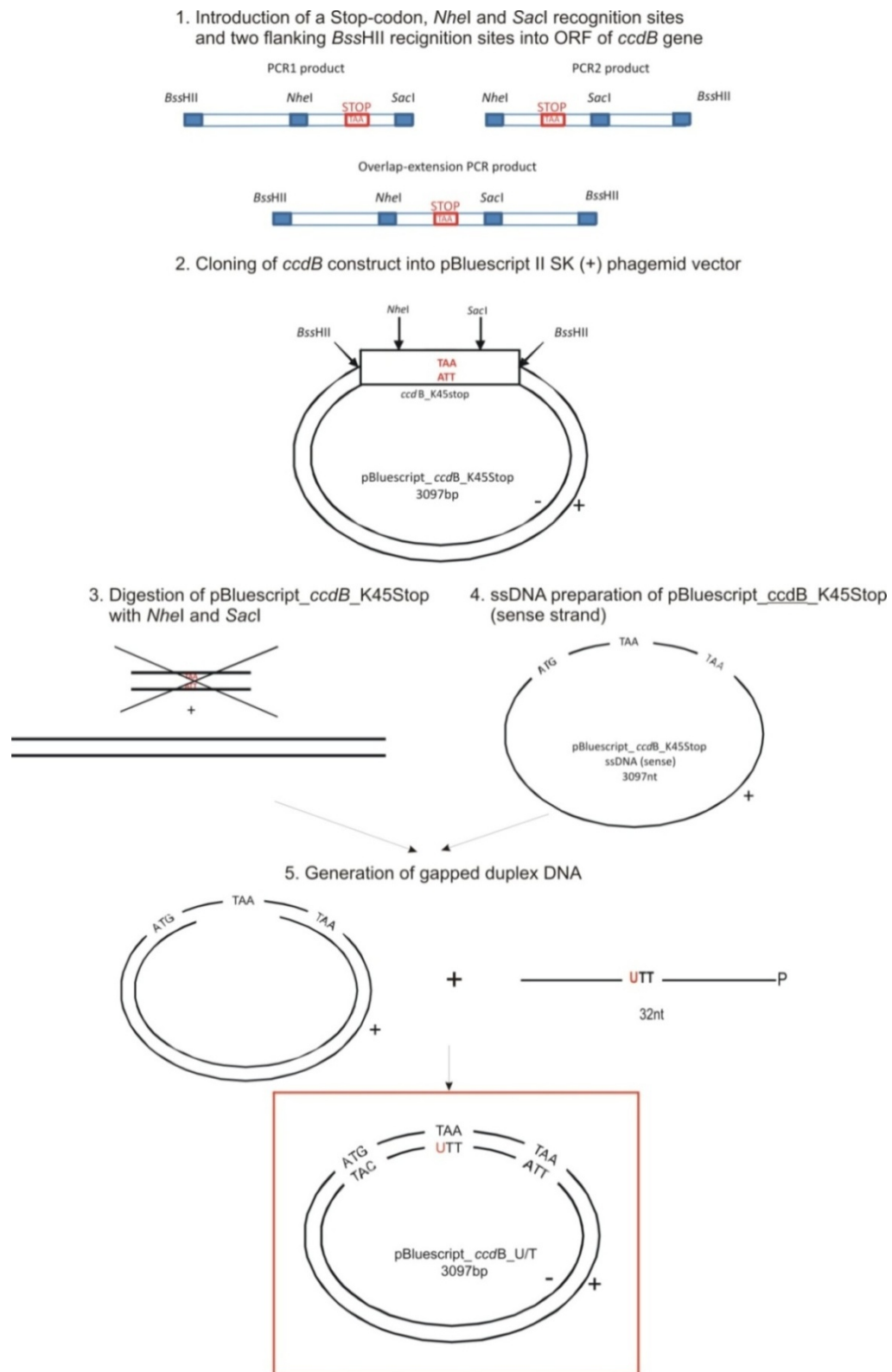


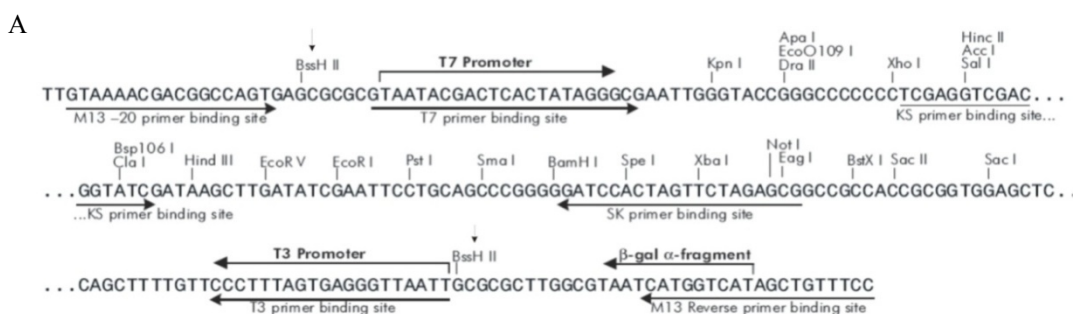
Figure 3.22: Schematic representation of heteroduplex DNA construction steps.

Site-directed mutagenesis by overlap extension using PCR (2.2.2.2.5) was employed to obtain *ccdB* gene with two restriction endonuclease sites and stop codon introduced within the gene sequence (Figure 3.22 (1)). *ccdB* is encoded by the F-plasmid of *E. coli*, therefore

E. coli NM522 (2.1.1.12) DNA was used as template for the amplification of *ccdB* gene. Overlap extension mutagenesis involved 2 mutagenic primers containing *NheI* and *SacI* restriction sites and the stop codon. Each primer was used in a separate PCR reaction with an outer flanking primer carrying *Bss*HIII restriction site. In this manner two halves of *ccdB* containing 62 bp long complementary to each other region were generated. Next, 2 PCR product were put together where they anneal in the 62 bp region of complementarity and prime off each other. After the final PCR on this template with 2 outer flanking primers containing *Bss*HIII restriction sites the full length *ccdB* with the stop codon, *NheI*, *SacI* and 2 flanking *Bss*HIII restriction sites was obtained. Stop codon (TAA) was introduced into *ccdB* by replacing the lysine 45 (K45) codon (AAA). Both *NheI* and *SacI* restriction sites were introduced into *ccdB* without affecting the amino acid sequence of CcdB protein. This construct is designated as *ccdB_K45Stop* henceforth.

As next, PCR product was inserted into the pJET1.2 cloning vector and the insert sequence was verified (for sequence see Appendix 7.3.5). Then, the *ccdB_K45Stop* construct re-cloned into the *Bss*HIII site of pBluescript II SK (+) vector (Figure 3.22 (2), for method refer to 2.1.3.8). pBluescript II SK (+) is a phagemid vector; the sense strand (ssDNA) of this vector can be rescued using the helper phage M13K07 (2.1.2.4). The sense strand of the vector is also the sense-strand of the β -galactosidase gene (*lacZ*). This feature makes this vector useful for the purpose of heteroduplex DNA construction. When *ccdB_K45Stop* is successfully cloned, CcdB protein will be fused with the N-terminal 8 amino acids of LacZ protein and the expression of fusion protein will be regulated under the control of *lac* promoter.

Cloning of *ccdB_K45Stop* into *Bss*HIII restriction sites of the pBluescript II SK (+) (Figure 3.23A), provides ligation of the insert in both directions. It was expected that approximately 50% of transformants will contain the vector with insert ligated in desired orientation that will enable expression of the inserted gene. However, none of the 24 clones that were sequenced, contained the insert in desired orientation (for sequences see Appendix 7.4.1) (Figure 3.23B).



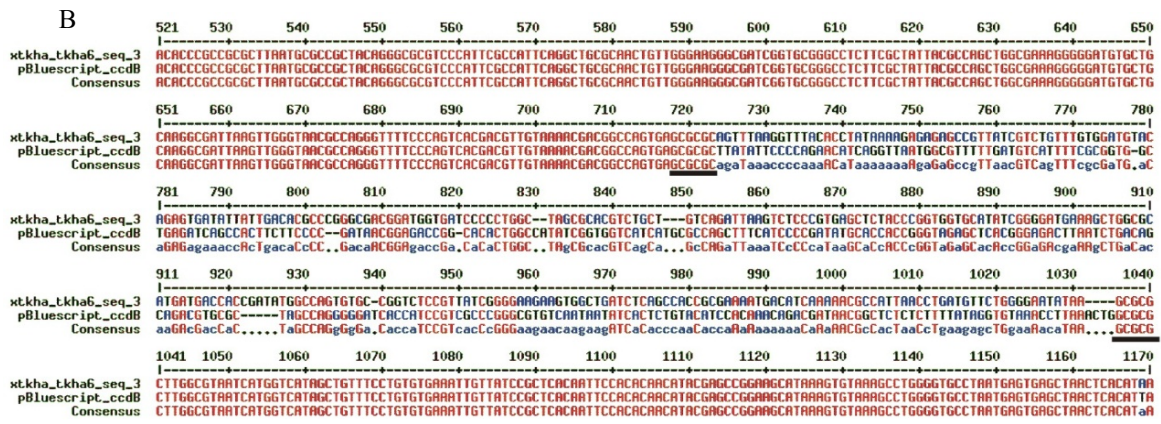


Figure 3.23: A: Multiple cloning site of pBluescript II SK (+) vector (adapted from pBluescript II Phagemid vectors; Instruction Manual, Stratagene, USA). 2 *Bss*HII sites are marked with arrows. **B:** Alignment of the obtained sequence to the expected sequence. *ccdB_K45Stop* is cloned in undesired orientation. 2 *Bss*HII sites are underlined. Sequence alignment was done with MultAlin online software (2.1.13).

In addition, the ligation mixture of *ccdB_K45Stop* and pBluescript II SK (+) was introduced into *E. coli* DH5 α and TOP10 strains (2.1.1.1) by transformation and colony-PCR (2.2.2.2.1) were performed. Several colony-PCRs also confirmed that all clones contained *ccdB_K4Stop* ligated in undesired orientation. One of these colony-PCRs is shown in Figure 3.24.

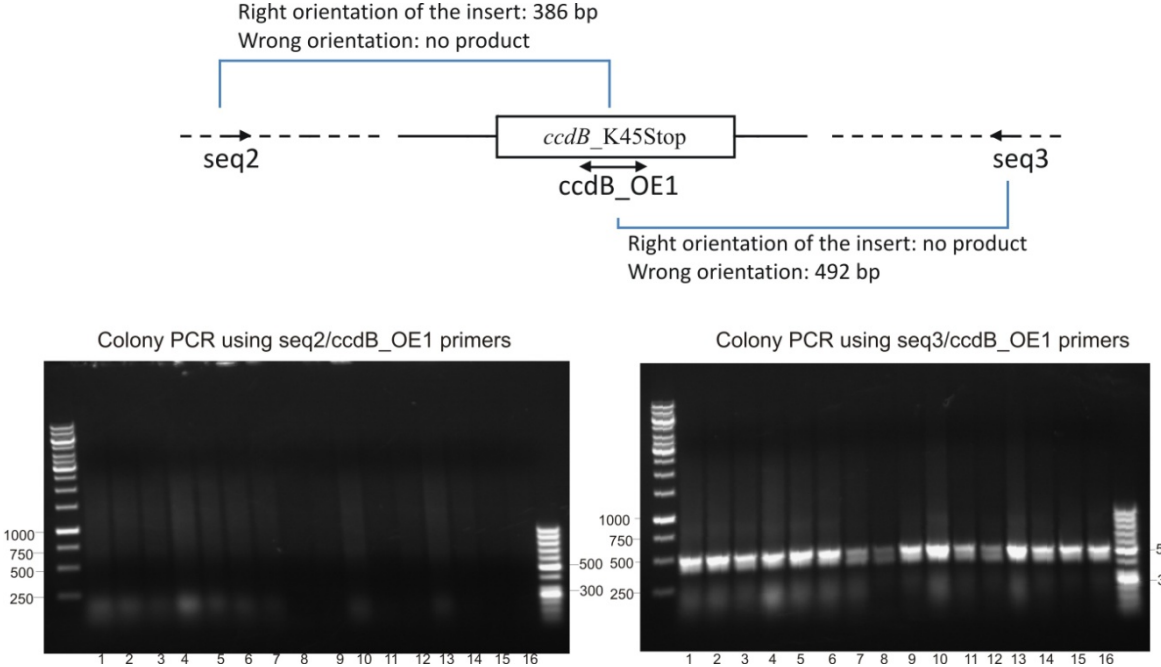


Figure 3.24: Colony PCR with *E. coli* colonies carrying *ccdB_K45Stop* ligated into pBluescript II SK (+) vector. Above is the schematic representation of primer combinations used for PCR and expected product sizes. 1-16: numbers given to colonies used for PCR. Colony-PCR was performed as described in section 2.2.2.2.1 and applied onto the agarose gel (2.2.2.4).

These results (Figure 3.21) suggest that the pBluescript II SK (+) with *ccdB_K45Stop* insert in the desired orientation expresses a short peptide that is possibly lethal for the cell

and only those clones that contain pBluescript II SK (+) with *ccdB_K45Stop* insert in wrong orientation survived. To verify this suggestion, *E. coli lacI^Q* strain TOP10F' (2.1.1.1.4) was transformed with *ccdB_K45Stop* and pBluescript II SK (+) after ligation. The *lacI^Q* mutation leads to continuously expressed repressor of the *lac* promoter causing inhibition of protein expression controlled under this promoter.

Colony-PCR with transformants revealed that 9 colonies, out of 16, contain the *ccdB_K45Stop* construct inserted in the desired orientation (Figure 3.25).

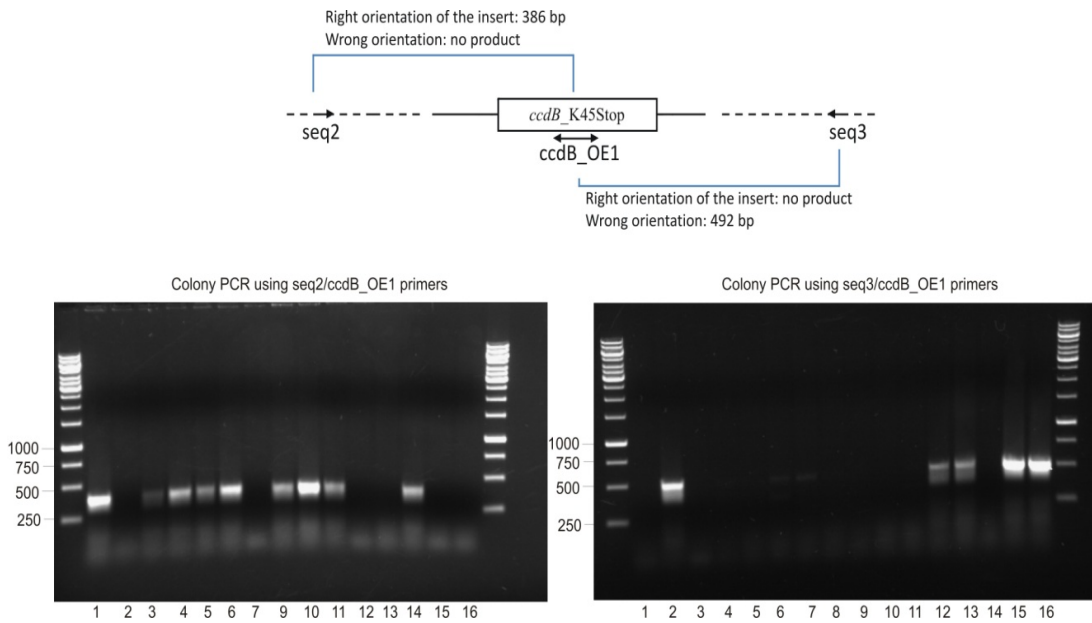


Figure 3.25: Colony PCR with *E. coli* TOP10F' colonies carrying *ccdB_K45Stop* ligated into pBluescript II SK (+) vector. Above is the schematic representation of primer combinations used for the PCR and explanation of product sizes. 1-16: numbers given to colonies used for the PCR. Colony-PCR was performed as described in section 2.2.2.2.1 and applied onto the agarose gel (2.2.2.4).

Sequencing of the clones that were positive in colony-PCR confirmed the right orientation of *ccdB_K45Stop* in pBluescript II SK (+) vector (Figure 3.23) (for sequences: Appendix 7.4.2).

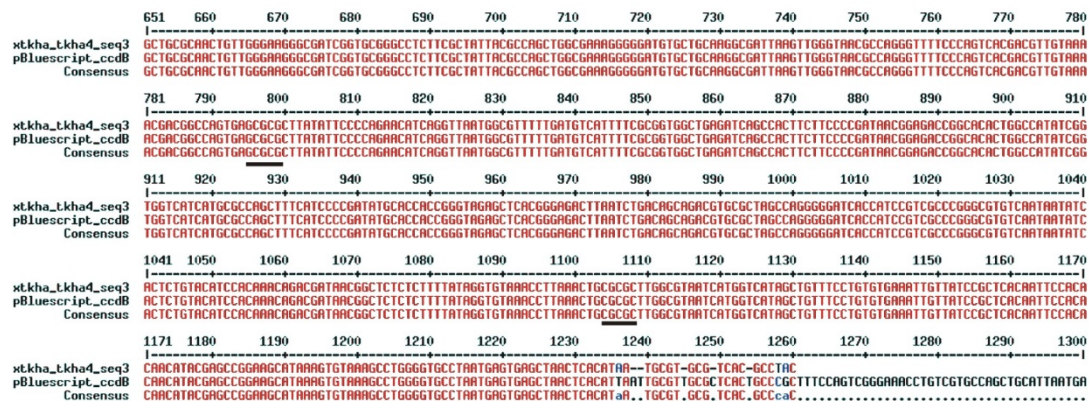


Figure 3.26: Alignment of the obtained sequence to the expected sequence. *ccdB_K45Stop* is cloned in desired orientation. 2 *Bss*HII sites are underlined. Sequence alignment was done with MultAlin online software (3.1.13).

Taken together these results imply that there is a negative selection in *E. coli* non-*lacI*^Q cells against the clones with desired orientation of the insert. Re-transformation of *E. coli* DH5 α and TOP10 cells (2.1.1.1) with the plasmid DNA obtained from *lacI*^Q strain did not yield in any colonies (Table 3.7). This confirmed previously obtained results that the presence of the vector containing *ccdB_K45Stop* in desired orientation is lethal for bacteria.

DH5 α	TOP10	TOP10 F'
0	0	1.3*10 ⁶

Table 3.7: Re-transformation efficiency of *E. coli* strains (number of transformants per 1 μ g DNA). pBluescript II SK (+) vector with *ccdB_K45Stop* cloned in desired orientation isolated from the *E. coli* TOP10F' cells was used for re-transformation.

Native CcdB is an 11.7 kDa protein (101 amino acids long) which is a part of *ccd* (*control of cell death*) system encoded by F plasmid in *E. coli*. *Ccd* system is one of the three systems that guarantee preferential growth of F-plasmid carrying cells in a bacterial population by killing newborn bacteria that have not inherited a copy of F-plasmid at cell division (post-segregational killing) (Afif *et al.*, 2001). If the action of CcdB is not prevented by CcdA protein, another part of *ccd* system, it traps and poisons the DNA-gyrase cleavable complex (Bernard *et al.*, 1993) by forming tight non-covalent complex and thus blocking the passage of *E. coli* and bacteriophage T7 polymerases (Chritchlow *et al.*, 1997). This suggests that CcdB converts gyrase into a DNA poison and kills bacteria by causing DNA lesions leading to double-strand breaks in the DNA (Loris *et al.*, 1999). Numerous publications describe that only the C-terminal 3 amino acids of CcdB (W99, G100, I101) are responsible for the “killer function” of this protein (Bahassi *et al.*, 1995; Bahassi *et al.*, 1999; Loris *et al.*, 1999; Critchlow *et al.*, 1997). More recently it was shown that the tryptophan 99 (W99) makes the actual contact with arginine 462 (R462) of GyrA protein (Dao-Thi *et al.*, 2005).

MTMITPSAQFKVYTYKRESRYRLFVDVQSDIIDTPGRRMVIPLASARLLSD

Figure 3.27: Amino acid sequence encoded by *ccdB_K45Stop*. N-Terminal 8 amino acids of LacZ are shown in red. CcdB_K45Stop polypeptide has a theoretical pI of 9.81 (calculated on ProtParam software, 2.1.13), with 8 positively charged (in green) and 5 negatively charged (in blue) amino acids.

Bahassi *et al.* (1995) showed that the expression of the first 20 or 60 amino acids of CcdB (CcdB_Q21Amber mutant or CcdB_W61-Amber mutant, respectively) have no cytotoxic

effect on *E. coli* (Bahassi *et al.*, 1995). The question, however, why 44 N-terminal amino acids of CcdB expressed in *E. coli* are being toxic remains open.

It is known that CcdB in complex with CcdA participates in autoregulation of *ccd* operon by binding to a DNA segment in the promoter region and CcdB may contain a partial DNA-binding motif (De Feyter *et al.*, 1989). The secondary structure and surface charge distribution of CcdB_K45Stop polypeptide possibly provide it with the increased DNA binding ability. Thus, unspecific but very tight binding of CcdB_K45Stop to the DNA may result in blockage of replication or transcription processes leading to cell death. Comprehensive elucidation of CcdB_K45Stop toxicity effect on *E. coli* cells requires further investigations that are beyond the purpose of this study.

Because of toxicity of the truncated CcdB protein, its use as selection tool for ExoA with acquired DNA uridine endonuclease activity was disapproved. On the other hand, this selection approach may work if other *E. coli* lethal genes will be engaged.

3.5 ExoA triple mutant and selection of its stable variant by genetic complementation

Structural basis of uridine recognition mechanism of Mth212 was not clarified when this project started. The directed evolution is a powerful tool for the modification of enzyme activities with no requirement of comprehensive understanding of structure-function relationship and as such this method was chosen to study uridine recognition by providing ExoA with DNA uridine endonuclease activity. Unfortunately, the use of this method met little success due to inability to select the particular protein from the library (Sections 3.2 - 3.4). Therefore, it was attempted to provide ExoA with the DNA uridine endonuclease activity by means of directed mutagenesis.

Rational design to obtain DNA uridine endonuclease activity was based on recent results of crystallographic studies of Mth212 (Lakomek, 2009; Lakomek *et al.*, 2010) and Mth212-mutants (Smolorz, 2009). These studies proposed a model of potential uridine recognition and/or discrimination mechanism where an additional pocket close to active centre is responsible for uridine recognition. Amino acid residues asparagine-114, glycine-115, lysine-116, lysine-125, asparagine-153, serine-171 and glycine-172 of Mth212 build the surface of this additional pocket (Figure 3.28).

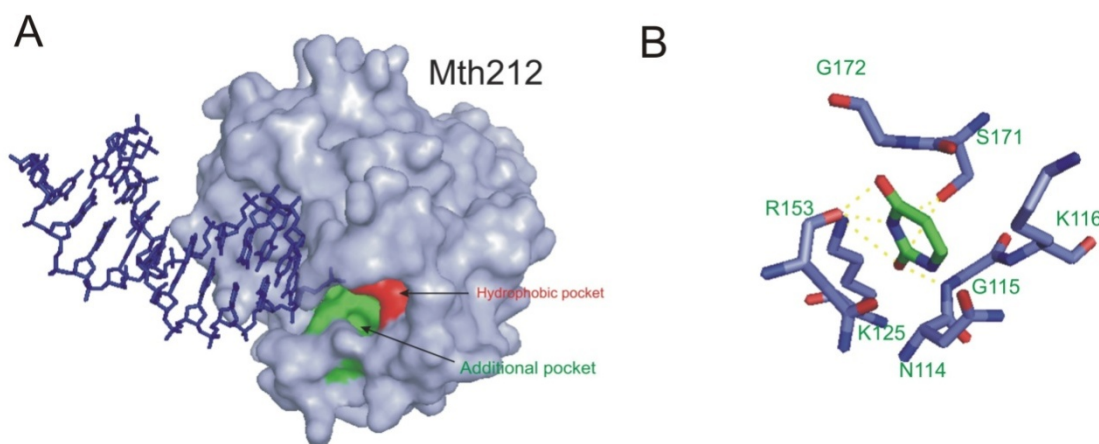


Figure 3.28: **A:** A *surface* representation of Mth212 molecule (protein A, 3GA6) with hydrophobic pocket outlined with W205, W219 and L221 residues (colored in red) and additional pocket outlined with N114, G115, K116, K125, N153, S171 and G172 residues (colored in green). **B:** A close-up view of Mth212 amino acids constituting additional pocket and their possible hydrogen bondings with uracil base. Pictures were generated using PyMol software and PDB-file 3GA6 (Lakomek *et al.*, 2010).

In order to determine ExoA amino acid residues homologous to amino acid residues that constitute the additional pocket of Mth212 multiple alignment of ExoA with other exonuclease III homologs including Mth212 was carried out and respective amino acids were then engrafted into Table 3.8.

Mth212	Mma3148	Af_ExoIII	ExoIII	ExoA	APE1
N114	N115	Q108	Q112	N109	N174
G115	G116	G109	G113	S110	A175
K116	K117	F110	E114	R111	G176
K125	K126	K120	K125	R120	R185
N153	N154	N148	N153	N147	N212
S171	S172	C167	C177	A165	A230
G172	G173	-	S178	G166	G231

Table 3.8: Amino acids of exonuclease III homologs (Mma3148 from *M. mazei*, Af_ExoIII from *A. fulgidus*, ExoIII from *E. coli*, APE1 from *H. sapiens* and ExoA from *B. subtilis*) homologous to amino acid residues constituting additional pocket of Mth212 from *M. thermoautotrophicus*. Residues that are conserved in respect of Mth212 residues are highlighted in blue; ExoA residues that were mutated are in red. Multiple sequence alignment was performed with CLUSTAL W2.0.12 software (2.1.13).

Table 3.8 shows that ExoA differs from Mth212 in respect of uridine recognition pocket constituting amino acids in residues serine-110, arginine-111 and arginine-120 (designated as S110, R111 and R120 henceforth) and alanine-165. Directed mutagenesis of S110, R111 and R120 residues of ExoA into G110, K111 and K120 respectively was found rational. ExoA alanine-165 was not targeted for mutagenesis since Mth212/S171T and Mth212/S171A mutant studies revealed relatively low contribution of this amino acid residue to uridine recognition (Smolorz, 2009).

3.5.1 Generation and purification of the ExoA S110G_R111K_R120K triple and R120K single mutants

In order to test whether S110G, R111K, R120K amino acid exchanges in ExoA will provide it with DNA uridine endonuclease activity *exoA_S110G_R111K_R120K* mutant (designated as ExoA triple mutant henceforth) was constructed by Site-directed mutagenesis by overlap extension using PCR (2.2.2.2.5) and the construct was then cloned into pASK-08 expression vector (2.1.3.5).

Lysine-125 in Mth212 which corresponds to arginine-120 in ExoA was shown to have important role in uracil recognition, explicitly taking part in discrimination against cytosine (S. Smolorz, 2009). To test whether exchanging arginine-120 into lysine can alone result in DNA uridine endonuclease activity R120K single mutant of ExoA was generated by site-directed Quick-change[®] mutagenesis (2.2.2.2.4). This mutation as well as all other site-specific mutations was verified by DNA sequence analysis (Appendix 7.5.1). For protein production WT *exoA*, R120K single and triple mutants were cloned as C-terminal 6xHis-tagged proteins into pASK-08 vector and introduced into *E. coli* NM522 Δ *ung* (2.1.1.1) cells.

As shown in Figure 3.29, wild-type ExoA (30 kDa) was detected in the supernatant of the crude extract and relative small amount of this protein was in the pellet. Compared to this, a large amount of R120K single mutant was detected in the pellet and only a small amount of this protein remained in the supernatant indicating that this protein can be isolated and purified from a large scaled culture. In contrast, the triple mutant was only detected in the pellet containing insoluble proteins, but not in the supernatant, or the amount of this protein in the supernatant is too small to be detected on the SDS-PAGE (2.2.3.1).

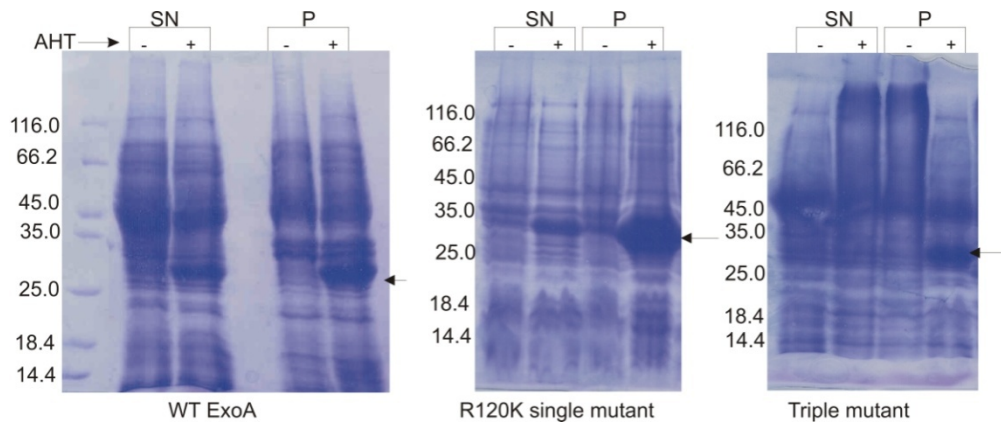


Figure 3.29: SDS-PAGE analysis of protein test expressions. Crude cell extracts of *E. coli* NM522 Δ ung overexpressing wild-type ExoA, ExoA R120K and ExoA triple mutant on 15% SDS-PAGE. SN: supernatant, P: pellet; +/- with or without induction with anhydrotetracycline (AHT); ExoA protein band (30kDa) is indicated with arrow. Crude cell extracts were isolated as described in section 2.2.3.3.

It is believed that stabilizing mutations tend to deactivate, whereas activating mutations tend to destabilize (Arnold, 1998). It can be suggested that the mutations introduced into ExoA sequence contributed to come extent to catalytic activity of enzymes, however enhanced activity came along with less stability and/or low solubility.

As next, it was tried to improve the solubility of the triple mutant during protein expression. Occasionally, induction of protein expression for a long time can result in misfolding and subsequent aggregation into inclusion bodies. Therefore, duration of the induction time was decreased. This attempt did not improve solubility of the triple mutant in a small-scale expression experiment, even after 4 hours of induction the protein was not present in the supernatant (Figure 3.30).

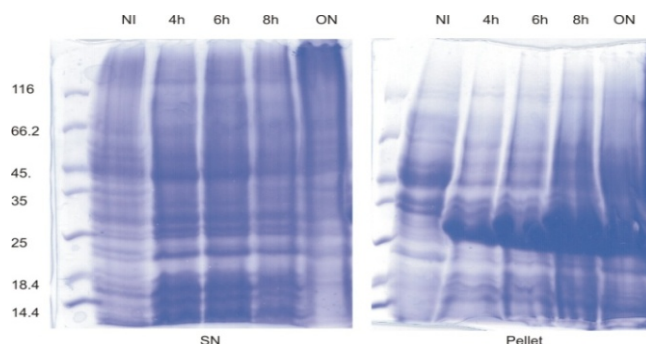


Figure 3.30: 15% SDS-PAGE analysis of *E. coli* NM522 Δ ung cell extracts overexpressing ExoA triple mutant. SN: supernatant; NI-not induced; 4h, 6h, 8h: 4, 6, 8 hours of induction with AHT, respectively; ON-overnight incubation with inducer. Crude cell extracts were done as described in section 2.2.3.3.

With the hope that the supernatant contains a small amount of the triple mutant that cannot be resolved by Coomassie stain, it was tried to isolate this protein from the supernatant of cells in a large-scale purification (2.1.1.13).

ExoA triple mutant protein extracts was made as described in 2.2.3.5 and the protein was purified using IMAC (2.2.3.6; Figure 3.31), followed by Heparin affinity chromatography (2.2.3.7; Figure 3.32). Purification of wild-type ExoA and R120K single mutant was performed by same way. At the end, purified proteins were concentrated to a final volume of 500 μ l and analyzed by SDS-PAGE (Figure 3.33).

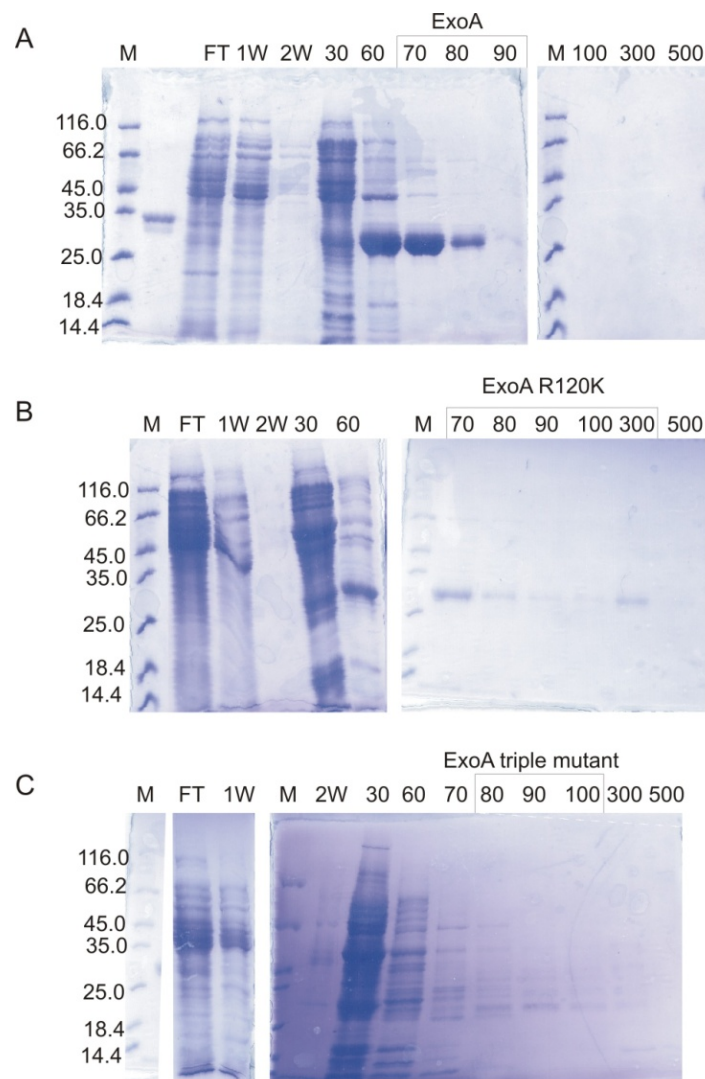


Figure 3.31: 15% SDS-PAGE analysis of IMAC fractions. **A:** WT ExoA, **B:** ExoA R120K single mutant, **C:** ExoA triple mutant. IMAC was carried out using 5 ml columns packed with Chelating Sepharose™ Fast Flow as described in section 2.2.3.6.

M: Protein Molecular Weight Marker (2.1.5.2); FT: Flow-through fraction. 1W and 2W: Column wash fractions. 30-500: Protein fractions eluted with 30-500 mM imidazole in IMAC wash buffer (2.1.9). Brackets indicate fractions pooled for subsequent purification.

As expected, a large amount of wild-type ExoA protein (Figure 3.28A) and a relative small

amount of R120K single mutant (Figure 3.31B) were obtained after purification by IMAC. IMAC elution fractions of ExoA triple mutant (Figure 3.31C) contained several proteins, including an almost invisible protein band of expected molecular weight (~30 kDa) that could be concentrated by next step of purification. Therefore, either of the IMAC fractions that contain partly purified proteins, WT ExoA, R120K single mutant, and the triple mutant were subjected to a Heparin affinity chromatography.

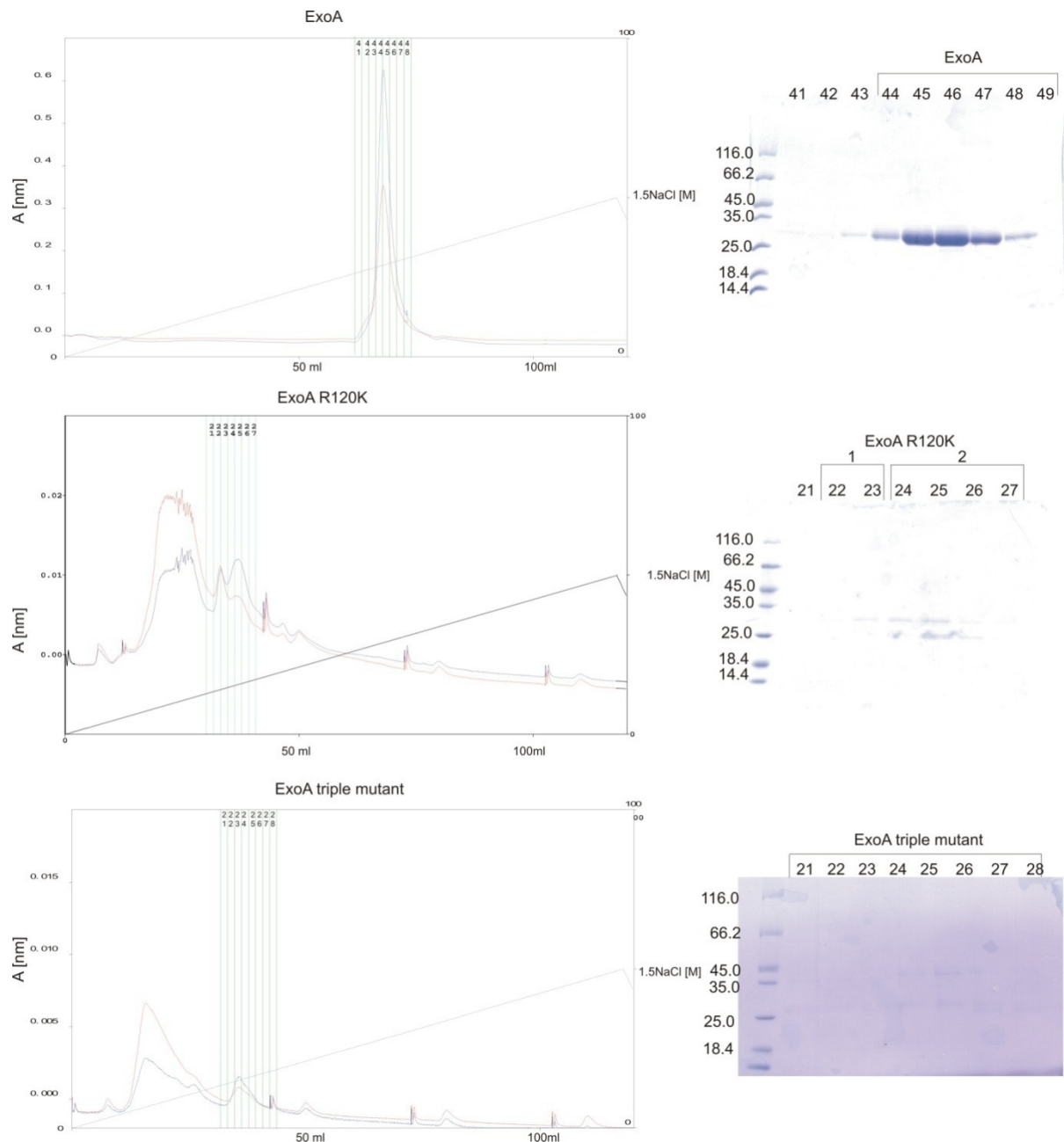


Figure 3.32: Elution profiles of ExoA, ExoA R120K single and ExoA triple mutants purification by Heparin affinity chromatography are shown on the left. Heparin chromatography was performed on BioCAD™ Workstation (Applied Biosystems) using POROS® HS 20 μm column (10 mm x 100 mm, 7.89 ml) at a 4 ml/min flow rate. Left ordinate: absorption at 260 nm (red) and 280 nm (blue); Right ordinate: concentration of NaCl in mol [M]; Abscissa: elution volume in ml. Green lines and numbers above the chromatogram indicate fractions that were analysed by 15% SDS-PAGE shown on the right. Brackets above the gel indicate fractions pooled and concentrated (Figure 3.33).

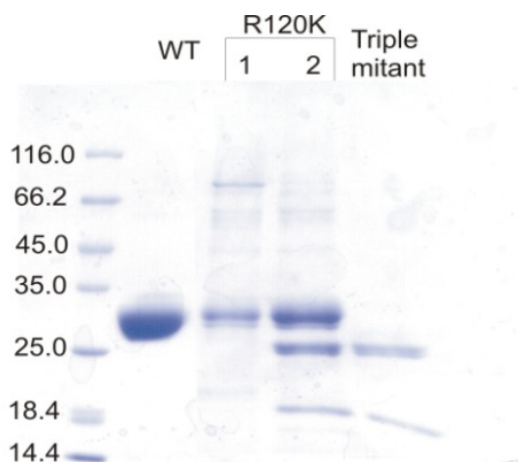


Figure 3.33: 15% SDS-PAGE analysis of purified and concentrated proteins purification. Wild-type ExoA (WT), 2 fractions of ExoA R120K single mutant (R120K) and ExoA triple mutant were concentrated to final volume of 500 μ l. 5 μ l of wild-type ExoA, 20 μ l of each single and triple mutant solutions is applied onto gel.

At the end, the fractions of Heparin affinity chromatography representing the main peak of elution profile (Figure 3.32) were concentrated and analyzed by SDS-PAGE. As shown in Figure 3.33, highly purified WT ExoA, two protein solutions of partly purified R120K single mutant, and a triple mutant solution containing a protein band of 25 kDa and 20 kDa that differed from the expected size were obtained. Interestingly, one the two protein solutions of R120K single mutant (2. fraction of R120K in Figure 3.30) contains same sized protein bands indicating that they may be resulted from N-terminal degradation of ExoA mutants that possibly did not alter the activity of the mutants.

3.5.2 Activity assays with ExoA variants

In order to study the effect of R120K and S110G_R111K_R120K substitutions on the enzymatic activity of ExoA single mutant and ExoA triple mutant, purified protein solutions (Figure 3.33) were analysed by endonuclease assay. The assay was performed as described in 2.2.2.9 using 40-mer double-stranded DNA oligonucleotide substrates containing an AP/G (where AP is an abasic site analogue), U/G, U/C and U/T mismatches as well as U/A natural base pair at position 24. Reaction products obtained during endonuclease assays were analysed under denaturing conditions by 11% A.L.F.-polyacrylamid gel electrophoresis (A.L.F.-PAGE, see section 2.2.2.5) (Figure 3.34C-F).

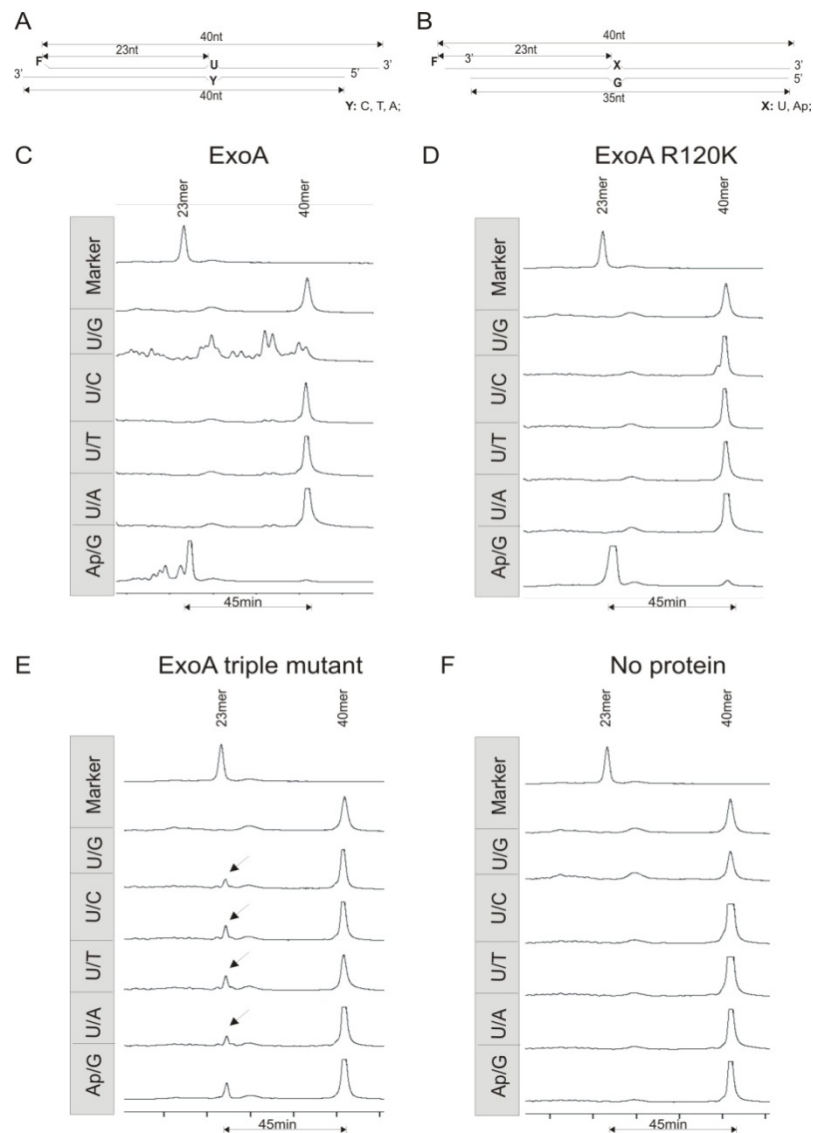


Figure 3.34: A.L.F.-PAGE of endonuclease assays with ExoA, ExoA R120K single and ExoA triple mutants. **A-B:** Schematic representation of substrates used in the assay. Ap/G and U/G containing substrates are blunt-ended, whereas U/C, U/T and U/A containing substrates have 5 nucleotides long 3' overhang. **C-F:** A.L.F.-PAGE analysis of endonuclease assays with ExoA (**C**), ExoA R120K single mutant (**D**) and ExoA triple mutant (**E**). **D:** Endonuclease assay in absence of protein. 0.24pmol of substrate was incubated with purified protein (Figure 3.33, amount of enzyme used for assay: 0.24 pmol of ExoA, 1 μ l of R120K and 5 μ l of triple mutant) for 15 min at 37°C in 50 μ l of endonuclease buffer (2.1.9).

Wild-type ExoA showed strong AP-endonuclease (with Ap/G substrate) and 3'-5' exonuclease (with blunt-ended Ap/G and U/G substrates) activities. No 23-mer product was observed with uracil containing substrates (Figure 3.34C). This result is in agreement with results of ExoA activity assays made in the beginning of present study (Sections 3.1.1 and 3.1.2). ExoA R120K single mutant exhibited AP-endonuclease activity similar to wild type ExoA, however, its 3'-5' exonuclease activity was severely decreased. No 23-mer product was observed with uracil containing substrates as well (Figure 3.34D).

Activity assay with ExoA triple mutant revealed 23-mer product with all 4 uracil containing substrates (indicated with arrows on Figure 3.34E). Processing of uracil in all 4

substrates was of similar rate and was comparable with the processing of AP-site analog in Ap/G substrate. Substrate containing hypoxanthine mispaired with guanine was not processed by ExoA triple mutant (data not shown).

This asks the question whether this uracil specific activity can be assigned to ExoA triple mutant. On the SDS-PAGE (Figure 3.33) of purified ExoA triple mutant protein solution showed 2 protein bands of approximately 20 and 25 kDa, but not a band of the expected size (30kDa). The origin of these 2 proteins is unclear. Whether these 2 proteins were responsible for the uracil specific activity is equivocal as well, since ExoA R120K single mutant protein solution also showed the presence of these 2 bands in addition to the 30kDa ExoA band. To test if these 2 protein bands may be variants of ExoA which underwent N-terminal processing, Western Blot analysis (2.2.3.2) was done.

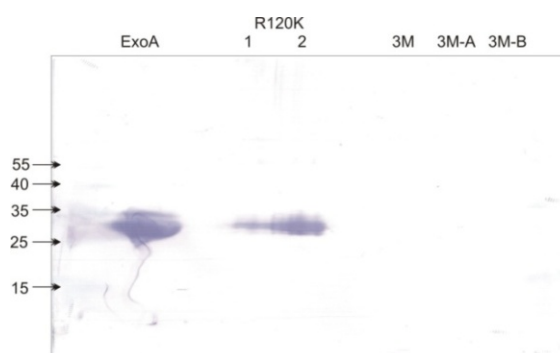


Figure 3.35: Western Blot analysis with ExoA, ExoA R120K single and ExoA triple mutants. All ExoA variants carry C-terminal 6xHis-tag; antibodies used for Western Blot were Penta-His antibody and anti-mouse AP-conjugated IgG. 3M, 3M-A, 3M-B: different preparations of ExoA triple mutant. 2 μ l of wild-type ExoA and 20 μ l of all other protein solutions were loaded onto gel. PageRuler™ Prestained Protein Ladder (2.1.5.2) was used as protein molecular weight standard.

The 20 and 25 kDa protein bands were not detectable in both ExoA single and triple mutant solutions by Western blot (Figure 3.35), indicating that probably non of these two bands originate from ExoA or that ExoA mutant was degraded from the C-terminus containing the 6xHis-tag.

3.5.3 Attempts to optimize production of ExoA triple mutant protein

To improve the yield of ExoA triple mutant experimental conditions were modified and tested. (1) Incubating *E. coli* cells during protein overexpression at low temperature can reduce the rate of protein synthesis thus giving the cells more time for proper folding of proteins. (2) Decreasing incubation time after induction can reduce protein loss due to degradation by proteases. (3) Addition of protease inhibitors can prevent degradation of proteins thereby improving the yield of overexpressed protein. (4) Heat shock of a cell

culture prior to induction can increase expression of chaperones that is needed for proper folding of protein molecules (Chen *et al.*, 2002).

Unfortunately, all above mentioned modifications did not improve the yield of ExoA triple mutant. As illustrated in Figure 3.36, neither decrease of incubation temperature to 25°C (A) nor heat shock of cells at 42°C prior to induction of protein expression (B) had any effect on the yield of the triple mutant as a soluble protein. Effect of other conditions on protein expression are not presented here, as they exhibited similar pattern as in Figures 3.24, 3.25, namely no ExoA triple mutant appearance in the supernatant of cell extracts.

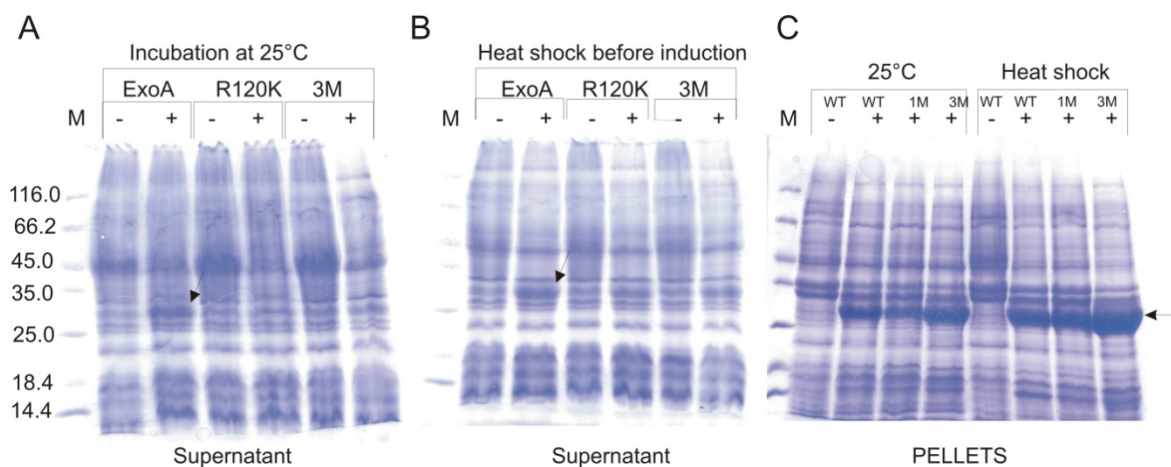


Figure 3.36: Effect of low incubation temperature (A) and heat shock prior to induction (B) on the yield of ExoA triple mutant. Crude cell extracts of *E. coli* NM522 Δ ung overexpressing ExoA (WT), ExoA R120K and ExoA triple mutant (3M) were analyzed by 15% SDS-PAGE. M: Protein Molecular Weight Marker; +/-: with or without induction with anhydrotetracycline (AHT); ExoA protein band (30kDa) is indicated with an arrow. Crude cell extracts were done as described in section 2.2.3.3.

3.5.4 ExoA quadruple (S110G_R111K_D145N_R120K) mutant production, purification and activity assays

ExoA triple mutant protein solution exhibited uracil specific activity. In order to assign this activity to ExoA triple mutant and exclude the possibility of contamination with *E. coli* enzymes an inactive variant of ExoA triple mutant (ExoA_S110G_R111K_R120K_D145N, designated as quadruple mutant henceforth) can be produced under the same conditions as ExoA triple mutant (Section 3.5.1). If uracil specific activity is abolished in the protein solution of ExoA quadruple mutant, it will support the proposition that ExoA triple mutant has acquired DNA uridine endonuclease activity.

Conserved amino acid residues aspartate-210 in APE1 and aspartate-151 in Mth212 are known to be essential residues for the catalytic function of these enzymes (Rothwell *et al.*,

2000; Georg *et al.*, 2006). Substitution of this aspartate into asparagine leads to the loss of all catalytic activities in these proteins. Amino acid sequence alignment of human APE1, Mth212 and ExoA (Figure 3.1, Section 3.1.1) revealed aspartate-145 in ExoA to be the equivalent residue.

The replacement of aspartate at 145 by asparagines (D145N), an inactivating mutation, was introduced into *exoA_S110G_R111K_R120K* by site-directed Quick-change[®] mutagenesis (2.2.2.2.4) and the presence of mutation was verified by DNA sequence analysis (for sequence Appendix 7.5.2). ExoA quadruple mutant protein was produced under same conditions as that used for the triple mutant (Section 3.5.1). Figure 3.37 summarizes the purification steps of ExoA quadruple mutant.

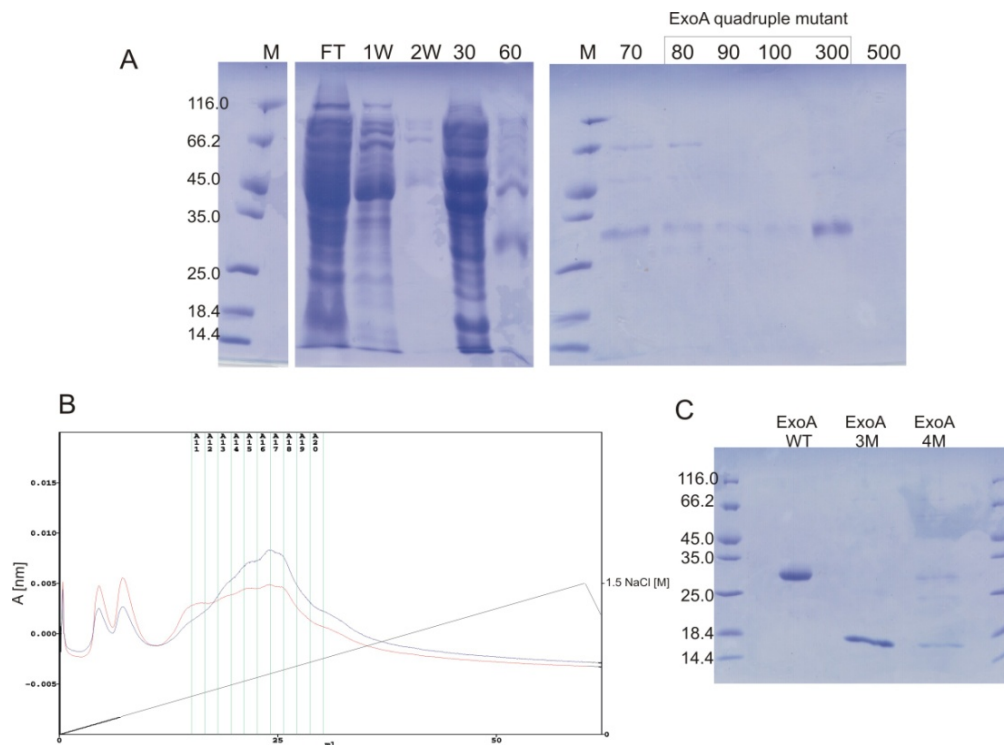


Figure 3.37: Purification of ExoA quadruple mutant. **A:** 15% SDS-PAGE of IMAC fractions. M: Molecular weight marker, FT: Flow-through fraction. 1W and 2W: Column wash fractions. 30-500: Protein fractions eluted with 30-500 mM imidazole in wash buffer (2.1.9). Brackets indicate fractions pooled for subsequent purification **B:** Elution profile of the ExoA quadruple mutant purification by Heparin affinity chromatography. Left ordinate: absorption at 260nm (red) and 280 nm (blue); right ordinate: concentration of NaCl in mol [M]; abscissa: elution volume in ml. Numbers above the chromatogram indicate fractions that were pooled and concentrated to final volume of 350 μ l. **C:** 15% SDS-PAGE of purified wild type ExoA, ExoA triple mutant (3M) and ExoA quadruple mutant (4M).

As shown on Figure 3.37C, D145N mutation had modest influence on the yield of the protein as faint band of 30kDa size was present on SDS-PAGE. This may be a result of a subtle stabilization of the protein structure thus making it more soluble in comparison to ExoA triple mutant.

Endonuclease activity assays (2.2.3.10) were performed to test the ExoA quadruple mutant

protein solution for activity against uracil in DNA (Figure 3.38).

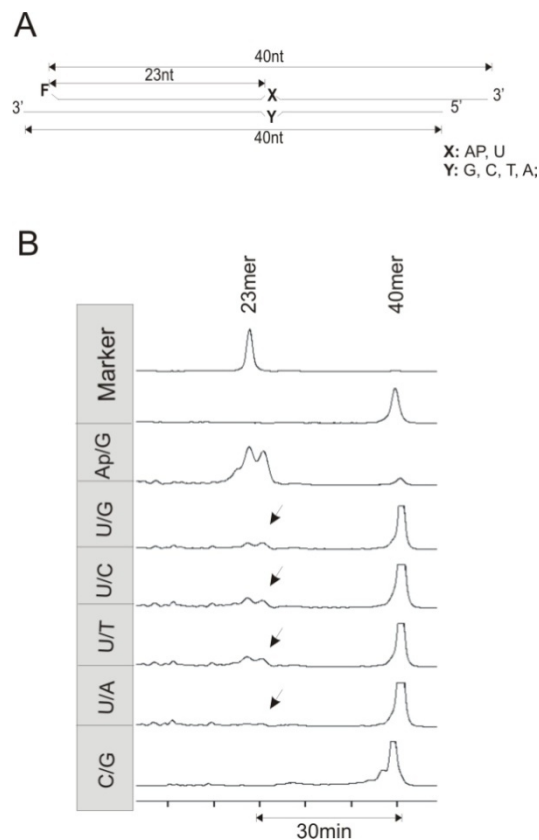


Figure 3.38: A.L.F.-PAGE of endonuclease assays with ExoA quadruple mutant. **A:** Schematic representation of substrate used in the assay. **B:** A.L.F.-PAGE analysis of endonuclease assays quadruple mutant. 0.24pmol of substrate was incubated with 2.5 μ l of protein solution (Figure 3.37C) for 20 min at 37°C in 50 μ l of endonuclease buffer (2.1.9).

A.L.F.-PAGE analysis showed the presence of 23-mer product peak with ExoA quadruple mutant protein solution incubated with uracil containing substrates (indicated with arrows on Figure 3.38). In addition to the 23-mer product, a 22-mer product and series of shorter products were observed which can be considered as the product of 3'-5' exonucleolytic degradation of the main 23-mer product. Significantly large product peak with AP/G substrate indicates the presence of an enzyme with AP-endonuclease activity in the protein solution. Since D145N mutation must have abolished all catalytic activities of ExoA, this result suggests possible contamination with an AP-endonuclease of *E. coli* and its notably strong activity excludes the possibility of spontaneous revertants of ExoA.

Taken together these results suggest that the uracil specific activity detected in ExoA triple mutant protein solution may originate from contamination with *E. coli* enzymes: uracil-DNA glycosylase other than UNG (uracil N-glycosylase, *E. coli* Family 1 UDG) and AP-endonuclease. However, it does not inevitably imply that ExoA triple mutant does not exhibit DNA uridine endonuclease activity.

3.5.5 Design of selection procedure of a stable variant of ExoA triple mutant

The assumption is that ExoA has acquired DNA uridine endonuclease activity due to S110G, R111K, and R120K mutations. However, this activity of ExoA cannot be demonstrated, because these mutations concurrently contributed to conformational destabilization of the protein leading to its aggregation in inclusion bodies.

The goal is to improve conformational stability of ExoA triple mutant through introduction of additional mutations and thus obtain pure protein to ascertain whether ExoA triple mutant exhibits DNA uridine endonuclease activity. Library of randomized ExoA triple mutant variants and a selection approach to identify the stable protein are required.

The idea for genetic selection of a stable ExoA triple mutant was based on increased sensitivity of *E. coli* $\Delta xthA$ cells to Mitomycin C than wild-type cells (Cunningham *et al.*, 1986). Overexpression of an AP-endonuclease, Mma3148 from *M. mazei* in particular, in those cells contributes to the resistance to this antibioticum (S. Ber, 2009). Thus, ExoA triple mutant variants that have acquired mutations that compensate the destabilizing effect of the three mutations can be selected by growing on Mytomycin C. Expression of a stable variant of ExoA triple mutant in *E. coli* $\Delta xthA$ cell will lead to the cell growth on Mitomycin C, whereas other cells do not grow. This approach rests on an assumption that the three mutations did not affect AP-endonuclease activity of ExoA.

A critical prerequisite to this approach is an evidence that overexpression of wild-type ExoA leads to the resistance of *E. coli* $\Delta xthA$ cells to Mitomycin C. It is known that overexpression of the *E. coli* exonuclease III homolog, XthA, in $\Delta xthA$ cells is toxic due to unknown reasons. It is possible that overexpressed XthA binds unspecificly to DNA leading to replication / transcription arrest and consequently to cessation of cell growth (Ber, 2009). Therefore, it must be ensured that ExoA variants can be overexpressed in $\Delta xthA$ cells.

3.5.6 *E. coli* $\Delta xthA$ strain and cytotoxicity of overproduced proteins

To test the cytotoxic effect of overexpressed ExoA, ExoA triple mutant, ExoA quadruple mutant or Mth212, corresponding genes were inserted into pASK-08 vector and introduced into *E. coli* BW25113 $\Delta xthA$ (2.1.1.1) by transformation and transformants were plated in the presence or absence of anhydrotetracycline (AHT) inducer.

pASK_08		pASK_exoA		pASK_exoA_D145N		pASK_exoA_3M		pASK_exoA_4M		pASK_mth212	
-	+AHT	-	+AHT	-	+AHT	-	+AHT	-	+AHT	-	+AHT
8,3*10 ⁴	1.1*10 ⁵	3*10 ⁵	0 (2,8*10 ⁵)	3,4*10 ⁵	70	7,8*10 ⁴	10	6,5*10 ⁴	10	1,9*10 ⁵	30

Table 3.9: Transformation efficiency in *E. coli* BW25113 Δ xthA cells (number of transformants per μ g DNA). 100ng of DNA was used for transformation. -/+ AHT: transformants plated on agar medium with or without AHT inducer. Colonies of pASK_exoA in *E. coli* Δ xthA (shown in red) were very small, and could be counted only after 2 days of incubation at 37°C. pASK_exoA_3M: *exoA* containing S110G, R111K, R120K mutations; pASK_exoA_4M: *exoA* containing S110G, R111K, R120K, D145N mutations;

No transformants were obtained under conditions when wild-type ExoA, ExoA mutants as well as Mth212 were overexpressed in *E. coli* BW25113 Δ xthA cells (Table 3.9). To rule out the possibility of reduced transformation efficiency due to the inability to establish plasmid DNA in the cell, colonies grown on agar medium without inducer were transferred into liquid medium and overnight culture was plated on agar medium with or without inducer.

	-	+AHT
pASK_exoA_D145N	1,04*10 ⁷	44
pASK_exoA_3M	9.5*10 ³	9

Table 3.10: Number of colonies of *E. coli* Δ xthA cells carrying pASK_exoA_D145N and pASK_exoA_3M (*exoA* containing S110G, R111K, R120K mutations) vectors. Overnight cell culture was diluted and plated on agar medium with and without AHT inducer.

When the same number of cells containing pASK_exoA_D145N vector is plated on agar medium with or without inducer, only 44 cells (=0.0004% of cells) were grown on medium with inducer, indicating that overexpression of inactive ExoA in *E. coli* Δ xthA cells in fact leads to cessation of cell growth (Table 3.10). Number of cells overexpressing ExoA triple mutant on agar medium with inducer is only 9, however, it makes 0.1% of cells grown on agar medium without inducer. This shows that a relative high number of cells survived overexpression of the ExoA triple mutant compared to overexpression of the inactive ExoA, which supports our previous result demonstrating that the ExoA triple mutant is very unstable: *E. coli* Δ xthA cells survive the overexpression of this protein because the protein is rapidly aggregated into inclusion bodies.

From experiments of *E. coli* BW25113 Δ xthA transformation it could be seen that overexpression constructs of wild-type ExoA as well as of ExoA mutants and Mth212 cannot be established in those cells (Table 3.9). Same observation was made when *E. coli* XthA was attempted to be expressed in the same strain: expression of both wild-type and inactive mutant of XthA lead to cell death. However, cells that acquired nonsense

mutations, frameshift mutations or mutations that lead to destabilization of the protein tertiary structure within *xthA* gene survived (Ber, 2009). This, *per se*, is surprising since XthA is a natural cell constituent. Why overexpression of an exonuclease III homolog results in cell death? It can be tentatively explained by fact that exonuclease III homologs are multifunctional nucleases and too much nuclease activity spills over into unspecific action thus lethally damaging the genome. However, observation that overexpression of inactive variant of ExoA also caused cell death (Table 3.10) along with results of Ber (2009) that inactive variant of XthA was lethal as well do not support this explanation.

Since it is known that inactivating amino acid exchange from aspartate to asparagine in exonuclease III homologs did not affect the DNA binding property of these proteins and even stabilize the substrate binding (Rothwell, 2000; Ciiradeva, 2009) it can be suggested that exonuclease III homologs when overexpressed unspecifically bind to DNA thus inhibiting binding of other essential proteins to DNA. From this, it can be assumed that this lethal effect should be observed in any kind of genetic background as long as it allows for sufficiently high gene expression.

However, contrary to this assumption, *E. coli* Δ *ung* strain has been routinely employed for overproduction of exonuclease III homologs without any problems (this work, Sections 3.1.2 and 3.5.1; Schomacher *et al.*, 2006; Ber, 2009; Ciiradaeva, 2009). From this it can be deduced that the possible explanation for the lethal effect lies in a phenotypic specialty of the Δ *xthA* genotype. It was shown that *E. coli* Δ *xthA* cells exhibit hyper-rec phenotype (Zieg *et al.*, 1978). The question is whether the molecular reasons of this hyper-rec phenotype and the lethal effect of exonuclease III overexpression can be brought together in a plausible model. Below it was attempted to address this question.

- Crystallographic studies of Mth212 (in collaboration with department of Prof. Ficner) revealed strong binding affinity of this protein to DNA ends, since in crystal structures of Mth212 in complex with dsDNA oligonucleotide protein was invariably bound in an exonuclease-like binding mode (Lakomek *et al.*, 2010). Furthermore, the same binding mode was reported for crystal structure of exonuclease III homolog from *A. fulgidus* in complex with dsDNA oligonucleotide (Schmiedel *et al.*, 2009), thus implying that exonuclease III homologs strongly bind to DNA ends.
- The hyper-rec phenotype of *E. coli* Δ *xthA* cells may be due to one or both of the following reasons: (1) single-strand breaks emerge when class I AP-endonuclease with associated glycosylase activity, such as Nth, MutM, or Nei remove damaged

bases from DNA with concomitant generation of DNA breaks 3' to the AP-site. In *E. coli*, exonuclease III and endonuclease IV process the unusual DNA 3'-ends (3'-dRp, 3'-phosphate) that emerge as a result of this glycosylase/AP-lyase pathway. Significantly, exonuclease III accounts for more than 95% of the total activity in *E. coli* crude extracts for removal of 3'-blocking ends (Demple *et al.*, 1986). In the absence of exonuclease III, endonuclease IV is alone responsible for removing DNA 3'-blocking ends otherwise the single-strand break will be converted to a double-strand break by an encounter with a replication fork or by the generation of a nearby nick on the opposite strand. This would induce recombinational repair by the RecBCD pathway. (2) in RecBCD recombination pathway, RecBCD binds specifically to DNA double-strand end (Kowalczykowski, 2000). In wild-type cells, such ends may be targets of competition between RecBCD and exonuclease III (Centore *et al.*, 2008). In such case, exonuclease III suppresses, to some extent, recombination and the deletion of the *xthA* gene would relieve this suppression.

- By the time cells of a $\Delta xthA$ strain are prepared for transformation, their genomes are laced with single strand breaks of the nature outlined above. After transformation, replication resumes and expression of the plasmid-borne exonuclease III gene starts. The single strand breaks are converted to double strand breaks which are in need of recombinational repair. This however, is frustrated by the large amounts of exonuclease III now present and competing with RecBCD for the DNA ends. This renders the double strand breaks lethal.

This model is in accord with all known facts of biochemistry of exonuclease III homologs and of genetics of $\Delta xthA$ mutants. It makes the following specific prediction: The lethal effect of *exoA* (or homolog) overproduction on $\Delta xthA$ cells is transient in nature and confined to the time window immediately following transformation. In other words, it should be possible to stably establish overproduction constructs of *exoA* (or homologs) with no expression of host *xthA* in the production phase of the transgene under any of the following regimes: (1) instead of employing a $\Delta xthA$ host, use gene regulation and bring down expression of the host *xthA* gene to (near) zero only after transformation. (2) introduce the *xthA* deletion into a wild type strain already transformed with the overproduction construct. (3) use a $\Delta xthA$ host that overproduces the RecBCD functions. (4) Repress *exoA* (*xthA*) transgene expression during transformation of a $\Delta xthA$ host and tune up expression only later and slowly. For lack of time, however, none of these predictions could be tested.

Remarkably, Hadi and Wilson III (2000) observed same extreme cytotoxicity of Ape2, a human AP-endonuclease with high sequence homology to *E. coli* XthA, when overexpressed in *E. coli* cells. Site-specific mutagenesis of catalytic residues as well as depletion of unique C-terminal domain of this protein provided little alleviation from the observed cytotoxicity. However, since they did not specify whether this effect was observed in $\Delta xthA$ cells it is difficult to discuss about their results in connection with this work.

To conclude this sub-section, generation of a stable variant of the ExoA triple mutant by selection of *E. coli* $\Delta xthA$ cells carrying the random library is impossible under utilized experimental conditions due to cytotoxic effect of protein overexpression on these cells.

4 Summary

Mth212, an exonuclease III homolog from the archaeon *Methanothermobacter thermoautotrophicus*, compensates the lack of a DNA uracil glycosylase (UDG) in this organism by catalyzing direct strand incision next to a uridine residue in the DNA, a reaction substituting in a single step the consecutive action of a UDG and an apurinic-/apyrimidinic (AP)-endonuclease in base excision repair (BER). What structural solution was found for Mth212 to possess this unique activity was unknown. To elucidate this question, an approach to convert ExoA from *B. subtilis*, an exonuclease III homolog without specific activity against uridine in DNA, into DNA uridine endonuclease was taken. Prior to this study, directed mutagenesis of amino acid residues of another exonuclease III based on the apo structure of Mth212 was met with limited success, and, therefore, a particular approach employing directed evolution was proposed. Directed evolution of enzymes requires efficient selection procedure. The *exoA* mutant libraries in *E. coli* and *B. subtilis* were generated and different selection strategies to identify the ExoA with acquired DNA-U activity were developed and tested.

1. *Selection in B. subtilis using PBS2 bacteriophage.* Because of the unique feature of bacteriophage PBS1 to inherently possess uracil in its DNA, this bacteriophage was the foremost candidate for creating selection pressure on bacterial cells carrying the library of mutated proteins. For this approach, lytic derivative of PBS1 (named PBS2) was required. Although intensely studied in the last decades, PBS2 bacteriophage is no longer available in the scientific community. Therefore, it was attempted to mutagenize PBS1 into a variant exhibiting same lytic activity as PBS2 by means of UV-irradiation. Approximately 2×10^6 plaques were screened for a clear-plaque mutant, yet the desired mutant was not found. Although all other prerequisites for the selection of a protein with acquired activity were fulfilled, without lytic mutant of PBS1 this selection approach could not be utilized.

2. *Selection in E. coli using virulent P2vir1Ram3 bacteriophage with uracils introduced into DNA.* In this approach Ram3 mutation in the late gene of P2vir1Ram3 bacteriophage was used to protect cells carrying desired activity from the secondary infection with newly produced bacteriophages. It was believed that due to this mutation bacterial cells die without releasing new bacteriophages. However, the P2vir1Ram3 did not fulfill this requirement and therefore could not be employed in this selection approach.

3. *Selection in E. coli using heteroduplex DNA.* This approach was based on the ability of DNA uridine endonuclease to initiate repair of uracil containing mismatch. The

E. coli lethal gene *ccdB* was used in the generation of a heteroduplex DNA with a mismatched uridine residue (U/T) as a part of stop codon. In contrast to our expectations, cloning of *ccdB* gene containing the mismatch into the phagemid vector was lethal for *E. coli* despite of the stop codon present within the gene. This makes the use of this construct in this selection approach impossible.

Due to the problems that emerged during the development of above-discussed selection strategies, directed evolution of ExoA into DNA uridine endonuclease was not accomplished. Utilization of different *E. coli* bacteriophage (approach 2) and or construction of the heteroduplex DNA with a lethal gene other than *ccdB* (approach 3) may lead to successful selection approach for directed evolution. However, due to limited time these possible modifications were not attempted.

Rationally designed S110D, R111K and R120K exchanges in the protein sequence lead to insolubility of ExoA, thus the protein could not be produced and characterized and attempts to improve the solubility of triple mutant protein met no success. Genetic selection of a stable variant of this triple mutant protein in *E. coli* $\Delta xthA$ cells was attempted, yet cytotoxic effect of protein overexpression precluded accomplishing this task. Projecting these amino acid exchanges onto another exonuclease III homolog from a thermostable organism is likely to answer the question whether these amino acids contribute to DNA uridine endonuclease activity.

The question what makes Mth212 to a DNA uridine endonuclease remains open. Directed evolution, however, is one of the straightforward methods that can indeed clarify the mechanism of uridine recognition by Mth212. Further modifications such as use of different bacteriophages and or genes will improve the methods utilized in this work and will result in a successful selection ultimately leading to the elucidation of the structural roots lying underneath the unique activity.

5 Abbreviations

Amp	ampicillin
AP-	aprimidinic/apurinic site
APS	ammoniumperoxodisulfat
bp	base pair
BSA	<i>bovine serum albumin</i>
°C	degree Celsius
C-terminal	carboxy-terminal
DNA	deoxyribonucleic acid
dNTP	deoxyribonucleoside triphosphate
dsDNA	double stranded DNA
DTT	dithiothreitol
dYT	<i>double yeast tryptone</i>
EDTA	ethylenediaminetetraacetate
e.g.	<i>exempli gratiā</i> (for example)
EP	error-prone
g	gramm
h	hours
HEPES	4-(2-Hydroxyethyl)-1-piperazin-ethan-sulfonic acid
IMAC	immobilized metal ion affinity chromatography
IPTG	isopropyl- β -D-thiogalactopyranosid
kb	kilo-base pair
l	liter
LB	Luria Bertani
M	molar
Mr	relative molecular mass
ml, μ l	milli- (10^{-3}), micro- (10^{-6}) liter
min	minutes

μm , nm	micro- (10^{-6}), nano- (10^{-9}) meter
N-terminal	amino-terminal
OD	optical density x nm
ori	origin of replication
p	pico (10^{-12})
PAGE	polyacrylamide gel electrophoresis
PCR	polymerase chain reaction
PEG	polyethyleneglycol
Pfu-Polymerase,	DNA-Polymerase B from <i>Pyrococcus furiosus</i>
RT	room temperature
rpm	rotation per minute
sec	second
SDS	sodiumdodecylsulfat
ssDNA	single stranded DNA
T	temperature
t	time
Taq-Polymerase,	DNA-Polymerase from <i>Thermus aquaticus</i>
TEMED	N,N,N',N'-Tetramethylethylenamin
Tris	tris(hydroxymethyl)aminomethan
U	enzymatic activity unit
U-Endo	DNA-uridine-endonuclease
UDG	Uracil-DNA-Glycosylase
Ugi	Uracil-DNA-Glycosylase Inhibitor
Ung	Uracil-N-Glycosylase from <i>E. coli</i>
UV	ultraviolet
Vol.	volume
v/v	volume/volume
w/v	weight/volume

3D three-dimensional

DNA/RNA-Bases:

A Adenine

C Cytosine

G Guanine

T Thymine

U Uracil

Amino acids:

A / Ala Alanine

C / Cys Cysteine

D / Asp Aspartic Acid

E / Glu Glutamic Acid

F / Phe Phenylalanine

G / Gly Glycine

H / His Histidine

I / Ile Isoleucine

K / Lys Lysine

L / Leu Leucine

M / Met Methionine

N / Asn Asparagine

P / Pro Proline

Q / Gln Glutamine

R / Arg Arginine

S / Ser Serine

T / Thr Threonine

V / Val Valine

W / Trp Tryptophan

Y / Tyr Tyrosine

6 Literature

- Abedon, S. T.** (2008). Bacteriophage Ecology: population growth, evolution, and impact of bacterial viruses (Advances in Molecular and Cellular Microbiology). Cambridge: Cambridge University Press.
- Afif H., N. Allali, M. Couturier and L. Van Melderren** (2001). The ratio between CcdA and CcdB modulates the transcriptional repression of the *ccd* poison-antidote system. *Molecular Microbiology*, 41 (1), 73-82.
- Aharoni A., A. D. Griffiths and D. S. Tawfik** (2005). High-throughput screens and selections of enzyme-encoding genes. *Current Opinion in Chemical Biology*, 9, 210-216.
- An Q., P. Robins, T. Lindahl, D. E. Barnes** (2005). C→T mutagenesis and gamma-radiation sensitivity due to deficiency in the Smug1 and Ung DNA glycosylases. *The EMBO Journal*, 24, 2205-2213.
- Aprelikova O. and J. Jiricny** (1991). Effect of uracil situated in the vicinity of a mispair on the directionality of mismatch correction in *Escherichia coli*. *Nucleic Acids Research*, 19 (7), 1443-1447.
- Arnold, F. H** (1998). Design by Directed evolution. *Accounts of Chemical Research*, 31, 125-131.
- Bahassi E. M., M. H. O'Dea, N. Allali, J. Messens, M. Gellert and M. Couturier** (1999). Interactions of CcdB with DNA gyrase. Inactivation of GyrA, poisoning of the gyrase-DNA complex, and the antidote action of CcdA. *The Journal of Biological Chemistry*, 274 (16), 10936-10944.
- Bahassi E. M., M. A. Salmon, L. Van Melderren, P. Bernard and M. Couturier** (1995). F plasmid CcdB killer protein: *ccdB* gene mutants coding for non-cytotoxic proteins which retain their regulatory functions. *Molecular Microbiology*, 15 (6), 1031-1037.
- Barret T. E., R. Savva, G. Panayotou, T. Barlow, T. Brown, J. Jiricny, L. H. Pearl** (1998). Crystal structure of a G:T/U mismatch specific DNA glycosylase: mismatch recognition by complementary-strand interactions. *Cell*, 92, 117-129.
- Beckman R. A., A. S. Mildvan and L. A. Loeb** (1985). On the fidelity of DNA replication: manganese mutagenesis in vitro. *Biochemistry*, 24 (21), 5810-5817.
- Ber, S.** (2009). Biochemische, molekularbiologische und genetische Untersuchung über strukturelle Voraussetzungen für DNA U-Endonukleaseaktivität in der ExoIII-Familie von DNA Reparaturenzymen. Dissertation. *Georg August Universität Göttingen*.
- Bernard P., K. E. Kezdy, L. Van Melderren, J. Steyaert, L. Wyns, M. L. Pato, P. N. Hoggins and M. Couturier** (1993). The F plasmid CcdB protein induces efficient ATP-dependent DNA cleavage by gyrase. *Journal of Molecular Biology*, 234, 534-541.

- Bertani, L.** (1957). The effect of inhibition of protein synthesis on the establishment of lysogeny. *Virology*, 4, 53-71.
- Bichara M., J. Wagner and I. B. Lambert** (2006). Mechanisms of tandem repeat instability in bacteria. *Mutation Research/Fundamental and Molecular Mechanisms of Mutagenesis*, 598 (1-2), 144-163.
- Bhagwat A. S. and M. Lieb** (2002). Cooperation and competition in mismatch repair: very short patch repair and methyl-directed mismatch repair in *Escherichia coli*. *Molecular Microbiology*, 44, 1421-1428.
- Black M. E., T. G. Newcomb, H. M. Wilson and L. A. Loeb** (1996). Creation of drug-specific herpes simplex virus type 1 thymidine kinase mutants for gene therapy. *Proceedings of the Natural Academy of Sciences of United States of America*, 93 (8), 3525-3529.
- Brakmann S. and A. Schwienhorst** (2004). *Evolutionary Methods in Biotechnology*. Weinheim: WILEY-VCH Verlag GmbH & Co. KgaA.
- Brakmann S. and B. F. Lindemann** (2004). Generation of mutant libraries using random mutagenesis. In S. B. Schwienhorst, *Evolutionary methods in biotechnology* (S. 5-11). Weinheim: WILEY-VCH Verlag GmbH & Co. KgaA.
- Brigidi P., E. De Rossi, M. L. Bertani, G. Riccardi and D. Matteuzzi** (1990). Genetic transformation of intact cells of *Bacillus subtilis* by electroporation. *FEMS Microbiology*, 67, 135-138.
- Bron S., K. Murray, T. A. Trautner** (1975). Restriction and modification in *B. subtilis*. Purification and general properties of a restriction endonuclease from strain R. *Molecular and General Genetics*, 143 (1), 13-23.
- Cadwell R. C. and G. F. Joyce** (1994). Mutagenic PCR. *PCR Methods and Applications*, 3, 136-140.
- Cadwell R. C. and G. F. Joyce** (1992). Randomization of genes by PCR mutagenesis. *PCR Methods and Applications*, 2, 28-33.
- Campbell C. R., D. Ayares, K. Watkins** (1989). Single-stranded DNA gaps, tails and loops are repaired in *Escherichia coli*. *Mutation Research/Fundamental and Molecular Mechanisms of Mutagenesis*, 211 (1), 181-188.
- Calsou P., A. Villaverde and M. Difais** (1987). Activated RecA protein may induce expression of a gene that is not controlled by the LexA repressor and whose function is required for mutagenesis and repair of UV-irradiated bacteriophage lambda. *Journal of Bacteriology*, 169 (10), 4816-4821.
- Centore R. C., R. Lestini and S. J. Sandler** (2008). XthA (Exonuclease III) regulates loading of RecA onto DNA substrates in log phase *Escherichia coli* cells. *Molecular Microbiology*, 67 (1), 88-101.

- Chang A. C. Y. and S. N. Cohen** (1978). Construction and characterization of amplifiable multicopy DNA cloning vehicles derived from the P15A cryptic miniplasmid. *Journal of Bacteriology*, 134 (3), 1141-1156.
- Chang S. and S. N. Cohen** (1979). High frequency transformation of *Bacillus subtilis* protoplasts by plasmid DNA. *Molecular and General Genetics*, 168, 111-115.
- Chen J., T. B. Acton, S. K. Basu, G. T. Montelione and M. Inouye** (2002). Enhancement of the solubility of proteins overexpressed in *Escherichia coli* by heat shock. *Journal of molecular Microbiology and Biotechnology*, 4 (6), 519-524.
- Chen J-C., W. M. Rideout III and P. A. Jones** (1994). The rate of hydrolytic deamination of 5-methylcytosine in double-stranded DNA. *Nucleic Acids Research*, 22 (6), 972-976.
- Chritchlow S. E., M. H. O'Dea, A. J. Howells, M. Couturier, M. Gellert and A. Maxwell** (1997). The interaction of the F-plasmid killer protein, CcdB, with DNA gyrase: induction of DNA cleavage and blocking of transcription. *Journal of Molecular Biology*, 273, 826-839.
- Cirino P. C., K. M. Mayer and D. Umeno** (2003). Generating mutant libraries using error-prone PCR. *Methods in Molecular Biology*, 231, 3-9.
- Ciirdaeva E.** (2009). Investigations into the mode of action of the DNA uridine endonuclease Mth212 of *Methanothermobacter thermautotrophicus* Δ H. Dissertation. Georg August Universität Göttingen.
- Cordoba-Canero D., E. Dubois, R. A. Ariza, M-P- Doutriaux and T. Roldan-Arjona** (2010). *Arabidopsis* Uracil DNA Glycosylase (UNG) is required for base excision repair of uracil and increases plant sensitivity to 5-Fluorouracil. *The Journal of Biological Chemistry*, 285, 7475-7483.
- Cunningham R. P., S. M. Saporito, S. G. Spitzer and B. Weiss** (1986). Endonuclease IV (nfo) mutant of *Escherichia coli*. *Journal of Bacteriology*, 168 (3), 1120-1127.
- Cutting S. M. and P. Youngman** (1994). Gene transfer in Gram-Positive bacteria. In *Methods for general and molecular bacteriology* (S. 348-364). Washington, DC: American Society for Microbiology.
- Dao-Thi M-H., L. Van Melderen, E. De Genst, H. Afif, L. Buts, L. Wyns. R. Loris** (2005). Molecular basis of gyrase poisoning by the addiction toxin CcdB. *Journal of Molecular Biology*, 348 (5), 1091-1102.
- Davidson J. F., J. Anderson, H. Guo, D. Landis and L. A. Loeb** (2002). Applied molecular evolution of enzymes involved in synthesis and repair of DNA. In S. B. Johnson, *Directed Molecular Evolution of Proteins: or How to Improve Enzymes for Biocatalysis* (S. 281-307). Wiley-VCH Verlag GmbH & Co. KGaA.
- De Bont R. and N. van Larebeke** (2004). Endogenous DNA damage in humans: a review of quantitative data. *Mutagenesis*, 19 (3), 169-185.

- De Feyter R., C. Wallace, D. Lane** (1989). Autoregulation of the *ccd* operon in the F plasmid. *Molecular and General Genetics*, 218, 481-486.
- Demple B. A., A. Johnson and D. Fung** (1986). Exonuclease III and endonuclease IV remove 3' blocks from DNA synthesis primers in H₂O₂-damaged *Escherichia coli*. *Proceedings of the Natural Academy of Sciences of United States of America*, 83, 7731-7735
- Di Noia J. M., C. Rada, M. S. Neuberger** (2006). SMUG1 is able to excise uracil from immunoglobulin genes: insight into mutation versus repair. *The EMBO Journal*, 25, 585-595.
- Dower W. J., J. F. Miller and C. W. Ragsdale** (1988). High efficiency transformation of *E. coli* by high voltage electroporation. *Nucleic Acids Research*, 16, 6127-6145.
- Dowding J. E. and D. D. Hopwood** (1973). Temperate bacteriophage for *Streptomyces coelicolor* A2(2) isolated from soil. *Journal of General Microbiology*, 78, 349-359.
- Duncan B. K. and J. Miller** (1980). Mutagenic deamination of cytosine residues in DNA. *Nature*, 287, 560-561.
- Duncan B. K. and B. Weiss.** (1982). Specific mutator effects of *ung* (uracil-DNA glycosylase) mutations in *Escherichia coli*. *Journal of Bacteriology*, 151 (2), 750-755.
- Duncan B. K. and H. R. Warner** (1977). Metabolism of uracil-containing DNA: Degradation of bacteriophage PBS2 DNA in *Bacillus subtilis*. *Journal of Virology*, 22 (3), 835-838.
- Eckert K. A. and T. A. Kunkel** (1990). High fidelity DNA synthesis by the *Thermus aquaticus* DNA polymerase. *Nucleic Acids Research*, 18, 3739-3744.
- El-Deiry W. S., K. M. Downey and A. G. So** (1984). Molecular mechanisms of manganese mutagenesis. *Proceedings of the Natural Academy of Sciences of United States of America*, 81, 7378-7382.
- Fields P. I. and R. E. Yasbin** (1980). Involvement of deoxyribonucleic acid polymerase III in W-reactivation in *Bacillus subtilis*. *Journal of Bacteriology*, 144 (1), 473-475.
- Friedberg E. C., G. C. Walker, W. Siede, R. D. Wood, R. A. Schultz, T. Ellenberger** (2006). DNA Repair and Mutagenesis. Second edition. Washington, D.C.: ASM Press.
- Fromant M., S. Blanquet and P. Plateau** (1995). Direct random mutagenesis of gene-sized DNA fragments using Polymerase Chain Reaction. *Analytical Biochemistry*, 224, 347-353.
- Fromme J. C. and G. L. Verdine** (2004). Base Excision Repair. In W. Yang, Advances in protein chemistry. Volume 69. DNA repair and replication (S. 1-28). San Diego: Elsevier Academic Press.

- Gabbar S., M. Wyszynski and A. S. Bhagwat** (1994). A DNA repair process in *Escherichia coli* corrects U:G and T:G mismatches to C:G at sites of cytosine methylation. *Molecular and General Genetics*, 243, 244-248.
- Gelfand D. H. and T. H. White** (1990). In PCR Protocols: A guide to methods and applications (S. 129-141). San Diego: Academic Press.
- Georg J., L. Schomacher, J. P. Chong, A. I. Majernik, M. Raabe, H. Urlaub, S. Müller, E. Ciirdaeva, W. Kramer and H-J. Fritz** (2006). The *Methanothermobacter thermoautotrophicus* ExoIII homologue Mth212 is a DNA uridine endonuclease. *Nucleic Acids Research*, 34 (18), 5325-5336.
- Gläsner W., R. Merkl, V. Schellenberger, H-J. Fritz** (1995). Substrate preferences of Vsr DNA mismatch endonuclease and their consequences for the evolution of the *Escherichia coli* K-12 genome. *Journal of Molecular Biology*, 245, 1-7.
- Hadi M. Z. and D. M. Wilson III** (2000). Second human protein with homology to the *Escherichia coli* abasic endonuclease III. *Environmental and Molecular Mutagenesis*, 36, 312-324.
- Hanahan, D.** (1985). DNA Cloning I. A Practical Approach. New York: Oxford University Press/IRL Press.
- Harris R. S., S. K. Petersen-Mahrt, M.S. Neuberger** (2002). RNA editing enzymes APOBEC1 and some of its homologs can act as DNA mutators. *Molecular Cell*, 10, 1247-1253.
- Hendrich B., U. Hardeland, H-H. Ng, J.Jiricny, A. Bird** (1999). The thymine glycosylase MBD4 can bind to the product of deamination at methylated CpG sites. *Nature*, 401, 301-304.
- Hilvert D., S. V. Tayoler and P. Kast** (2002). Using Evolutionary strategies to investigate the structure and function of chorismate mutases. In S. B. Johnson, Directed Molecular Evolution of Proteins: or How to Improve Enzymes for Biocatalysis (S. 29-62). Wiley-VCH Verlag GmbH & Co. KGaA.
- Hinks J. A., M. C. Evans, Y. De Miguel, A. A. Sartori, J. Jiricny and L. H. Pearl** (2002). An iron-sulphur cluster in the family 4 uracil DNA glycosylases. *Journal of Biological Chemistry*, 277, 16936-16940.
- Hitzeman R. A., and A. R. Price** (1978). *Bacillus subtilis* bacteriophage PBS2-induced DNA polymerase, its purification and assay characteristics. *The Journal of Biological Chemistry*, 253 (23), 8518-8525.
- Horst J-P., and H-J. Fritz** (1996). Counteracting the mutagenic effect of hydrolytic deamination of DNA 5-methylcytosine residues at high temperature: DNA mismatch N-glycosylase Mig.Mth of the thermophilic archaeon *Methanobacterium thermoautotrophicum* THF. *The EMBO Journal*, 15 (19), 5459-5469.

- Hoseki J., A. Okamoto, R. Masui, T. Shibata, Y. Inoue, S. Yokoyama and S. Kuramitsu** (2003). Crystal structure of a family 4 uracil-DNA glycosylases from *Thermus thermophilus* HB8. *Journal of Molecular Biology*, 333, 515-526.
- Ischenko A. A. and M. K. Sapparbaev** (2002). Alternative nucleotide incision repair pathway for oxidative DNA damage. *Nature*, 415, 183-187.
- Ishiwa H. and H. Shibahara-Sone** (1986). New shuttle vectors for *Escherichia coli* and *Bacillus subtilis*. IV. The nucleotide sequence of pHY300PLK and some properties in relation to transformation. *Japanese Journal of Genetics*, 61, 515-528.
- Jackson L.A. and L. A. Loeb** (2001). The contribution of endogenous sources of DNA damage to the multiple mutations in cancer. *Mutation Research*, 477 (1-2), 7-21.
- Jaenisch R. and A. Bird** (2003). Epigenetic regulation of gene expression: how the genome integrates intrinsic and environmental signals. *Nature Genetics*, 33 Suppl., 245-254.
- Jansohn, M.** (2006). Gentechnische Methoden. Eine Sammlung von Arbeitsanleitungen für das molekularbiologische Labor. Spektrum Akademischer Verlag.
- Kahn M. L., R. Ziermann, G. Deho, D. W. Ow, M. G. Sunshine and R. Calendar** (1991). Bacteriophage P2 and P4. *Methods in Enzymology*, 204, 264-280.
- Katz G. E., A. R. Price and M. J. Pomerantz** (1976). Bacteriophage PBS2-induced inhibition of uracil-containing DNA degradation. *Journal of Virology*, 20 (2), 535-538.
- Kavil B., M. Otterlei, G. Slupphaug, H. E. Krokan** (2007). Uracil in DNA - general mutagen, but normal intermediate in acquired immunity. *DNA Repair*, 6, 505-516.
- Kavli B., O. Sundheim, M. Akbari, M. Otterlei, H. Nilsen, P. A. Aas, L. Hagen, H. E. Krokan, G. Slupphaug** (2002). hUNG2 is the major repair enzyme for removal of uracil from U:A mismatches, and U in single-stranded DNA, with hsMUG1 as a broad specificity backup. *The Journal of Biological Chemistry*, 277, 39926-39936.
- Kosaka H., J. Hoseki, N. Nakagawa, S. Kuramitsu, R. Masuri** (2007). Crystal structure of family 5 uracil-DNA glycosylase bound to DNA. *Journal of Molecular Biology*, 373 (4), 839-850.
- Kowalczykowski S. C.** (2000). Initiation of genetic recombination and recombination-dependent replication. *Trends in Biochemical Sciences*, 25, 156-165
- Kramer B., W. Kramer and H-J. Fritz** (1984). Different base/base mismatches are corrected with different efficiencies by the methyl-directed DNA mismatch-repair system of *E. coli*. *Cell*, 38, 879-887.
- Krokan H. E., F. Drablos and G. Slupphaug** (2002). Uracil in DNA - occurrence, consequences and repair. *Oncogene*, 21, 8935-8948.

- Kunkel, T.** (1992). DNA replication fidelity. *Journal of Biological Chemistry*, 267, 18251-18254.
- Laemmli, U. K.** (1970). Cleavage of structural proteins during the assembly of the head of bacteriophage T4. *Nature*, 227, 680-685.
- Lakomek, K.** (2009). Structural characterization of the lysosomal 66.3 kDa protein and of the DNA repair enzyme Mth0212 by means of X-ray crystallography. Dissertation. Georg August University of Göttingen.
- Lakomek K., A. Dickmanns, E. Ciirdaeva, L. Schomacher and R. Ficner** (2010). Crystal structure analysis of DNA uridine endonuclease Mth212 bound to DNA. *Journal of Molecular Biology*, 399, 604-617.
- Lauer G. D. and L. C. Klotz** (1976). Molecular weight of bacteriophage PBS2 DNA. *Journal of Virology*, 18 (3), 1163-1164.
- Linderoth N. A., B. Julien, K. E. Flick, R. Calendar and G. E. Christie** (1994). Molecular cloning and characterization of bacteriophage P2 genes R and S involved in tail completion. *Virology*, 200, 347-359.
- Lindahl, G.** (1971). On the control of transcription of bacteriophage P2. *Virology*, 46, 620-633.
- Lindahl T. and B. Nyberg** (1972). Rate of depurination of native deoxyribonucleic acid. *Biochemistry*, 11 (19), 3610-3618.
- Lindahl, T.** (1993). Instability and decay of the primary structure of DNA. *Nature*, 362, 709-715.
- Lindahl T. and D. E. Barnes.** (2000). Repair of endogenous DNA damage. *Cold Spring Harbor Symp. Quant. Biol.*, 65, 127-133.
- Lindahl, T.** (2001). Keynote: Past, present and future aspects of base excision repair. *Progress in Nucleic Acid Research and Molecular Biology*, 68.
- Loris R., M-H. Dao-Thi, E. M. Bahassi, L. Van Melderen, F. Poortmans, R. Liddngton. M. Couturier and L. Wyns** (1999). Crystal structure of CcdB, a topoisomerase poison from *E. coli*. *Journal of Molecular Biology*, 285, 1667-1677.
- Love P. E. and R. E. Yasbin** (1984). Characterzation of the inducible SOS-like system of *Bacillus subtilis*. *Journal of Bacteriology*, 160 (3), 910-920.
- Lutz S. and S. J. Benkovic** (2002). Engineering protein evolution. In S. B. Johnson, Directed Molecular Evolution of Proteins: or how to improve enzymes for biocatalysis (S. 177-208). Wiley-VCH Verlag GmbH & Co. KGaA.
- Martin-Verstraete I., M. Debarbouille, A. Klier and G. Rapoport** (1994). Interactions of wild-type and truncated LevR of *Bacillus subtilis* with the upstream activating sequence of the levanase operon. *Journal of Molecular Biology*, 241, 178-192.

- Meinken C., H-M. Blencke, H. Ludwig and J. Stülke** (2003). Expression of the glycolytic *gapA* operon in *Bacillus subtilis*: differential syntheses of proteins encoded by the operon. *Microbiology*, 149, 751-761.
- Miura A. and J. Tomizawa** (1970). Mutation and recombination of bacteriophage lambda: effect of ultraviolet radiation. *Proceedings of the National Academy of Sciences of United States of America*, 67 (4), 1744-1726.
- Mol C. D., S. P. S. Parikh, C. D. Putnam, T. P. Lo and J. A. Tainer** (1999). DNA repair mechanisms for the recognition and removal of damaged DNA bases. *Annual Review of Biophysics and Biomolecular Structure*, 28, 101-128.
- Mol C. D., T. Izumi, S. Mitra and J. A. Tainer** (2000). DNA-bound structures and mutants reveal abasic DNA binding by APE1 and DNA repair coordination (corrected). *Nature*, 403, 451-456.
- Msadek T., F. Kunst, A. Klier and G. Rapoport** (1991). DegS-DegU and ComP-ComA Modulator-Effector pairs control expression of the *Bacillus subtilis* pleiotropic regulatory gene *degQ*. *Journal of Bacteriology*, 173 (7), 2366-2377.
- Nedderman P. and J. Jiricny** (1994). Efficient removal of uracil from G-U mispairs by the mismatch-specific thymine DNA glycosylase from HeLa cells. *Proceedings of the National Academy of Sciences of United States of America*, 91, 1642-1646.
- Olsen L. C., R. Aasland, H. E. Krokan and D. E. Helland** (1991). Human uracil-DNA glycosylase complements *E. coli ung* mutants. *Nucleic Acids Research*, 19 (16), 4473-4478.
- Pace C. N., F. Vajdos, L. Fee, G. Grimsley and T. Gray** (1995). How to measure and predict the molar absorption coefficient of a protein. *Protein Science*, 4, 2411-2423.
- Palmer B. R. and M. G. Marinus** (1994). The *dam* and *dcm* strains of *Escherichia coli*: a review. *Gene*, 143 (1), 1-12.
- Palva I., P. Lehtovaara, L. Kääriäinen, M. Sibakov, K. Cantell, C. H. Schein, K. Kashiwagi, C. Weissmann** (1983). Secretion of interferon by *Bacillus subtilis*. *Gene*, 22 (2-3), 229-235.
- Parikh S. S., C. D. Mol, G. Slupphaug, S. Bharati, H. E. Krokan, J. A. Tainer** (1998). Base excision repair initiation revealed by crystal structures and binding kinetics of human uracil-DNA glycosylase with DNA. *The EMBO Journal*, 17, 5214-5226.
- Patel P. H. and L. A. Loeb** (2000). DNA polymerase active site is highly mutable: evolutionary consequences. *Proceedings of the National Academy of Sciences of United States of America*, 97 (10), 5095-5100.
- Pearl, H. P.** (2000). Structure and function in the uracil-DNA glycosylase superfamily. *Mutation Research*, 460, 165-181.
- Pruss G. J. and R. Calendar** (1978). Maturation of bacteriophage P2 DNA. *Virology*, 86 (2), 454-467.

- Rastogi R. P., Richa, A. Kumar, M: B. Tyagi and R. P. Sinha** (2010). Molecular mechanisms of ultraviolet radiation-induced DNA damage and repair. *Journal of Nucleic Acids*, Published online 2010 December 16. doi:10.4061/2010/592980.
- Rice K. C. and K. W. Bayles** (2008). Molecular control of bacterial death and lysis. *Microbiology and Molecular Biology Reviews*, 72 (1), 85-109.
- Roberts J. D. and T. A. Kunkel** (1996). Chapter 7. Fidelity of DNA replication. In M. L. DePamphilis, *DNA Replication in Eukaryotic Cells* (S. 217-247). New York: Cold Springs Harbor Laboratory Press.
- Rothwell D. G., B. Hang, M. A. Gorman, P. S. Freemont, B. Singer, I. D. Hickson** (2000). Substitution of Asp-210 in HAP1 (APE/Ref-1) eliminates endonuclease activity but stabilises substrate binding. *Nucleic Acids Research*, 28 (11), 2207-2213.
- Ruiz-Laguna J., M. J. Prieto-Alamo, C. Pueyo** (2000). Oxidative mutagenesis in *Escherichia coli* strains lacking ROS-scavenging enzymes and/or 8-oxoguanine defenses. *Environmental and Molecular Mutagenesis*, 35 (1), 22-30.
- Salas-Pacheco J. M., B. Setlow, P. Setlow and M. Pedraza-Reyes** (2005). Role of the Nfo and ExoA apurinic/aprimidinic endonucleases in protecting *Bacillus subtilis* spores from DNA damage. *Journal of Bacteriology*, 187 (21), 7374-7381.
- Sandigursky M., and W. A. Franklin** (1999). Thermostable uracil-DNA glycosylase from *Thermotoga maritima*, a member of a novel class of DNA repair enzymes. *Current Biology*, 9, 531-534.
- Sandigursky M., and W. A. Franklin** (2000). Uracil DNA glycosylase in the extreme thermophile *Archaeoglobus fulgidus*. *Journal of Biological Chemistry*, 275, 19146-19149.
- Sanger F., S. Nicklen, A. R. Coulson** (1977). DNA sequencing with chain terminating inhibitors. *Proceedings of the National Academy of Sciences of United States of America*, 74, 5463-5467.
- Santos S. B., C. M. Carvalho, S. Sillankorva, A. Nicolau, E. C. Ferreira and J. Azeredo** (2009). The use of antibiotics to improve phage detection and enumeration by the double-layer agar technique. *BMC Microbiology*, 9 (148), doi:10.1186/1471-2180-9-148.
- Sartori A. A., A. Fitz-Gibbon, H. Yang, H. Miller and J. Jiricny** (2002). A novel uracil-DNA glycosylase with broad substrate specificity and an unusual active site. *The EMBO Journal*, 21, 3182-3191.
- Sartori A. A., P. Schär, S. Fitz-Gibbon, J. H. Miller and J. Jiricny** (2001). Biochemical characterization of uracil-processing activities in the hyperthermophilic archaeon *Pyrobaculum aerophilum*. *Journal of Biological Chemistry*, 276, 29979-29986.
- Sasaki I. and G. Bertani** (1965). Growth abnormalities in Hfr derivatives of *Escherichia coli* strain C. *Journal of General Microbiology*, 40, 365-376.

- Savva R., K. McAuley-Hecht, T. Brown, L. H. Pearl** (1995). The structural basis of specific base-excision repair by uracil-DNA glycosylase. *Nature*, 373, 487-493.
- Schmiedel R., B. Kuettner, A. Keim, N. Sträter and T. Greiner-Stöffele** (2009). Structure and function of an AP endonuclease from *Archaeoglobus fulgidus*. *DNA Repair*, 8 (2), 219-231.
- Schomacher L., A. K. Schürer, E. Ciirdaeva, P. McDermott, J. P. J. Chong, W. Kramer, H-J. Fritz** (2010). Archaeal DNA uracil repair via direct strand incision: A minimal system reconstituted from purified components. *DNA Repair*, 9, 438-447.
- Schomacher L., J. P. J. Chong, P. McDermott, W. Kramer and H-J. Fritz** (2009). DNA uracil repair initiated by the archaeal ExoIII homologue Mth212 via direct strand incision. *Nucleic Acids Research*, 37 (7), 2283-2293.
- Shafikhani S., R. A. Siegel, E. Ferrari and V. Schellenberger** (1997). Generation of large libraries of random mutants in *Bacillus subtilis* by PCR-based plasmid multimerization. *Biotechniques*, 23 (2), 304-310.
- Shenoy S., K. C. Ehrlich and M. Ehrlich** (1987). Repair of thymine-guanine and uracil-guanine mismatched bases in bacteriophage M13mp18 DNA heteroduplexes. *Journal of Molecular Biology*, 197 (4), 617-626.
- Shida T, T. Ogawa, N. Ogasawara, and J. Sekiguchi** (1999). Characterization of *Bacillus subtilis* ExoA protein: a multifunctional DNA-repair enzyme similar to the *Escherichia coli* exonuclease III. *Bioscience, Biotechnology and Biochemistry*, 63 (9), 1528-1534.
- Singleton P. and D. Sainsbury** (2006). Dictionary of Microbiology and Molecular Biology. Third edition, revised. West Sussex: John Wiley & Sons Ltd.
- Slepecky R. A. and H. E. Hemphill** (2006). The Genus *Bacillus* - Nonmedical. In M. D. al., Prokaryotes, Third edition (S. 530-562). Springer Science + Business Media, LLC.
- Smolorz, S.** (2009). Untersuchungen zum Problem der spezifischen Erkennung des Substrat-Uracilrestes durch die zur ExoIII-Familie gehörende Uridin-Endonuklease Mth212 aus *Methanothermobacter thermoautotrophicus*. Diplomarbeit. Georg August Universität Göttingen.
- Starkuviene V., and H. J. Fritz** (2002). A novel type of uracil DNA glycosylases mediating repair of hydrolytic DNA damage in the extremely thermophilic eubacterium *Thermus thermophilus*. *Nucleic Acids Research*, 30, 2097-2102.
- Starkuviene, V.** (2001). Identification and characterization of thermostable uracil glycosylases from the archaeon *Methanobacterium thermoautotrophicum* and the bacterium *Thermus thermophilus*. Dissertation, Georg-August Universität Göttingen.

- Steege D. A. and J. I. Horabin** (1983). Temperature inducible amber suppressor: construction of plasmids containing the *Escherichia coli* SerU- (SupD-) gene under control of the bacteriophage labmd PL promoter. *Journal of Bacteriology*, 155 (3), 1417-1425.
- Suenaga H., M. Goto and K. Furukawa** (2004). DNA shuffling. In S. B. Schwiienhorst, Evolutionary methods in biotechnology (S. 13-24). Weinheim: WILEY-VCH Verlag GmbH & Co. KgaA.
- Sunshine M. G., M. Thorn, W. Gibbs, R. Calendar and B. Kelly** (1971). P2 phage amber mutants: Characterization by use of a polarity suppressor. *Virology*, 46 (3), 691-702.
- Takahashi, I.** (1963). Transducing phages for *Bacillus subtilis*. *Journal of General Microbiology*, 31, 211-217.
- Trevors J. T., B. M. Chassy, W. J. Dower and H. P. Blaschek** (1992). Electrotransformation of bacteria by plasmid DNA. In Guide to Electroporation and Electrofusion (S. 265-290). San Diego: Academic Press.
- Vartanian J-P., M. Henry and S. Wain-Hobson** (1996). Hypermutagenic PCR involving all four transitions and a sizeable proportion of transversions. *Nucleic Acids Research*, 24 (14), 2627-2631.
- Verri A., P. Mazzarello, G. Biamonti, S. Spadari and F. Focher** (1990). The specific binding of nuclear protein(s) to the cAMP responsive element (CRE) sequence (TGACGTCA) is reduced by the misincorporation of U and increased by desamination of C. *Nucleic Acids Research*, 18, 5775-5780.
- Walker, G. C.** (1978). Inducible reactivation and mutagenesis of UV-irradiated bacteriophage P22 in *Salmonella typhimurium* LT2 containing the plasmid pKM101. *Journal of Bacteriology*, 135 (2), 415-421.
- Wang Z. and D. W. Mosbaugh** (1989). Uracil DNA glycosylase inhibitor gene of bacteriophage PBS2 encodes a binding protein specific for uracil DNA glycosylase. *Journal of Biological Chemistry*, 264, 1163-1171.
- Wang T-W., H. Zhu, X-Y. Ma, t. Zhang, Y-S. Ma and D-Z. Wei** (2006). Mutant library construction in directed molecular evolution. *Molecular Biotechnology*, 34, 55-68.
- Wanner R. M., D. Castor, C. Güthlein, E. C: Böttger, B. Springer, J. Jiricny** (2009). The uracil DNA glycosylase UdgB of *Mycobacterium smegmatis* protects the organism from the mutagenic effects of cytosine and adenine deamination. *Journal of Bacteriology*, 191 (20), 6312-6319.
- Warner H. R., B. K. Duncan, C. Garret and J. Neuhard** (1981). Synthesis and metabolism of uracil-containing deoxyribonucleic acid in *Escherichia coli*. *Journal of Bacteriology*, 145 (2), 687-695.
- Weigle, J. J.** (1953). Induction of mutations in a bacterial virus. *Proceedings of the Natural Academy of Sciences of United States of America*, 39, 628-636.

- Weiss B. and L. Grossman** (1987). Phosphodiesterases involved in DNA repair. *Advances in Enzymology*, 60, 1-34.
- Xia G., L. Chen, T. Sera, M. Fa, P. G. Schulz, F. E. Romesberg** (2002). Directed evolution of novel polymerase activities: mutation of a DNA polymerase into an efficient RNA polymerase. *Proceedings of the National Academy of Sciences of United States of America*, 99 (10), 6597-6602.
- Xiao G. Y., M. Tordova, J. Jagadeesh, A. C. Drohat, J. T. Stivers, G. L. Gilliland** (1999). Crystal structure of *Escherichia coli* uracil DNA glycosylase and its complexes with uracil and glycerol: structure and glycosylase mechanism revisited. *Proteins: Structure, Function and Genetics*, 35, 13-24.
- Xue G-P., J. S. Johnson, B. P. Dalrymple** (1999). High osmolarity improves the electrotransformation efficiency of the gram-positive bacteria *Bacillus subtilis* and *Bacillus licheniformis*. *Journal of Microbiological Methods*, 34, 183-191.
- Yang H., S. Fitz-Gibbon, E. M. Marcotte, J. H. Tai, E. C. Hyman and J. H. Miller** (2000). Characterization of a thermostable DNA glycosylase specific for U/G and T/G mismatches from the hyperthermophilic archaeon *Pyrobaculum aerophilum*. *Journal of Bacteriology*, 182, 1272-1279.
- Yoon J. H., C. S. Lee, T. R. O'Connor, A. Asui and G. P. Pfeifer** (2000). The DNA damage spectrum produced by simulated sunlight. *Journal of Molecular Biology*, 299, 681-693.
- Zieg J., V. F. Maples and S. R. Kushner** (1978). Recombination levels of *Escherichia coli* K-12 mutants deficient in various replication, recombination, or repair genes. *Journal of Bacteriology*, 134 (3), 958-966.
- Zierman R., B. Bartlett, R. Calendar and G. E. Christie** (1994). Functions involved in bacteriophage P2-induced host cell lysis and identification of a new tail gene. *Journal of Bacteriology*, 176 (16), 4974-4984.

7 Appendix

In Appendix Section original sequencing data are given (refer to the attached CD). Chromatograms are saved in .ab1 format and can be viewed by employing enclosed Chromas Lite 2.01 software. Vector sequences are given in .docx files as well as in .gb format, supported by Vector NTI software.

7.1 Vector sequences

7.2 Sequences of cloned error-prone PCR products

7.2.1 Sequences to Approach 1 (Results and Discussion, 3.2)

7.2.2 Sequences to Approach 2 (Results and Discussion, 3.3)

7.2.3 Sequences to Approach 3 (Results and Discussion, 3.4)

7.3 Verification of different clonings

7.3.1 Sequence of *exoA* with *SphI* restriction site removed

7.3.2 Sequence of cloned *serU132* tRNA gene

7.3.3 Sequence of cloned *R* gene from P2vir1Ram3 bacteriophage

7.3.4 Sequence of cloned *R* gene from P2vir1 bacteriophage

7.3.5 Sequences of *ccdB_K45* construct cloned into pJET1.2

7.4 Cloning of *ccdB_K45* construct into pBluescript II SK (+) phagemid vector

7.4.1 Sequences of *ccdB_K45* construct cloned into pBluescript II SK (+) in undesired orientation

7.4.2 Sequences of *ccdB_K45* construct cloned into pBluescript II SK (+) in desired orientation

7.5 Sequences to directed mutagenesis of ExoA

7.5.1 Sequences of ExoA single and triple mutants

7.5.2 Sequence of ExoA quadruple mutant

7.6 *exoA* sequences from survived $\Delta xthA$ transformants

7.7 Nucleotide and amino acid sequences of *exoA*

Acknowledgements

Prof. Dr. Hans-Joachim Fritz is the first I would like to thank to. I thank you for accepting me as a PhD student in your research group, for your keen supervision, motivating discussions and encouragement.

I would like to thank Dr. Wilfried Kramer. Thank you for being co-referent of the thesis, for your valuable remarks on the theoretical and practical aspects of the work, for all advices and help.

I also wish to express my gratitude to my colleagues at the department Dr. Anke Schürer, Dr. Christopher Ede, Steffen Schubert, Nils Krietenstein, Sabine Smolorz, Sabrina Lehmann, who all helped me, taught me and motivated me throughout my work. My special thanks goes to Dr. Blagovesta Popova for her continuous help, and to my lab-mates Dr. Elena Ciirdaeva and Dr. Svetlana Ber for being not only the lab-mates but very good friends. You all being so nice and friendly had a great impact on me and my work.

Many thanks to Marita Kalck, Bettina Hucke, Christiane Preiß, Angelika Löffers for their readiness to help and the warm, friendly atmosphere. I greatly appreciate the work of Olaf Waase, Patrick Regin and Jarek Sobkowiak.

I would love to extent my warmest thanks to all my friends from Göttingen. There are too many people whom I am grateful to mention all here. But thanks to you all I always felt like at home in Göttingen. My special thanks goes to Dr. Byambajav Buyandelger, Altantsetseg Tsendsuren, Khishigjargal Mookhor and Oyunsanaa Byambasuren whose help and support have been invaluable.

I wish to strongly express my thanks to the DAAD, Deutscher Akademischer Austausch Dienst, especially the Referat 423. Without the financial support from DAAD I would not be writing these words.

Last but never the least I would like to thank my family. To my beloved grandmother Sonya, who is always praying for me, I dedicate this work. I am deeply grateful to my dearest parents, my best advisers, to whom I am always their little baby. Without my Mom I would never have stepped into this fascinating field, and I can't thank her enough for that. I thank my beloved and respected grandparents, uncles and aunts, my two little sisters, whose love, support and belief in me give me the strength to go forward.

Curriculum vitae

Name: Khaliun Tseden
Date of birth: 11.11.1983
Place of birth: Greifswald, Germany
Nationality: Mongolian

1990-2000	Primary and secondary Mongolian-Russian joint school Nr. 3
2000-2004	Study of Biotechnology with major in Genetics at the Faculty of Biology, National University of Mongolia.
2004	Bachelor of Science (B.Sc.) degree in Biology. Diploma work: "Optimisation and employment of RAPD-PCR for populational genetics study of <i>Ochotona daurica</i> ".
2004-2005	Experimental work at the Institute of Human Genetics, Georg-August University of Göttingen
2005-2006	Study for the Master of Science (M. Sc.) degree in Biology at the Faculty of Biology, National University of Mongolia. Master thesis: "Premature translation of transition protein 2 mRNA causes sperm abnormality and male infertility."
2006-2007	Teaching assistant at the Faculty of Biology, National University of Mongolia
2007-2011	German Academic Exchange Service (DAAD) fellow
October 2007-till date	PhD study at the Institute of Microbiology and Genetics, Georg-August University of Göttingen under supervision of Prof. Dr. Hans-Joachim Fritz